

CRUSTAL STRUCTURE OF INDIA AND ADJOINING REGIONS USING RAYLEIGH WAVE DISPERSION

A THESIS

*submitted in fulfilment of the
requirements for the award of the degree*

of

DOCTOR OF PHILOSOPHY

in

APPLIED GEOPHYSICS

By

P. K. S. CHAUHAN



DEPARTMENT OF EARTH SCIENCES
UNIVERSITY OF ROORKEE
ROORKEE-247,667 (INDIA)

FEBRUARY, 1994

Gratis

CANDIDATE'S DECLARATION

I hereby certify that the work, which is being presented in this thesis entitled "CRUSTAL STRUCTURE OF INDIA AND ADJOINING REGIONS USING RAYLEIGH WAVE DISPERSION" in fulfilment of the requirement for the award of the Degree of Doctor of Philosophy, submitted in the Department of Earth Sciences of the University, is an authentic record of my own work carried out during a period from March, 1988 to February, 1994 under the supervision of Prof. V.N. Singh.

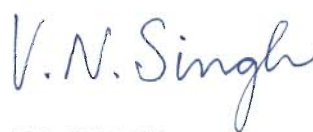
The matter embodied in this thesis has not been submitted by me for the award of any other Degree.

Candidate's Signature.

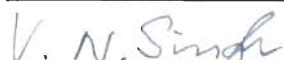

(P. K. S. CHAUHAN)

This is to certify that the above statement made by the candidate is correct to the best of my knowledge.

Signature of Supervisor.


(V.N. SINGH)
Professor
Department of Earth Sciences
University Of Roorkee
ROORKEE -247667,INDIA

The Ph.D. viva-voce examination of Mr. P.K.S.Chauhan, Research Scholar was held on 6-2-1995.


Signature of Guide


Signature of External Examiner.

ABSTRACT

Among the different methods which have been used to deduce crustal structure from seismic observations, the use of surface wave dispersion holds a prominent place. This method has been used since early 1950's. The development of the method of computing theoretical Rayleigh wave dispersion curves by Haskell and its subsequent improvement by other workers, establishment of long period seismographs by Ewing's group at Colombia, development of the improved techniques to compute group velocity dispersion curves from seismograms and establishment of global digital seismograph network, which yields high quality data have been the important landmarks in the history of surface wave dispersion studies.

A Wide Band Seismological Observatory, established at the Department of Earth Sciences, University of Roorkee, Roorkee in October, 1982, has yielded a unique data set of earthquake records. The seismographs installed at this observatory have a flat velocity response from 0.2 to 20.0 seconds, which enables these to generate analog records of local as well as distant seismic events with equal fidelity. The Rayleigh waves recorded by these seismographs have been found to span a period range of 3.0 to greater than 20.0 seconds. This provides a valuable opportunity to use short period Rayleigh waves to get refined models of the crustal structure at shallow depths.

The crustal structure of India and surrounding regions has been investigated by a number of workers. A variety of methods has been used to compute group velocity dispersion curves from Rayleigh wave data recorded by various types of seismographs at different locations. In the present study Rayleigh waves recorded

at Roorkee have been processed using multiple filter technique to get group velocity dispersion curves and to deduce crustal structure. For this purpose 18 earthquakes have been selected from seven source zones in and around India. All of which have produced well dispersed wave trains of Rayleigh waves.

Computer programs have been written for implementation of multiple filter technique, which includes computation of response of seismographs and its use in applying instrumental correction in frequency domain. The validity of this technique was tested by applying it to synthetic seismograms generated for given dispersion curves of prescribed shape. Another set of computer programs were written to generate theoretical dispersion curves of Rayleigh waves for a layered earth model using Knopoff's method. In this program roots of the dispersion function have been located by pattern search method, and group velocity has been obtained by numerical differentiation.

Use of Rayleigh wave records at a single station to deduce the seismic velocity structures in different crustal regions is one of the important features of the present work. Earthquakes used in this study have occurred in Iran, Hindukush, Afghanistan- Tadzhakistan Border, Kirghizikstan, Tadzhakistan, Tibet, China and India-Bangladesh Border. The analog records have been digitized and the digital data so obtained were analysed to obtain Rayleigh wave group velocity dispersion curves. The observed dispersion curves have been matched with theoretical dispersion curves generated using Knopoff's method. No formal inversion of dispersion curves has been attempted. Rayleigh waves in the period range 3.0-50.0 seconds have been used. Short period Rayleigh waves have yielded better control on the thickness and velocity of top layer. The interpretation of dispersion is in terms of average crustal structure over the entire path between the respective

source region of earthquakes and the recording stations. The paths cross diverse tectonic provinces. For the purposes of interpreting observed dispersion curves all plausible crustal models have been examined and their theoretical group velocity dispersion curves derived for comparison with observed curves. The total absolute errors in the matching of observed and computed dispersion curves have been found to be below 10%. In the following paragraphs some important results have been described.

In the East Ganga Basin this study has revealed a crustal thickness of 40.0 km. which agrees with that found by earlier workers. The thickness of top most sedimentary layer has been found to be 5.0 km which contrasts with the value of 3.0 km found earlier. The path of Rayleigh waves from the epicentre of the only event used is confined entirely to the East Ganga Basin.

The Rayleigh wave paths from three events in east China cross part of the Tibet plateau and Himalayan ranges. Over this path the average crustal thickness is about 61.0 km with a low speed layer at the top and another low speed layer in the depth range of 21.0–36.0 km. The shear wave velocity in the low velocity layer in the crust is only 3.71% less than that in the layer above.

The three events in the Tibet region have their epicentre almost north of Roorkee. The paths of Rayleigh waves have a substantial fraction in Tibetan Plateau and also cross Himalayan ranges. The dispersion data for Tibet region suggest the presence of low velocity layer at a depth of 20.0–40.0 km. The presence of the low speed layer has been suggested by a few other workers. The shear wave velocity in this layer has been found to be 3.71% less than that in the layer above. The average crustal thickness turns out to be 65.0 km.

The dispersion curves from four earthquakes from the Afghanistan region suggest a three layer crust with a total thickness of about 66.0 km. For the Hindukush region from which five events have been analysed, a four layer crust with total thickness of about 71.0 km is found. A thin velocity layer of 6.0 km thickness at a depth of 30.0 km has also been found, the presence of this has also been suggested on the basis of body wave studies. A thin layer at the top is found in both these cases.

An average crustal thickness of 46.0 km. is suggested in the region which includes part of Iran, Pakistan and Western Ganga Basin. No previous study exists with which these results could be compared. Some geophysical studies in the Western Ganga Basin have revealed an average crustal thickness in the range of 38.0- 45.0 km.

The present study has demonstrated the usefulness of using Rayleigh waves from Wide Band Observatory to deduce crustal structure in that the details of near surface layers have become more refined.

Non availability of sufficient number of events with well developed dispersed Rayleigh wave trains has been one of the main limitations of this study.

ACKNOWLEDGEMENTS

With a profound sense of reverence and gratitude I express my indebtedness to Prof V.N. Singh for his outstanding guidance, immense help and unflinching moral support invariably required for the completion of such a monumental task as the present one. He offered for my liberal use his precious time, acumen and expertise; despite his extremely busy schedule. He encouraged me in moments of despair, inspired me when, at times, I felt severely demotivated. Needless to say, without his "*sharing the cross*", this work could not see the light of the day.

I express my gratitude towards Prof A.K. Jain, Head of the Department, for his kind help in providing me the departmental facilities as and when required. I am grateful to Prof K. N. Khattri, Prof B. B. S. Singhal and Late Prof R. K. Goel, all ex-Heads, for their invaluable help.

I am thankful to Prof R. Chander, Dr. P. K. Gupta and Dr(Mrs) I. Sarkar for their constructive criticism and suggestions at various stages of the work.

With tremendous respect I bow before the memory of Sri Shiv Shankar Sharma, my school teacher, who led me from mediocrity to the path of perpetual accomplishments. He infused in me the confidence and the will to work untiringly and to attain success in all my endeavours-academic or personal.

I affectionately recall the invaluable help, assistance and moral support provided to me by all my friends and colleagues during the course of the work. Those who deserve special mention include Anil Semwal, Vasundhara, Tarun, Sandeep, Ajay, Shrikant, Sanjeev, Rajesh Tripathi, Prakhar and Abid. A special note of thanks to Vasundhara for taking pains in finalising the chapters.

"The man is a history-making animal, who can neither repeat his past nor leave it behind." I fondly recall, at this crucial moment, my long association with beloved Bharat Bhushan, Manendra and Rajesh, who had been beside me in all events of joy and sorrow during my stay at Roorkee. It was kind of a perfect human interaction where we shared emotionally and intellectually. I treasure for a lifetime the memories of the times spent with them.

I am thankful to Shasshank, Kamesh and Nair for extending whole-hearted help and assistance during the preparation of this document.

From a well-knit family emerges a well-endowed personality. I consider myself fortunate in the sense I have always enjoyed the blessings, trust and love of a whole spectrum of elders in the family. Besides my parents and parents-in-law, these include Arun and Sunil Bhai, Sneh and Anjali Bhabhi, sisters Sushamadi and Manishi and respected jijaji Dharm Singh I also lovingly recall tiny bundles of joy and sweetness Mini, Mishu, Abhi, Chintu and Pintoo.

"Pain when expressed loses its glory." My better half silently suffered in solitude when I pursued research for long hours. Her perseverance and understanding and love were the foundation stones over which I built many a castles of achievement. It would not have been possible to finish this work without her love and patience.

It seems a bit awkward to me to give formal and verbal expression to my feelings for my parents and parents-in-law. They, as many in typical Indian family still continue to be, have been guiding light and unlimited source of love and inspiration for me since my infancy. Additionally, they have had complete confidence in me and

my capabilities, and always encouraged me to go ahead and take a plunge whenever I revealed my ideas and plans before them. And in the instances of adverse odds, and their have been quite a few, they have never let me down and advised to try with renewed vigour. Secretly, I have always tried to emulate them; and my ambition is to reach their level of exaltation in humanness.

Finally, I express my thankfulness to all others who helped me at various points in time, and are not mentioned here explicitly.

A handwritten signature in blue ink, appearing to read 'Pradeep' with a flourish at the end.

(PRADEEP CHAUHAN)

CONTENTS

CONTENTS	Page No.
CERTIFICATE	
ABSTRACT	
ACKNOWLEDGEMENTS	
CONTENTS	
LIST OF FIGURE CAPTIONS	
LIST OF TABLES	
CHAPTER - 1 INTRODUCTION	1
1.1 General	1
1.2 Motivation	5
1.3 Literature Review	6
1.3.1 Theoretical Studies	6
1.3.2 Data Analysis	7
1.3.3 Crustal Structure	7
1.3.4 Indian Crust	9
1.3.5 Thickness of Crust in India and Surrounding Region	9
1.3.6 Velocity Structures	17
1.4 Plan of Thesis	17
CHAPTER - 2 SOME ASPECTS OF RAYLEIGH WAVE DISPERSION AND ITS MEASUREMENTS	19
2.1 Introduction	19
2.2 Rayleigh Waves on the surface of a semi elastic solid	19
2.3 Rayleigh waves on the surface of a layered half space	20
2.4 Phase and Group Velocity	22

2.4.1	Phase Velocity	22
2.4.2	Group Velocity	23
2.5	Determination of Phase and Group Velocity	28
2.5.1	Phase Velocity	28
2.5.2	Group Velocity	28
2.5.2.1	The Classical Approach	28
2.5.2.2	Spectrograph Method	29
2.5.2.3	Moving Window Method	29
2.6	Multiple Filter Technique	30
2.7	Inversion of Rayleigh Wave Data	36
CHAPTER - 3	COMPUTATION OF RAYLEIGH WAVE SYNTHETIC DISPERSION CURVES	37
3.1	Introduction	37
3.2	Haskell Method	38
3.3	Knopoff's Method	46
3.4	Discussion	49
3.5	Synthetic Dispersion Curves	54
CHAPTER - 4	COMPUTATION OF RAYLEIGH WAVE GROUP VELOCITY DISPERSION CURVE	55
4.1	Introduction	55
4.2	The Wide Band Seismological Observatory	55
4.2.1	Seismometer Response	56
4.3	Selection of Data Set	61
4.4	Computational Aspects of Multiple Filter Technique	61
4.5	Test of Computer Program MFT	68
4.5.1	Synthetic Seismogram	68
4.5.1.1	First Method	68

4.5.1.2 Second Method	71
4.5.2 Results of the Tests	78
CHAPTER - 5 ANALYSIS AND INTERPRETATION OF RESULT	79
5.1 Introduction	79
5.2 Analysis of Results and Their Interpretation	82
5.2.1 India Bangladesh Border Region	82
5.2.2 China Region	87
5.2.3 Tibet Region	93
5.2.4 Afghanistan Region	100
5.2.5 Hindukush Region	106
5.2.6 Iran Region	112
5.3 Comments	117
CHAPTER - 6 CONCLUSIONS	118
APPENDIX - I	120
REFERENCES	125

LIST OF FIGURE CAPTIONS

FIGURE NO.	DESCRIPTION	PAGE NO.
Figure-2.1	Typical phase velocity and group velocity curve for layered earth.	27
Figure-3.1	Layered earth model for continental structure	39
Figure-3.2	Synthetic Group Velocity Dispersion Curve for Model-1.	51
Figure-3.3	Synthetic Group Velocity Dispersion Curve for Model-2.	52
Figure-3.4	Synthetic Group Velocity Dispersion Curve for Model-3.	53
Figure-4.1	Velocity Response of the Wide Band Seismograph System. The Displacement and Acceleration Response are also given in the figure.	58
Figure-4.2	Epicentre Map of events selected in the present study.	62
Figure-4.3	Flow chart for Multiple Filter Technique.	64
Figure-4.4	(a) The digitized seismogram for Tibet earthquake of October, 31st, 1982. (b) Seismogram after instrumental Correction.	65
Figure-4.5	Group Velocity Dispersion Curve for China Region obtained in the present study. The solid line	69

shows the best fit line of the fourth order polynomial. * represents the observational points.

- Figure-4.6 Assumed Phase and Group velocity dispersion curve for generating synthetic seismogram for the test of program MFT. 72
- Figure-4.7 Synthetic Seismogram using Chander et al.(1968) formula. For the dispersion curve given in figure 4.6. the seismogram is generated without taking instrument effect into account. 72
- Figure-4.8 Synthetic Seismogram without taking instrument effect into account, using Bullen and Bolt(1985) Formula. The assumed dispersion curve for this seismogram is shown in figure 4.9 74
- Figure-4.9 Assumed Phase and Group velocity Dispersion Curve for generating Synthetic seismogram for testing the program MFT. 74
- Figure-4.10 Comparison of computed and assumed dispersion curves. The computed dispersion curve is 75

obtained after applying the program MFT.

- Figure-4.11 Assumed Phase and Group velocity dispersion curves set (ii) and (iii) used in the construction of Synthetic Seismograms for the test of program MFT. 76
- Figure-4.12 Assumed Phase and Group velocity dispersion Curves set (iv) and (v) used in the construction of Synthetic Seismograms for the test of program MFT. 77
- Figure-5.1 Wave path for Rayleigh waves in East Ganga Basin region. (Map modified after (Gansser, 1993)) 83
- Figure-5.2 Group velocity dispersion data of East Ganga Basin is plotted over average dispersion curve for Mid Continental type of Crust (After Brune, 1969) 84
- Figure-5.3 (a) The seismogram for India Bangladesh Border region earthquake of April, 13 1989, for 481 sec. duration. (b) Group velocity dispersion curve for East Ganga Basin. * represents the observed data and solid line represents the theoretical model. 85

- Figure-5.4 Proposed shear velocity model for East Ganga Basin. Complete model for this region is shown in the upper part of the figure. Dashed line shows the velocity model given by Chaudhary(1966). 86
- Figure-5.5 Wave path for Rayleigh waves in China region.(Map modified after (Gansser, 1993) 88
- Figure-5.6 Average Group velocity dispersion data of China Region is plotted over average dispersion curve for Mid Continental type of Crust(After Brune, 1969) 89
- Figure-5.7 (a) The seismogram for China region earthquake of April, 25 1989, for 660 sec. duration. (b) Average Group velocity dispersion curve for China Region. * represents the observed data and solid line represents the theoretical model. 91
- Figure-5.8 Proposed shear velocity model for China Region. Complete model for this region is shown in the upper part of the figure. 92
- Figure-5.9 Wave path for Rayleigh waves in Tibet region.(Map modified after (Gansser, 1993) 95

- Figure-5.10 Average Group velocity dispersion data of Tibet Region is plotted over average dispersion curve for Mid Continental type of Crust(After Brune, 1969) 96
- Figure-5.11 Average Group velocity dispersion data of Tibet Region is plotted over average dispersion curve for Alpine type of Crust(After Brune, 1969) 97
- Figure-5.12 (a) The seismogram for Tibet Region earthyquake of October, 31 1982, for 419 sec. duration. (b) Average Group velocity dispersion curve for Tibet Region. * represents the observed data and solid line represents the theoretical model. 98
- Figure-5.13 Proposed shear velocity model for Tibet Region. Complete model for this region is shown in the upper part of the figure. Dashed lines show the velocity models given by Chen and Molnar(1981) and Chun and Yoshii(1977). CM1 corresponds th 55 km crust, CM2 correspons to 70 km crust while CY1 is for 68 km crust. 99

Figure-5.14	Wave path for Rayleigh waves in Afghanistan region.(Map modified after (Gansser, 1993)	101
Figure-5.15	Average Group velocity dispersion data of Afghanistan Region is plotted over average dispersion curve for Mid Continental type of Crust(After Brune, 1969)	102
Figure-5.16	Average Group velocity dispersion data of Afghanistan Region is plotted over average dispersion curve for Alpine type of Crust(After Brune, 1969)	103
Figure-5.17	(a) The seismogram for Afghanistan-Tadzhakistan Border region earthquake of February, 27 1983, for 360 sec. duration. (b) Group velocity dispersion curve for Afghanistan Region . * represents the observed data and solid line represents the theoretical model.	104
Figure-5.18	Proposed shear velocity model for Afghanistan Region. Complete model for this region is shown in the upper part of the figure.	105
Figure-5.19	Wave path for Rayleigh waves in Hindukush region.(Map modified after (Gansser, 1993)	107

Figure-5.20	Average Group velocity dispersion data of Hindukush Region is plotted over average dispersion curve for Mid Continental type of Crust(After Brune, 1969)	108
Figure-5.21	Average Group velocity dispersion data of Hindukush Region is plotted over average dispersion curve for Alpine type of Crust(After Brune, 1969)	109
Figure-5.22	(a) The seismogram for Hindukush Region earthquake of July, 03 1984, for 363 sec. duration. (b) Group velocity dispersion curve for Hindukush Region Basin. * represents the observed data and solid line represents the theoretical model.	110
Figure-5.23	Proposed shear velocity model for Hindukush Region. Complete model for this region is shown in the upper part of the figure.	111
Figure-5.24	Wave path for Rayleigh waves in Iran region.(Map modified after (Gansser, 1993)	113
Figure-5.25	Average Group velocity dispersion data of Iran Region is plotted over average dispersion curve for Mid Continental type of Crust(After Brune, 1969)	114

Figure-5.26 (a) The seismogram for Iran earthquake of July, 12 1983, for 602 sec. duration. (b) Group velocity dispersion curve for Iran Region. * represents the observed data and solid line represents the theoretical model. 115

Figure-5.27 Proposed shear velocity model for Iran Region. Complete model for this region is shown in the upper part of the figure. 116

LIST OF TABLES

TABLE NO.	DESCRIPTION	PAGE NO.
Table 1.1	Classification of Various Crustal Type	8
Table 1.2	Velocity structure of Indian Peninsula, Central part. (After Bhattacharya, 1974)	10
Table 1.3	Velocity structure of Indian Peninsula, Western Ghats. (After Bhattacharya, 1974)	10
Table 1.4	Velocity structure of Central India. (After Bhattacharya, 1981)	11
Table 1.5	Velocity structure of Central India. (After Singh, 1987)	11
Table 1.6	Velocity structure for Ganga Basin. (After Chaudhary, 1966)	12
Table 1.7	Velocity structure for Western Ganga Basin. (After Chun, 1986)	12
Table 1.8	Velocity structure for Northern India. (After Singh, 1987)	13
Table 1.9	Velocity structure for Bay of Bengal. (After Brune and Singh, 1986)	14
Table 1.10	Velocity structure for Tibetan Plateau. (After Chun and Yoshii, 1977)	15
Table 1.11	Velocity structure for Tibetan Plateau. (After Chen and Molnar, 1981)	15

Table 1.12	Velocity structure for Northern and Central Indian ocean. (After Singh, 1988)	16
Table 3.1	Model parameters for the computation of Synthetic dispersion curves	50
Table 4.1	Hypocentral parameters of earthquakes selected in the present study.	59
Table 4.2	Regionwise distribution of earthquakes selected in the study.	60
Table 4.3	Error analysis for the MFT program for synthetic dispersion sets	73
Table 5.1	Regionwise distribution of earthquakes in six regions under present study.	80

CHAPTER-1

INTRODUCTION

1.1 GENERAL

Man's knowledge of earth under his feet has grown very slowly compared to his knowledge about the heavenly bodies which are much more fascinating. Investigations into the earth's internal structure had to wait till suitable means of making appropriate observations on its surface were available. When earthquake seismograms were examined closely it became clear that they could be utilized for learning about earth's internal structure. The travel times of compressional and shear waves that propagate through the earth's interior led Oldahm to discover, in 1906, the liquid core of the earth, and Mohorovicic, in 1909, to determine the thickness of the earth's crust. Since then much more data from many disciplines such as gravity, geomagnetism, heat flow measurements, etc. in addition to seismology has been collected and analysed to obtain more detailed knowledge about earth's interior.

The knowledge of the earth's interior developed in somewhat lopsided manner. The structure of the earth's deep interior was revealed earlier than that of the crust. Again the structure of the continental crust which is very accessible for geoscientist's investigations is less well known than that of the oceanic crust. The two types of the crust, continental and oceanic, differ in many respects, the former being much older and heterogeneous than the latter. Both the continental and the oceanic crusts are well defined and are well separated from the underlying mantle by a well demarcated discontinuity, the so called Mohorovicic discontinuity. The

continental crust is composed of sediments, gneisses, granites and granodiorite in its upper part and gabbro, amphibolites and granulites in its lower part.

The sedimentary rocks form the uppermost layer of the crust. This layer is altogether absent in some regions, whereas in others thick sedimentary sequences are found, which tend to change in their deeper parts into diagenetically modified, often metamorphosed, rock units, and cannot be distinguished from the real crystalline crust on the basis of their velocities.

Seismically the crust is defined by velocities of compressional waves less than 7.8 km/s or by shear wave velocities less than 4.3 km/s. The crustal rocks are characterised by density values less than 3.1 gm/cc (Messiner, 1986). The average thickness of continental crust is about 35.0 km and thus it forms only a thin shell of the earth. However this thin shell is very important for all scientific investigations.

In some areas an intracrustal boundary, known as the Conrad discontinuity, has been found. This has been defined as the boundary between the upper and lower continental crust. The P- wave velocity in the upper crust is less than 6.3–6.5 km/s whereas in the lower part of the continental crust this velocity exceeds 6.5 km/s.

The crustal structure has been investigated using analysis of seismological data, refraction and reflection seismic measurements, gravity, electromagnetic and magnetotelluric measurements, magnetic methods, geothermal observations, stress measurements, geological mapping, laboratory measurements of seismic wave velocities at high pressure and high temperatures, creep measurements and age determination. Of these, the seismic methods based on natural and controlled sources, have played a very prominent role in unravelling the structure of

continental crust. Seismic refraction measurements have helped in determining the velocity structure of the crust, specially in its deeper part. Improvements in techniques of conducting seismic refraction experiments and data processing coupled with advancements in methods of interpretation have yielded earth models with 3-5 different layers, some times dipping or showing velocity gradients or low velocity zones in the middle crust. Seismic reflection studies of crustal structure are characterised by the high structural resolution and the information which it yields about deeper reflections. Most of the improvements in collecting, processing and interpreting seismic reflection data is an offshoot of its use in oil exploration. The velocity structure which has emerged from such controlled source measurements to a depth of 50.0 km. as given by (Meissner,1986), is as follows;

P-wave Velocity(V_p)	Composition
$V_p < 5.7$ km/s	Sediments or near Crystalline rocks
$5.7 < V_p < 6.4$ km/s	Upper crust, (gneisses, granites)
$6.4 < V_p < 7.1$ km/s	Lower Crust (diorites, gabbros, amphibolites, granulites)
$7.1 < V_p < 7.8$ km/s	Lower most crust in shield and platform areas.
$V_p > 7.8$ km/s	Upper most mantle (peridotite)

Studies of earthquake seismograms recorded at seismological observatories all

over the world have been most valuable in understanding the structure and deformational history of the crust and upper mantle. Studies of the pattern of global seismicity have been instrumental in the development of the theory of plate tectonics, and in mapping plate boundaries. Body wave travel times from near and local earthquakes and surface wave dispersion studies have yielded a wealth of information about crustal velocity structure. The analysis of surface wave dispersion in general and those of Rayleigh wave in particular have yielded valuable information about upper mantle, particularly shear wave velocities, low velocity zones and density stratification.

Surface waves form the longest and most prominent portion of a seismogram generated by a shallow earthquake. Surface waves traverse areas with diverse geological structures and as they propagate they carry with them the information about the properties of these areas. This is reflected in the characteristics of the long dispersed wave train which is observed on a seismogram. Surface waves constitute an important source of information about earthquake size through surface wave magnitude M_s , and about the earthquake source through seismic moment tensor. Surface wave observations are being utilised in the investigations of lateral inhomogeneities and elastic anisotropy of the earth's mantle.

Rayleigh waves are the simplest and well known example of surface waves. They exist in the presence of a free surface such as earth's surface. In a homogeneous half space Rayleigh waves are non dispersive i.e., their velocity does not depend on frequency. However in a layered earth these waves show strong dispersion and give rise to a long dispersed wave train on a seismogram. Vertical component seismograms of shallow focus earthquakes display prominently the Rayleigh waves unaffected by Love waves.

1.2 MOTIVATION

A Wide Band Seismological Observatory was established at the Department of Earth Sciences in October, 1982. This yielded a unique data set of earthquakes seismograms for both local and distant events. The broad band seismographs installed at this observatory have a flat velocity response between 0.2 to 20.0 seconds. This makes it possible to record surface wave trains with periods as short as 2.0 seconds. Thus these records present a good opportunity to study short period Rayleigh waves which can yield valuable information about velocity structure of upper crustal layers. This was the starting point in taking up present investigation.

A survey of literature revealed that not many studies of the crustal structure of India and surrounding regions have been done. Of these only three studies have made use of multiple filter technique in analysing dispersed wave trains. An important step in this direction was taken when Rayleigh waves of an earthquake with its epicentre in Afghanistan Tadjhakistan border region and recorded at Roorkee were analysed by Tokhi(1987) in the course of an M.Tech. dissertation. This study, though quite limited in its scope, acted as a catalyst in embarking upon the present investigation. It was thought that if suitable earthquakes are selected having good azimuthal distribution and their Rayleigh wave dispersion characteristics are analysed using seismograms of Wide Band Seismological Observatory at Department of Earth Sciences, University of Roorkee, Roorkee and employing multiple filter technique, it would give additional information about regional crustal velocity structure. The studies were accordingly planned and a set of 18 earthquakes in seven source zones was finally selected for detailed investigations. In the present work, group velocity dispersion curves of Rayleigh waves have been computed and compared with theoretical dispersion curves

generated for given velocity models.

1.3 LITERATURE REVIEW

The use of seismic surface waves in the study of earth's interior was started in early 1950's. The development of Haskell(1953) method of computing the surface wave dispersion function and installation of long-period seismographs world-wide by Ewing's group at Columbia constituted some of the early advances. Since then the use of surface waves of both Rayleigh and Love types in the study of the earth's interior has made rapid progress. A major breakthrough in this direction was the availability of fast digital computers and the installation of Global Digital Seismograph Network which provided high quality data for later studies.

1.3.1 Theoretical Studies

The earliest study carried for surface wave dispersion analysis was initiated by Thomson(1950) which was later extended by Haskell(1953) for the perfectly elastic multilayered media. The first implementation of Haskell's method was done by Dorman et al.(1960) on first generation computers and by Press et al.(1961) on second generation computers. The optimization of this method for computer application was treated by Schwab and Knopoff(1970), who discussed in detail the loss of precision and other problems in this method. Among other attempts dealing with improvements in the computational aspects of Haskell method the most notable is that of Watson(1970) reduced Δ - matrix extension, which is the fastest and contains the loss of precision control feature. Knopoff(1964) gave an alternate method for treating the problem posed by Haskell(1953). The computer implementation of Knopoff's method was performed by Randall(1967). The computer application and optimization of the Knopoff's method was carried out by

Schwab(1970). A considerable saving of computer time was achieved with the help of improvements suggested and carried out by Schwab(1970).

1.3.2 Data Analysis

On the observational front two types of studies were conducted by various workers in the field of surface wave analysis i.e., phase-velocity and group-velocity dispersion studies. Among the different methods suggested for phase-velocity determination the most notable are the two station method(classical approach) by Sato(1955), method of summation and multiplication of records by Bloch and Hales(1968), triangular array method by Press(1956b) and frequency-wavenumber method by Linville and Laster(1967). The early determination of the group-velocity was carried out by the classical Peak and Trough Method(Brune,1960). Later developments include the use of electrical analogue spectrograph by Ewing et al.(1959). Use of Fourier transform is exemplified by the Moving Window Method(Iyer,1964, Landisman et al., 1969), FTAN Method(Levshin et al., 1972) and the Multiple Filter Technique (Dziewonski et al.,1969). Most of the group velocity determination are carried by the Multiple Filter Technique which has also been used in the present investigations.

1.3.3 Crustal Structure

Santo(1963) and Brune(1969) have given a classification of the crust and mantle on the basis of surface wave studies. The most important parameters used in classifying the various types of crust are: crustal thickness, upper mantle P, velocity, tectonic characteristics, sediment thickness and the water depth(in case of oceanic crust). The classification of various crustal types as suggested by Brune(1969) has been shown in Table - 1.1.

TABLE - 1.1

CRUSTAL TYPES

Crustal Type	Crustal Thickness Km.	Pn Velocity Km/sec	Tectonic Characteristics	Geological Features
A. Shield	35	8.3	Very stable	Little or no sediment exposed batholithic rocks of Precambrian age.
B. Mid-continent	38	8.2	Stable	Moderate thickness of post-Precambrian sediments.
C. Basin-range	30	7.8	Very unstable	Recent normal faulting, volcanism and intrusion; high mean elevation.
D. Alpine	55	8.0	Very unstable	Rapid recent uplift, relatively recent intrusion; high mean elevation.
E. Great island arc	30	7.4-7.8	Very unstable	High volcanism, intense folding and faulting.
F. Deep ocean basin	11	8.1-8.2	Very stable	Very thin sediments overlying basalts, linear magnetic anomalies, no thick Paleozoic sediments.
G. Shallow water mid-ocean ridge	10	7.4-7.6	Unstable	Active basaltic volcanism little or no sediments.

(Based on Brune, 1969)

1.3.4 Indian Crust

Many workers e.g., Chaudhary(1966,67), Gupta and Narain(1967), Chatterji(1971), Negi and Singh(1973), Tandon(1973), Bhattacharya(1971,74,81), Chen and Molnar(1975,81), Chun and Yoshii(1977), Romanowicz(1982), Chun(1986), and Singh(1987,88) have deduced the crustal structure of India and surrounding regions with the help of surface wave dispersion studies. The computation of group velocity has mostly been carried out by the classical peak and trough method. Some workers, e.g., Singh(1987) have used Multiple Filter Technique. The Indian ocean crust has been studied by Nag(1967), Sourio(1981) and Singh(1988) with the help of surface wave dispersion.

1.3.5 Thickness of crust in India and surrounding region

For the purpose of this section the surface waves studies of Indian crust have been grouped into following types.

- (a) Peninsular region
- (b) Gangetic Plain
- (c) Himalayan Region
- (d) Bay of Bengal
- (e) Tibetan Plateau
- (f) Indian Ocean Region

In the peninsular region estimates of crustal thickness vary from 41.0 to 50.0 km. The higher value for crustal thickness has been found in the Western Ghat region and lower value in the central portion. This region has been studied by Bhattacharya(1971,74,81), Tandon(1973) and Singh(1987).

TABLE - 1.2

INDIAN PENINSULA, CENTRAL PART
(After Bhattacharya, 1974)

Layer No.	Thickness (Km.)	P - wave velocity (Km/sec.)	S - wave velocity (Km/sec.)	Density (gm/cc)
1.	12.0	5.57	3.95	2.60
2.	29.0	6.44	3.92	3.01
.....				
3.	19.0	8.24	4.73	3.30
4.	40.0	8.24	4.8"	3.30
5.	20.0	8.30	4.8"	3.30
6.	40.0	8.30?	4.8"	3.40
7.	60.0	8.40	4.55	3.40
8.	60.0	8.40	4.55	3.50
9.	60.0	8.50	4.75	3.50
10.	20.0	8.50	4.75	3.60
11.	40.0	8.60	4.75	3.60
12.	100.0	9.10	5.10	3.90
13.	180.0	9.20	5.40	4.10
14.	20.0	10.00	5.80	4.20
15.	-	11.00	6.30	4.30

TABLE - 1.3

INDIAN PENINSULA, WESTERN GHATS
(After Bhattacharya, 1974)

Layer No.	Thickness (Km.)	P - wave velocity (Km/sec.)	S - wave velocity (Km/sec.)	Density (gm/cc)
1.	16.0	6.00	3.50	2.63
2.	36.0	6.60	3.98	3.15
.....				
3.	48.0	8.24	4.73	3.30
4.	40.0	8.24	4.64	3.30
5.	20.0	8.30	4.64	3.30
6.	40.0	8.30	4.64	3.40
7.	-	11.00	6.30	4.30

TABLE - 1.4

CENTRAL INDIA
(After Bhattacharya, 1981)

Layer No.	Thickness (Km.)	P - wave velocity (Km/sec.)	S - wave velocity (Km/sec.)	Density (gm/cc)
1.	20.4	5.78	3.530	2.60
2.	18.3	6.58	3.916	3.01
.....				
3.	61.3	8.19	4.603	3.30
4.	20.0	8.30	4.603	3.30
5.	20.0	8.30	4.603	3.40
6.	80.0	8.40	4.570	3.40
7.	60.0	8.40	4.550	3.50
8.	60.0	8.50	4.550	3.50
9.	20.0	8.50	4.700	3.60
10.	40.0	8.60	4.700	3.60
11.	-	9.10	5.300	3.70

TABLE - 1.5

CENTRAL INDIA
(After Singh, 1987)

Layer No.	Thickness (Km.)	P - wave velocity (Km/sec.)	S - wave velocity (Km/sec.)	Density (gm/cc)
1.	19.0	5.81	3.40	2.72
2.	11.0	6.42	3.70	2.82
3.	11.0	6.66	3.94	2.95
4.	03.0	4.60	2.50	3.24
.....				
5.	20.0	8.10	4.35	3.40
6.	20.0	8.20	4.40	3.40
7.	20.0	8.20	4.45	3.40
8.	95.0	8.40	4.15	3.30
9.	40.0	8.40	4.25	3.40
10.	40.0	8.50	4.45	3.50
11.	20.0	8.50	4.65	3.60
12.	40.0	8.60	4.75	3.60
13.	100.0	9.10	5.10	3.90
14.	-	10.00	5.80	4.20

TABLE - 1.6

GANGA BASIN
(After Chaudhary, 1966)

Layer No.	Thickness (Km.)	P - wave velocity (Km/sec.)	S - wave velocity (Km/sec.)	Density (gm/cc)
1.	3.0	3.98	2.30	2.340
2.	17.0	6.15	3.55	2.817
3.	20.0	6.58	3.80	2.922

TABLE - 1.7

WESTERN GANGA BASIN
(After Chun, 1986)

Layer No.	Thickness (Km.)	P - wave velocity (Km/sec.)	S - wave velocity (Km/sec.)	Density (gm/cc)
1.	4.0	4.06	2.34	2.66
2.	6.0	5.31	3.06	2.72
3.	10.0	6.57	3.80	3.00
4.	20.0	6.89	3.98	3.08
.....				
5.	80.0	7.83	4.52	3.29
6.	80.0	8.08	4.66	3.34
7.	-	7.97	4.60	3.32

TABLE - 1.8

NORTHERN INDIA
(After Singh, 1987)

Layer No.	Thickness (Km.)	P - wave velocity (Km/sec.)	S - wave velocity (Km/sec.)	Density (gm/cc)
1.	4.0	3.50	1.65	1.82
2.	16.0	5.81	3.40	2.74
3.	15.0	6.42	3.70	2.82
4.	15.0	6.66	3.94	2.95
.....				
5.	20.0	8.10	4.45	3.40
6.	20.0	8.20	4.52	3.40
7.	95.0	8.40	4.40	3.30
8.	40.0	8.40	4.45	3.40
9.	40.0	8.50	4.60	3.50
10.	20.0	8.50	4.75	3.60
11.	40.0	8.60	4.75	3.60
12.	100.0	9.10	5.10	3.90
13.	-	10.00	5.80	4.20

TABLE - 1.9

BAY OF BENGAL
(After Brune and Singh, 1986)

Layer No.	Thickness (Km.)				P - wave velocity (Km/sec.)	S - wave velocity (Km/sec.)	Density (gm/cc)
	A	B	C	D			
1.	3.50	3.00	2.50	2.00	1.500	0.000	1.029
2.	0.25	0.25	0.25	0.25	1.651	0.345	-
3.	0.75	0.75	0.75	0.75	2.001	0.805	1.099
4.	2.25	2.75	2.25	3.50	3.303	1.518	1.797
5.	2.25	3.75	3.75	7.50	4.706	2.500	2.533
6.	9.00	11.00	17.50	22.00	6.813	3.940	2.738
7.	9.02	9.02	9.02	9.02	8.100	4.700	3.079
	27.02	30.52	37.02	45.02		MOHO	
8.	38.79	34.79	27.79	19.29	8.257	4.763	3.051
9.	100.30	100.30	100.30	100.30	8.001	4.800	3.014
10.	105.00	105.00	105.00	105.00	8.400	4.850	3.020
11.	105.20	105.20	105.20	105.20	8.837	5.050	3.030
12.	-	-	-	-	10.550	5.840	3.190

TABLE - 1.10

TIBET PLATEAU
(After Chun and Yoshii, 1977)

Layer No.	Thickness (Km.)	P - wave velocity (Km/sec.)	S - wave velocity (Km/sec.)	Density (gm/cc)
1.	03.5	4.50	2.60	2.40
2.	08.5	5.98	3.45	2.80
3.	16.0	5.98	3.42	2.80
4.	10.0	5.80	3.37	2.75
5.	30.0	6.30	3.64	2.90
6.	-	7.70	4.45	3.30

TABLE -1.11

TIBET PLATEAU
(After Chen and Molnar, 1981)

Layer No.	Thickness		Thickness		Thickness	
	A (Km.)	S-wave velocity (Km/sec)	B (Km.)	S-wave velocity (Km/sec)	C (Km.)	S-wave velocity (Km/sec)
1.	3.75	2.55	3.75	2.55	3.75	2.55
2.	16.25	3.40	41.25	3.40	41.25	3.40
3.	25.00	3.50	15.00	3.70	15.00	3.70
4.	10.00	3.70	10.00	3.90	25.00	3.90
5.	25.00	4.40	20.00	4.40	40.00	4.70
6.	10.00	4.47	10.00	4.41	-	4.38
7.	10.00	4.42	25.00	4.38		
8.	25.00	4.38	-	4.37		
9.	-	4.37				

TABLE - 1.12

NORTHERN AND CENTRAL INDIAN OCEAN
(After Singh, 1988)

Layer No.	Thickness (Km.)	P - wave velocity (Km/sec.)	S - wave velocity (Km/sec.)	Density (gm/cc)
1.	3.50	1.500	0.000	1.029
2.	0.85	1.651	0.345	1.029
3.	0.75	2.001	0.805	1.099
4.	0.80	3.303	1.518	1.797
5.	2.20	4.706	2.500	2.533
6.	15.00	6.813	3.940	2.738
.....				
7.	15.00	8.100	4.650	3.079
8.	40.00	8.160	4.763	3.051
9.	40.00	7.900	4.450	3.014
10.	50.00	7.800	4.300	3.014
11.	105.00	8.400	4.850	3.020
12.	-	8.837	5.050	3.030

Chaudhary(1966,67), Chatterjee(1971) and Chun(1986) have studied crustal structure in the Gangatic plains and have found crustal thickness between 40.0 and 43.0 km. The thinning of low velocity sediments along the southern margins of Gangatic basin has also been reported. Chun(1986) found the crust in western Ganga basin to have oceanic affinity.

In the Himalayan region a crustal thickness of 50.0 km has been reported(Negi and Singh, 1973; Singh, 1987). In Tibetan region a thickness of 45.0 km by Gupta and Narain(1967) and 70.0 km by Chun and Yoshii(1977) have been reported. Chen and Molnar(1981) have given the crustal thickness for Tibetan region: 55.0 km, 70.0 km and 85.0 km. Romanowicz(1982) gave a crustal thickness 65.0 km.

In the Indian ocean region a crustal thickness of 5.0-10.0 km in northern and central part has been reported by Nag(1967) and 23.0 km by Singh(1988) in the same region. Brune and Singh(1986) obtained a thickness of 35.0 km in the northern most part of the Bengal fan, 15.0 km in the ocean south of the southern tip of India and 20.0 km thick crust of more continental type at 20° N.

1.3.6 Velocity Structures

Velocity structures in different regions of India and its surroundings have been presented in the Table 1.2 to Table 1.12.

1.4 PLAN OF THESIS

Chapter - 2 deals with some aspects of the Rayleigh wave dispersion and the different methods of its analysis. The philosophy behind the Multiple Filter Technique is also discussed in it.

Chapter - 3, the theoretical aspects of the computation of Rayleigh wave dispersion method have been presented. The Haskell and Knopoff methods for computing the Rayleigh wave dispersion function have been discussed briefly.

Chapter - 4 deals with various steps involved in the analysis of the real data. The seismometer response and the selection of the data for the present study have also been discussed. The validation of the main program for implementing Multiple Filter Technique has been discussed with the help of synthetic seismograms.

Chapter - 5, deals the results and interpretation of observed dispersion curves. The velocity models for different regions which have been derived in the present study have also been presented.

Chapter - 6 gives the conclusions arrived at and the limitation of the work presented herein.

CHAPTER-2

SOME ASPECTS OF RAYLEIGH WAVE DISPERSION AND ITS MEASUREMENT

2.1 INTRODUCTION

In the present study the group velocity dispersion characteristics of Rayleigh waves recorded by seismographs at the Wide Band Seismological Observatory have been studied to deduce the crustal structure in India and surrounding regions. In the following paragraphs, some aspects of Rayleigh wave propagation and their dispersion characteristics have been outlined.

2.2 RAYLEIGH WAVES ON THE SURFACE OF A SEMI INFINITE ELASTIC SOLID

In 1885 Lord Rayleigh developed a theory of waves propagating on the free surface of a semi-infinite elastic solid. These waves are now known as Rayleigh waves. The waves propagate along the surface of semi infinite elastic solid with particles of the medium describing a retrograde elliptical motion in vertical plane. Their velocity is about 0.92 times that of the shear wave velocity in a homogeneous medium which has a Poisson's ratio equal to 0.25. The vertical component of particle displacement is about 1.5 times the horizontal component. The amplitude of particle motion diminishes with depth with horizontal component decreasing exponentially and changing sign at a depth of about 0.192 times the wavelength and the vertical

component decreasing exponentially throughout. The retrograde elliptical motion becomes prograde with change in sign of horizontal component.

The phase velocity c of Rayleigh waves in this case is given by following expression:

$$\left(2 - \frac{c^2}{\beta^2}\right)^2 - 4\left(1 - \frac{c^2}{\alpha^2}\right)^{1/2} \cdot \left(1 - \frac{c^2}{\beta^2}\right)^{1/2} = 0 \dots (2.1)$$

where α , β are compressional and shear wave velocities in the medium.

The above equation yields only one value of c/β lying between 0 and 1, if quantities under the squareroots have to remain non negative. This velocity ratio is a function of Poisson's ratio σ . For $\sigma = 0.25$, c turns out to be approximately 0.9194 β . The particle displacements at the surface of the semi infinite elastic solid are found to be such that horizontal component along the direction of propagation lags behind the vertical component by $\pi/2$.

2.3 RAYLEIGH WAVES ON THE SURFACE OF A LAYERED HALF SPACE

In the case of a layered earth model, Rayleigh waves are found to be dispersive, i.e. their velocity varies with wavelength. The waves are spread out over an interval in the form of a wave train characterised by both amplitude and frequency modulation. In the case of a single layer over a half space, where shear wave velocity in the half space is greater. The phase velocity of Rayleigh waves is determined by:

$$\Delta_R = 0 \quad \dots\dots(2.2)$$

where

$$\Delta_R = \begin{bmatrix} \gamma_1^2 & \gamma_1^2 & 0 & 2ikb_1 & -2ikb_1 & 0 \\ 2ika_1 & -2ika_1 & 0 & -\gamma_1^2 & -\gamma_1^2 & 0 \\ \gamma_1^2 e^{a_1 h} & \gamma_1^2 e^{-a_1 h} & -\gamma_2^2 e^{-a_2 h} & 2ikb_1 e^{b_1 h} & -2ikb_1 e^{-b_1 h} & 2ikb_1 e^{-b_2 h} \\ 2ika_1 e^{a_1 h} & -2ika_1 e^{-a_1 h} & 2ika_2 e^{-a_2 h} & -\gamma_1^2 e^{b_1 h} & -\gamma_1^2 e^{-b_1 h} & -\gamma_2^2 e^{-b_2 h} \\ ike^{a_1 h} & ike^{-a_1 h} & -ike^{-a_2 h} & -b_1 e^{b_1 h} & b_1 e^{-b_1 h} & -b_2 e^{-b_2 h} \\ a_1 e^{a_1 h} & -a_1 e^{-a_1 h} & a_2 e^{-a_2 h} & ike^{b_1 h} & ike^{-b_1 h} & -ike^{-b_2 h} \end{bmatrix}$$

$$\dots\dots(2.3)$$

where $a_i = (k^2 - k^2 \alpha_i)^{1/2}$; $b_i = (k^2 - k^2 \beta_i)^{1/2}$;

$$\gamma_i^2 = 2k^2 - k^2 \beta_i \quad , \quad i = 1, 2$$

When roots of equation(2.2) are determined numerically, it is found that one real root always lies between k_{R1} and k_{R2} , where $k_{R1} = w/c_{R1}$ and $k_{R2} = w/c_{R2}$, c_{R1} and c_{R2} being Rayleigh wave velocities of the layer and half space respectively($c_{R1} = 0.92 \beta_1$, $c_{R2} = 0.92 \beta_2$). Thus the velocity of Rayleigh waves of very short wavelength is about

nine-tenths of the shear wave velocity of layer. For very long wavelengths on the other hand, the Rayleigh wave velocity is nine-tenths of the shear wave velocity in the half space. For waves of intermediate wavelengths their velocity lies in between these two extremes.

There are other real and complex roots of equation(2.2) which have been discussed elsewhere, e.g., Pilant(1979). The real root as discussed above leads to fundamental mode Rayleigh waves and other roots give rise to higher shear modes. Of all the modes only the fundamental mode is without a cut off frequency, all frequencies from zero to infinity being propagated. All other modes have cut off frequency.

The case of 'n' layered half space, though more complex, can be dealt similarly. It is found that Rayleigh waves in this case exhibit a more complicated dispersion. Haskell(1953) has discussed this case in greater detail.

Due to their two dimensional nature, Rayleigh waves attenuate less rapidly with distance as compared to body waves. Their amplitudes diminish approximately by $r^{-1/2}$, where r is the epicentral distance. At great distances from the seismic disturbance, they carry much more energy than any other type of wave(Grant and West, 1965).

2.4 PHASE AND GROUP VELOCITY

2.4.1 Phase Velocity :-

As mentioned above Rayleigh waves observed in the earth show dispersion, i.e., their phase velocity is a function of frequency or wavelength. Since different

frequencies travel with different velocities, a spreading of waves is observed. The fact that the velocities of different frequencies are related to seismic wave velocities, and as of different layers in a layered earth model, is the basis of the use of dispersion of Rayleigh waves to study the properties of the earth's interior. Beginning with the early studies of Ewing and co-workers (Ewing et. al., 1959) surface wave dispersion of both Rayleigh and Love waves have been widely used for both regional and global studies of outer 1000 Km. of the earth.

It is common practice to express the velocity of Rayleigh wave propagation in dispersive wavetrains in terms of either phase velocity or group velocity. The phase velocity can be defined as the velocity of a wave at a specific frequency i.e.,

$$c = \omega/k \quad \dots\dots(2.4)$$

where ω = angular frequency and

k = angular wavenumber.

In case of a dispersive wave train of Rayleigh waves, the phase velocity is approximately equal to the velocity of its peaks, troughs, or zero crossings. Since average velocity in the earth increases as a function of depth, it is to be expected that waves with longer wavelengths will tend to have higher phase velocity. There are a number of methods available for measuring phase velocity.

2.4.2 Group Velocity :-

The concept of group velocity is associated with a wave packet. It is the velocity with which the maximum of a wave packet will travel in a dispersive medium. The peaks, troughs and zero crossings of a wave packet travel with phase velocity

whereas the wave packet as a whole travels with group velocity which in general is less than the phase velocity for most of the surface waves observed on seismogram. The group velocity, U , can be expressed as

$$U = \frac{dw}{dk} = c + k \frac{dc}{dk} \quad \dots\dots(2.5)$$

In terms of wavelengths

$$U = c - \lambda \frac{dc}{d\lambda} \quad \dots\dots(2.6)$$

The concept of group velocity of a dispersed wave train can also be explained in a different way as follows:

Let a seismic signal $f(t)$ consisting of fundamental Rayleigh mode be recorded by a seismic station at a distance r from the source, and azimuth θ from the source. The fourier transform of $f(t)$ is:

$$F(\omega) = \int_0^{\infty} f(t) \cdot \exp(-i\omega t) dt. \quad \dots(2.7).$$

The complex spectrum $F(\omega)$ can be written as:

$$F(\omega) = A(r, \theta, \omega) \cdot \exp[i\phi(r, \theta, \omega)] \quad \dots(2.8).$$

Where $A(r, \theta, \omega)$ is the amplitude spectrum and $\phi(r, \theta, \omega)$ is the phase spectrum. The amplitude spectrum depends on source mechanism of the earthquake, elastic and attenuation properties of the intervening medium and the amplitude response of the seismograph system at the recording station. The phase spectrum can be represented as

$$\phi(r, \theta, \omega) = k(\omega) \cdot r + \phi_0(\theta, \omega) + \phi_i(\omega) \quad \dots(2.9).$$

where $k(\omega)$ is the angular wavenumber, $\phi_0(\theta, \omega)$ is the source phase shift, and $\phi_i(\omega)$ is the instrumental phase shift. In order to describe the dispersive wave train in simple terms, the phase shifts ϕ_0 and ϕ_i are neglected and the inverse transform of equation(2.8) is written as

$$f(t) = \frac{1}{2\pi} \int_0^{\infty} A(r, \theta, \omega) \cdot \exp[i(\omega t - k(\omega)r)] d\omega \quad \dots(2.10).$$

The velocity of propagation of a monochromatic wave of frequency ω_0 can be found by setting the phase $\omega_0 t - k(\omega)r$ to a constant and then differentiating with respect to ω_0 , thus getting the equation

$$c(\omega_0) = \frac{\omega_0}{k(\omega_0)} \quad \dots\dots(2.11)$$

If the equation(2.10) is evaluated in the vicinity of ω_0 it is written as:

$$f(t)_{\omega_0} = \int_{\omega_0 - \epsilon}^{\omega_0 + \epsilon} A(r, \theta, \omega) \cdot \exp[i(\omega t - k(\omega)r)] d\omega \quad \dots(2.12).$$

The function $f(t)_{w_0}$ will be maximum when all the waves are in phase within the frequency band $(w_0 - e, w_0 + e)$ or

$$\frac{d}{dw} [wt - k(w)r]_{w=w_0} = 0 \quad \dots(2.13).$$

This yields the group travel time (t_{gr}) as:

$$t_{gr} = t_{w_0} = \left[\frac{dk(w)}{dw} \right]_{w=w_0} \cdot r \quad \dots(2.14).$$

and

$$U(w_0) = \left[\frac{dw}{dk(w)} \right]_{w_0} \quad \dots(2.15).$$

is the group velocity at $w=w_0$.

Fig.(2.1) shows some typical group velocity and phase velocity curves for simple layered media. The minimum in group velocity curves is known as Airy phase. As can be seen, wave with periods shorter than the period of Airy phase is characterised by reverse group velocity dispersion i.e., shorter periods will travel faster.

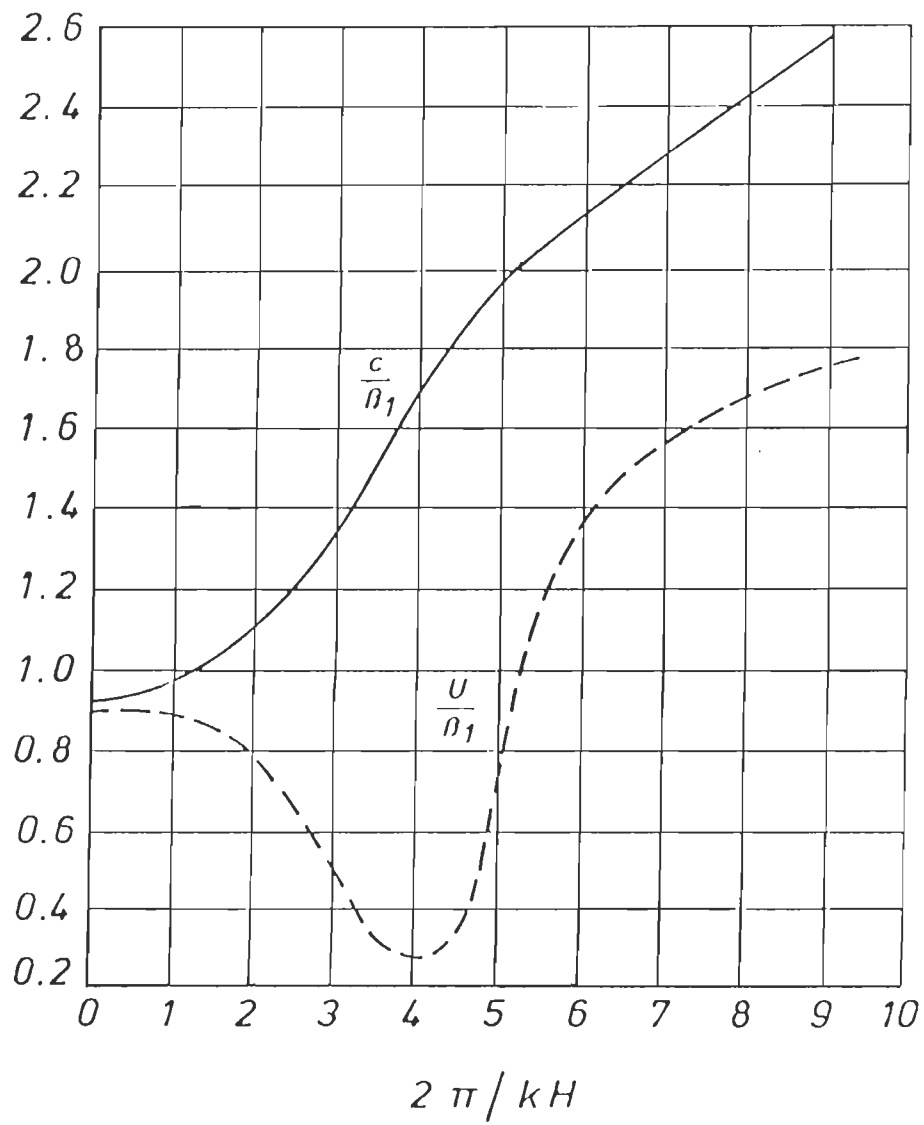


Figure-2.1 Typical phase velocity and group velocity curve for layered earth.

2.5 DETERMINATION OF PHASE AND GROUP VELOCITY

2.5.1 Phase Velocity

Several methods have been suggested to compute phase velocity from an observed wave train. At present such computations are carried out with the help of computers employing spectral techniques. Two station methods are in more common use. The two stations are so selected that they are aligned on a great circle path to the earthquake source. The time delays between station pairs of peaks, troughs or zero crossings for phases of different periods in the wave train are measured. Spectral techniques are in more common use, e.g., the one proposed by Bloch and Hales(1968), which involves measurement of group velocity prior to phase velocity determination. Methods based on single station and those based on tripartite stations have also been proposed.

2.5.2 Group Velocity

In the present study group velocity dispersion curves of Rayleigh waves have been used to deduce the crustal structure in India and surrounding regions. The group velocity of a surface wave at a frequency w is the velocity at which an envelop of a wave packet with frequency centered at w is transported. The wave packet comprising the group of waves has a continuous spectrum.

A number of methods exist for the determination of group velocity. Some of these are discussed below:

2.5.2.1 The Classical Approach: It is known as the Peak and Trough method or the graphical method. It consisted of determining instantaneous frequency at each time

point; following the method of Brune(1960); and then plotting a graph between frequency and time. This method presented some problems when the dispersive wave train consisted of contributions from other modes in addition to fundamental mode.

2.5.2.2 Spectrograph Method: An electrical analogue spectrograph was employed by Ewing(1959) which displayed the spectral variation of the analysed seismogram with time, and yielded directly a recording of group velocities as a function of frequency.

2.5.2.3 Moving Window Method: This method consists of choosing intervals(or time windows) of suitable length along the record and taking their fourier transform. The results are plotted as power or amplitude isolines in a graph with frequency as one co-ordinate and group velocity (average for each time interval) as the other co-ordinate. It is thus a representation of a time varying spectrum. The isolines display the dispersive properties of the waves.

Mathematically this method aims at calculating the moving fourier amplitude $F(w,\tau)$ from

$$F(w,\tau) = \int_{-\infty}^{\infty} f(t).w(t-\tau).exp(-iwt)dt \quad \dots\dots(2.16).$$

where τ is the time lag of the moving window $w(t-\tau)$.

For any given, constant frequency w , $F(w,\tau)$ is calculated for a series of τ values. From these various F values, that value of τ is chosen for which F attains its maximum value. This value of τ is the group arrival time corresponding to the chosen frequency, and leads to the calculation of group velocity. This method was employed by Iyer(1964) to analyse surface wave records of Chilean earthquake recorded at Kiruna in Sweden. Later the same method was used by Landisman et al.,(1969).

The success of this method depends on the length of the time window which controls resolution of period and time lag.

Instead of windowing in time domain as described above, it is also possible to employ windowing in frequency domain. This leads to Multiple Filter Technique which has been employed to determine Rayleigh wave group velocities in the present work. This technique is described below in greater detail.

2.6 MULTIPLE FILTER TECHNIQUE

In this section some basic aspects of the Multiple Filter Technique have been presented. The computational aspects of this technique have been presented in the next chapter.

The basic idea on which the Multiple Filter Technique is based, is the definition of group travel time as defined in equation(2.14). In order to get a wave packet centred at a frequency w_0 , the recorded dispersed wave train is filtered in frequency domain using a suitable filter centred around w_0 . The time at which the amplitude of this filtered trace is maximum yields the group travel time. Knowing the distance to the epicentre, the group velocity of the wave packet centred around w_0 can be determined.

In practice a filter trace $h_n(t)$ centred around a frequency w_n can be obtained by inverse fourier transform of the product of the spectrum of the recorded wave train and the spectrum of the band pass filter. This can be expressed in mathematical terms as follows:

$$h_n(t) = \frac{1}{2\pi} \int_{-\infty}^{+\infty} F(w).H(w,w_n).exp(iwt)dw \quad \dots(2.17)$$

where $H(w,w_n)$ is the response of a filter centred around w_n and $F(w)$ is the spectrum of the recorded dispersed wave train. A number of "central frequencies" w_n are chosen and corresponding $h_n(t)$ are obtained for determination of corresponding group travel times.

The success of the multiple filter technique depends on the choice of an appropriate filter function $H(w,w_n)$. A "box-car" was used by Kanamori and Abe(1968) as defined below.

$$H(w,w_n) = \begin{cases} 0 & \text{for } w < w_n - \Delta w \\ 1 & \text{for } w_n - \Delta w < w < w_n + \Delta w \\ 0 & \text{for } w > w_n + \Delta w \end{cases}$$

.....(2.18)

The use of Gaussian filters has been favoured by many investigators, e.g., Dziewonski et al.(1969). It is based on a property of a Gaussian filter by virtue of which, it causes the least loss of frequency domain resolution. According to the uncertainty principal(Papoulis, 1962),

$$\Delta t.\Delta w > (\pi/2)^{1/2} \quad \dots\dots\dots(2.19)$$

where D_t , D_w are respectively the time domain and frequency domain durations of a signal $f(t)$. The relation(2.19) holds if $f(t)$ vanishes at infinity faster than t^{-1} . The relation(2.19) means that if D_t is sought to be increased D_w must become smaller and vice versa. The equality in relation(2.19) holds for Gaussian signal defined as follows:

$$f(t) = (\alpha/\pi)^{1/2} \exp(-\alpha t^2) \quad \dots\dots\dots(2.20)$$

The following form of filter function $H(w, w_n)$ was chosen by Dziewonski et al.(1969).

$$H(w, w_n) = \exp\{-\alpha (w-w_n)^2/w_n^2\} \quad \dots\dots\dots(2.21)$$

The corresponding filtered trace $h_n(t)$ is given by

$$h_n(t) = \frac{1}{2\pi} \int_0^{\infty} A(w) \cdot \cos[k(w) \cdot r - wt] \\ * \exp\{-\alpha[(w-w_n)^2/w_n^2]\} \cdot dw. \\ \dots\dots\dots(2.22)$$

To evaluate the integral in equation(2.22), it is assumed, following Dziewonski and Hales(1972), that $A(w)$ and $k(w)$ can be represented in the vicinity of w_n by first order Taylor series expansion.

$$A(w) = A(w_n) + (dA/dw)w_n \cdot (w-w_n) = A_n + A_n' \cdot (w-w_n) \\ \dots\dots\dots(2.23)$$

$$k(w) = k(w_n) + (dk/dw)w_n.(w-w_n) = kn + kn'. (w-w_n)$$

.....(2.24)

The following form of $h_n(t)$ is then obtained

$$h_n(t) = g(w_n, t). \cos[kn.r - w_n.t + en(t)]$$

$$. \exp[-w_n^2 (kn'.r - t)^2 / 4\alpha] \quad \text{.....(2.25)}$$

where

$$g(w_n, t) = (\pi / 2)^{1/2} . w_n \{ An^2 + [An'.w_n (kn'.r - t)]^2 / 4\alpha \}^{1/2}$$

.....(2.26)

$$en(t) = \tan^{-1}[An'.w_n (kn'.r - t) / 2\alpha . An] \quad \text{.....(2.27)}$$

$$kn = \left(\frac{dk}{dw} \right)_{w_0} \quad An = \left(\frac{dA}{dw} \right)_{w_0} \quad \text{.....(2.28)}$$

For any signal $f(t)$, its instantaneous amplitude $a(t)$ and instantaneous phase $\phi(t)$ can be defined, after Goodman(1960), as

$$a(t) \cdot \exp\{i\phi(t)\} = f(t) + iq(t) \quad \dots\dots(2.29)$$

where $q(t)$ is the quardature signal of $f(t)$, the inphase signal. The quardature signal is defined as

$$q(t) = \frac{1}{2\pi} \int_{-\infty}^{+\infty} \exp[i(\omega t - \pi/2)]. F(\omega) \cdot d\omega \quad \dots\dots(2.30)$$

where $F(\omega)$ is the spectrum of $f(t)$.

The instantaneous amplitude $a(t)$ is then

$$a(t) = [f^2(t) + q^2(t)]^{1/2} \quad \dots\dots(2.31)$$

and its instantaneous phase is

$$\phi(t) = \tan^{-1} [q(t)/f(t)] \quad \dots\dots(2.32)$$

Applying the equations(2.29),(2.31) and (2.32) to $h_n(t)$ as given in equation(2.25), the instantaneous amplitude $a_n(t)$ and instantaneous phase $\phi_n(t)$ are obtained as:

$$a_n(t) = g(\omega_n, t) \cdot \exp[-\omega_n^2 (kn \cdot r - t)^2 / 4\alpha] \quad \dots\dots(2.33)$$

$$\phi_n(t) = \omega_n t - kn \cdot r - \epsilon_n(t). \quad \dots\dots(2.34)$$

Differentiating equation(2.33) with respect to time(t) and then equating the same to zero gives

$$t = r / \omega_n \quad \dots\dots(2.35)$$

$$\text{where } U_n = \frac{1}{k'n} = \left(\frac{dw}{dk} \right)_{\omega=\omega_n} \dots\dots(2.36)$$

This shows that the maximum of the envelope $a_n(t)$ corresponds to the group travel time of the energy associated with the frequency ω_n .

The above analysis is based on the assumption that $k(\omega)$ and $a(\omega)$ can be represented by their first order expansion as in equation(2.23) and equation(2.24), and second and higher order terms in the Taylor series expansion are neglected. If second order terms are included, the form of $a_n(t)$ becomes complicated. In that case the maximum of the envelope of $a_n(t)$ does not, in general, correspond exactly to group travel time. In case the first order approximations expressed in equation(2.23) and equation(2.24) are not valid, systematic errors will occur in the results(Dziewonski and Hales,1972).

The application of Multiple Filter Technique is most effective in case of multimode propagation i.e., when the wave trains belonging to two or more modes are mixed in time.

The success of Multiple Filter Technique depends on the selection of a particular filter width which should be as narrow as possible. The selection of a particular filter width is determined by the following factors:

- (i) level of noise
- (ii) character of dispersion curve, and
- (iii) the degree of contamination from energy belonging to

other modes of propagation.

The parameter α occurring in the expression(2.21) for filter response determines the filter width. A large value of α will make it difficult to resolve higher mode energy from the fundamental mode energy.

2.7 INVERSION OF RAYLEIGH WAVE DATA

The observed Rayleigh wave group velocity dispersion curves are matched with theoretical curves calculated for layered earth models to invert the Rayleigh wave seismograms. The models of earth structure so obtained are non-unique to some extent. The theoretical group velocity dispersion curves can be calculated using methods proposed by Thomson(1950), Haskell(1953) and Knopoff(1964). The next chapter presents some aspects of the methods mentioned above for generating theoretical group velocity dispersion curves.

CHAPTER-3

COMPUTATION OF RAYLEIGH WAVE SYNTHETIC DISPERSION CURVES

3.1 INTRODUCTION

The computation of Rayleigh wave synthetic dispersion curves constitutes the forward problem in theoretical seismology. The synthetic or theoretical dispersion curves are computed for layered earth models. By varying the parameters of the earth model a suite of dispersion curves can be obtained which can then be compared with observed dispersion curves. To solve the inverse problem, i.e., deducing earth structure from observed characteristics of surface wave dispersion, we match the observed dispersion curve with the synthetic dispersion curve. The earth models so obtained are generally non-unique. Various methods have been suggested for more efficient inversion of dispersion curves which aim at reducing the degree of non-uniqueness.

In the work presented here, observed dispersion curves have been matched with theoretical dispersion curves obtained using Knopoff's method (Schwab and Knopoff, 1972). A new method, the pattern search method, has been employed to search the roots of dispersion function. This method has the advantage, that the convergence is definite. In the following sections some important aspects, the theory of Thomson Haskell matrix method has been presented followed by Knopoff's method as discussed by Schwab (1970). Lastly some aspects of the computations of synthetic dispersion curves have been presented along with actual examples of such curves for three

typical models of earth crust.

3.2 HASKELL METHOD

A matrix formulation was developed by Haskell(1953) for phase velocity dispersion computation in case of Rayleigh waves. A layered earth model was considered for this purpose. Some aspects of this theory have been presented in this section. The layered earth model consists of n-1 layers resting on a half space which is termed the nth layer, as shown in Figure 3.1. The mth layer is characterised by a P-wave velocity α_m , S-wave velocity β_m , and density ρ_m , and thickness d_m . In the following Haskell's notation has been retained. However some of the relations have been presented in form of matrices.

The equations of motions are solved for each layer and u and w, the x and z components of displacements respectively are evaluated along with stress components, σ (normal) and τ (tangential) referred to the plane $z = \text{constant}$. In Haskell's paper the equations which have been solved are in terms of cubical dilatation Δ_m and rotation w_m (about y-axis) in the mth layer.

These equations are;

$$\frac{\partial^2 \Delta_m}{\partial x'^2} + \frac{\partial^2 \Delta_m}{\partial z'^2} = \frac{1}{\alpha_m^2} \frac{\partial^2 \Delta_m}{\partial t'^2} \quad \dots\dots(3.1)$$

$$\frac{\partial^2 w_m}{\partial x'^2} + \frac{\partial^2 w_m}{\partial z'^2} = \frac{1}{\beta_m^2} \frac{\partial^2 w_m}{\partial t'^2} \quad \dots\dots(3.2)$$

CONTINENTAL
MODEL

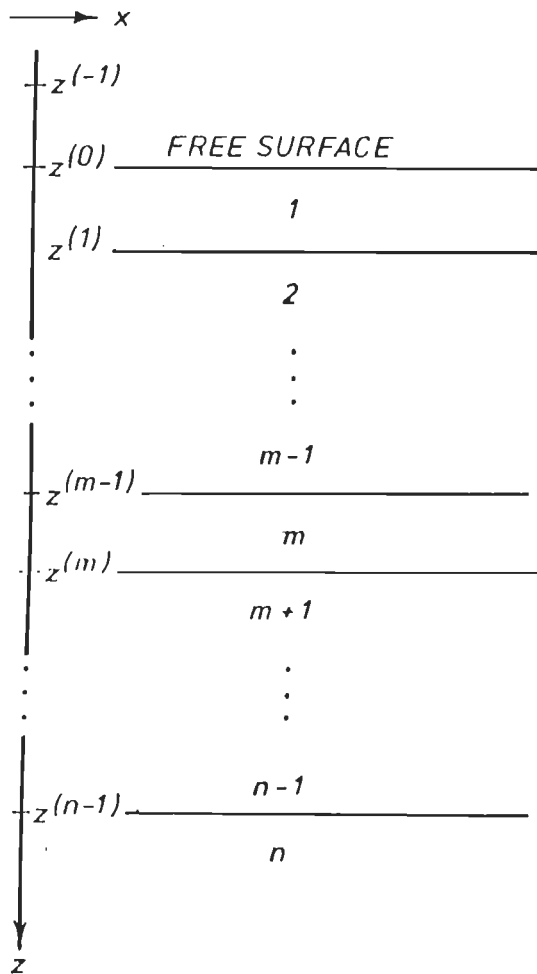


Figure-3.1 Layered earth model for continental structure

The solution of equation(3.1) and equation(3.2) are as follows;

$$\Delta_n = [\Delta'_n \exp(-ikr_{n,z}) + \Delta''_n \exp(ikr_{n,z})] \exp\{i(pt-kx)\}$$

.....(3.3)

$$w_n = [w'_n \exp(-ikr_{n,z}) + w''_n \exp(ikr_{n,z})] \exp\{i(pt-kx)\}$$

.....(3.4)

where p is the angular frequency, k is the angular wave number,

$$r_{n,z} = [(c/\alpha_n)^2 - 1]^{1/2} z$$

$$r_{n,z} = [(c/\beta_n)^2 - 1]^{1/2} z$$

and $\Delta'_n, \Delta''_n, w'_n, w''_n$ are constants. The parameter c is phase velocity and $r_{n,z}, r_{n,z}$ are real when $c > \alpha_n, \beta_n$ and imaginary when $c < \alpha_n, \beta_n$.

The displacement components u_n and w_n are obtained from Δ_n and w_n as follows:

$$u_n = - \frac{\alpha_n'}{p'} \frac{\partial \Delta_n}{\partial x} - 2 \frac{\beta_n'}{p'} \frac{\partial w_n}{\partial z} \quad \dots\dots\dots(3.5)$$

$$w_n = - \frac{\alpha_n'}{p'} \frac{\partial \Delta_n}{\partial z} + 2 \frac{\beta_n'}{p'} \frac{\partial w_n}{\partial x} \quad \dots\dots\dots(3.6)$$

The stress components σ and τ are given by

$$\sigma = p_1 [\alpha_1^2 \Delta_1 + 2\beta_1^2 \{(\alpha_1/p)^2 \cdot (\partial^2 \Delta_1 / \partial x^2) + 2(\beta_1/p)^2 \cdot (\partial^2 w_1 / \partial x \partial z)\}] \dots (3.7)$$

$$\tau = 2p_1 \beta_1^2 [-(\alpha_1/p)^2 \cdot (\partial \Delta_1 / \partial x \partial z) + (\beta_1/p)^2 \{(\partial^2 w_1 / \partial x^2) - (\partial^2 w_1 / \partial z^2)\}] \dots (3.8)$$

The boundary conditions involve continuity of displacements and stress at an interface. The continuity of displacement has been replaced by continuity of dimensionless quantities u/c and w/c . At the $n-1$ interfaces in the layered half space there will be $4(n-1)$ boundary conditions to be satisfied. At the free surface only two conditions need to be satisfied. So there will be $4n-2$ boundary conditions to be satisfied

On substituting equation(3.3) and equation(3.4) in equations(3.5 to 3.8) the resulting expressions are so modified that the constants $\Delta'_1, \Delta''_1, w'_1, w''_1$ appear as $\Delta'_1 + \Delta''_1, \Delta'_1 - \Delta''_1, w'_1 + w''_1$ and $w'_1 - w''_1$. The exponential terms involving r_{11} and r_{12} are converted into trigonometric functions, when $c > \alpha_1, \beta_1$ and hyperbolic functions when $c < \alpha_1, \beta_1$. In the m th layer bounded by $(m-1)$ th interface above and m th interface below, the following matrix relation is obtained;

$$U_{n-1} = E_n \cdot A_n \quad \dots\dots\dots(3.9)$$

$$\text{where } U_n = [\dot{u}_{n-1}/c, \dot{w}_{n-1}/c, \sigma_{n-1}, \tau_{n-1}]^T \dots\dots\dots(3.10)$$

$$A_n = [\Delta'_n + \Delta''_n, \Delta'_n - \Delta''_n, w'_n + w''_n, w'_n - w''_n]^T$$

$$\dots\dots\dots(3.11)$$

where E_n is the matrix

$$E_n = \begin{bmatrix} -(\alpha_n/c)^2 & 0 & -\gamma_n r_{n-1} & 0 \\ 0 & -(\alpha_n/c)^2 r_{n-1} & 0 & \gamma_n \\ -\rho_n \alpha_n^2 (\gamma_n - 1) & 0 & -\rho_n c^2 \gamma_n^2 r_{n-1} & 0 \\ 0 & \rho_n \alpha_n^2 \gamma_n r_{n-1} & 0 & -\rho_n c^2 \gamma_n (\gamma_n - 1) \end{bmatrix}$$

$$\dots\dots\dots(3.12)$$

$$\text{where } \gamma_n = 2(\beta_n/c)^2 \quad \dots\dots\dots(3.13)$$

In equation(3.9) the origin of z has been placed at $(m-1)$ th interface and U_{n-1} is evaluated at this interface. In the same manner setting $z = d_n$ in equation(3.9), another matrix relation is obtained as follows;

$$U_n = D_n \cdot A_n \quad \dots\dots\dots(3.14)$$

where $U_m = [\dot{u}_m/c, \dot{w}_m/c, \sigma_m, \tau_m]$ (3.15)

and

$D_m =$

$$\begin{bmatrix} -(\alpha_m/c)^2 \cos P_m & i(\alpha_m/c)^2 \sin P_m & -Y_m r_m \cos Q_m & iY_m r_m \sin Q_m \\ i(\alpha_m/c)^2 r_m \sin P_m & -(\alpha_m/c)^2 r_m \sin Q_m & -iY_m \sin Q_m & Y_m \cos Q_m \\ -p_m \alpha_m' (Y_m - 1) \cos P_m & ip_m \alpha_m' (Y_m - 1) \sin P_m & -p_m c' Y_m' r_m \cos Q_m & ip_m c' Y_m' r_m \sin Q_m \\ -ip_m \alpha_m' Y_m r_m \sin P_m & p_m \alpha_m' Y_m r_m \cos P_m & ip_m c' Y_m (Y_m - 1) \sin Q_m & -p_m c' Y_m (Y_m - 1) \cos Q_m \end{bmatrix}$$

.....(3.16)

where $P_m = kr_m d_m, Q_m = kr_m' d_m$ (3.17)

On eliminating $\Delta'_m + \Delta''_m$, etc. between expressions(3.9) and (3.14) the following relationship is obtained

$U_m = D_m E^{-1}_m U_{m-1}$ (3.18)

which relates displacements and stresses at the bottom of the mth layer to those at its top.

Applying the boundary conditions at the interface between (m-1)th layer and mth layer the relation obtained is as given below:

$U_m = a_m a_{m-1} U_{m-1}$ (3.19)

$$\text{where } a_n = D_n \cdot E^{-1}_n, a_{n-1} = D_{n-1} \cdot E^{-1}_{n-1} \dots\dots(3.20)$$

On repeated application of equation(3.19) the quantities at the bottom of (n-1)th interface are related to quantities at the free surface.

$$U_{n-1} = a_{n-1} a_{n-2} \dots\dots a_2 a_1 U_1 \dots\dots(3.21)$$

On using the inverse of the relation(3.9) in the nth layer, i.e., the half space, the column vector A_n is related to U_1 as follows;

$$A_n = E^{-1}_n a_{n-1} a_{n-2} \dots\dots a_2 a_1 U_1 \dots\dots(3.22)$$

The case under consideration is of Rayleigh waves which envisages vanishing of stress at $z = 0$ and absence of sources at infinity so that $\Delta''_n = w''_n = 0$. On substituting $\sigma = \tau = 0$, equation(3.19) becomes

$$B_n = J V_n \dots\dots(3.23)$$

$$\text{where } B_n = [\Delta'_n, \Delta'_n, w'_n, w'_n]^T \dots\dots(3.24)$$

$$V_n = [\dot{u}_n/c, \dot{w}_n/c, 0, 0]^T \dots\dots(3.25)$$

$$J = E^{-1}_n a_{n-1} a_{n-2} \dots\dots a_2 a_1 \dots\dots(3.26)$$

Elimination of Δ'_n and w'_n yields

$$\frac{\dot{u}_n}{\dot{w}_n} = \frac{J_{22} - J_{12}}{J_{11} - J_{21}} = \frac{J_{12} - J_{22}}{J_{21} - J_{11}} \quad \dots(3.27)$$

Equation(3.27) is the desired phase velocity dispersion relation since elements of matrix J are functions of c and k. This equation is modified to the following form

$$\frac{\dot{u}_n}{\dot{w}_n} = \frac{K}{L} = \frac{M}{N} \quad \dots\dots\dots(3.28)$$

It is found that $K = J_{22} - J_{12}$ and $N = J_{21} - J_{11}$ are always real whereas $L = J_{11} - J_{21}$ and $M = J_{12} - J_{22}$ are always imaginary for the case of surface waves. Thus the ratio \dot{u}_n/\dot{w}_n will always be imaginary and a phase difference of $\pi/2$ will exist between \dot{u}_n and \dot{w}_n . The particle motion is therefore elliptical. However the sense of motion may not be retrograde at all frequencies.

Equation(3.28) is used to compute c as a function of k. In earlier computation roots of $F(w,c) = K/L$ were found by fixing c and varying w or $k(=w/c)$ (Schwab and Knopoff, 1970). In later computations a set of frequencies were specified and iterations were carried out over velocities at each frequency. Earlier computations were done on IBM 7004 computer, and then on IBM 300 computer for overcoming loss of precision problems. Overflow problems also occurred which were controlled by layer reduction. Watson(1970) presented a most powerful variant of Thomson-Haskell formulation which is the fastest and keeps the loss of precision under control.

3.3 KNOPOFF'S METHOD

Knopoff(1964) proposed an alternate formulation of Rayleigh wave dispersion problem. The geometry of the problem is the same as in Haskell's method i.e., n-1 solid, perfectly elastic layers resting over a homogeneous elastic half space as shown in Figure 3.1. In the following paragraph the presentation follows Schwab(1970) closely. The column vector U_m and A_m are now defined as:

$$U_m = [c\dot{u}_m, c\dot{w}_m, \sigma_m, \tau_m]^T \quad \dots\dots\dots(3.29)$$

$$A_m = [-\alpha_m^2(\Delta'_m + \Delta''_m), -\alpha_m^2(\Delta'_m - \Delta''_m), \\ -2\beta_m^2(w'_m - w''_m), -2\beta_m^2(w'_m + w''_m)]^T \\ \dots\dots\dots(3.30)$$

The relation corresponding to equation(3.9) for mth layer is

$$U_m = E_m \cdot A_m \quad \dots\dots\dots(3.31)$$

where

$$E_m =$$

$$\begin{matrix} \cos pm & -i \sin pm & r_{m,1} \cos qm & -i r_{m,1} \sin qm \\ -i r_{m,1} \sin pm & r_{m,1} \cos pm & i \sin qm & -\cos qm \\ p_m(Y_m - 1) \cos pm & -i p_m(Y_m - 1) \sin pm & p_m Y_m r_{m,1} \cos qm & -i p_m Y_m r_{m,1} \sin qm \\ i p_m Y_m r_{m,1} \sin pm & -p_m Y_m r_{m,1} \cos pm & -i p_m(Y_m - 1) \sin qm & p_m(Y_m - 1) \cos qm \end{matrix} \\ \dots\dots\dots(3.32)$$

$$p_m = k r_{m-1} [z - z^{(m-1)}] \quad \dots\dots(3.33)$$

$$q_m = k r_{m-1} [z - z^{(m-1)}] \quad \dots\dots(3.34)$$

Vanishing of two stress components at $z = 0$, yields the Knopoff's submatrix $\Lambda_{(m)}$ which has the form

$$\Lambda_{(m)} = \begin{bmatrix} -p_i(Y_i-1) & 0 & -p_i Y_i r_{i-1} & 0 \\ 0 & p_i Y_i r_{i-1} & 0 & -p_i(Y_i-1) \end{bmatrix} \quad \dots\dots(3.35)$$

The continuity of displacements and stresses at the m th interface yields

$$\Lambda_m \cdot G_m = 0 \quad \dots\dots(3.36)$$

where G_m is obtained from A_m by adding four rows of coefficients $-\alpha'_{m+1}(\Delta'_{m+1} + \Delta''_{m+1})$ etc. The matrix Λ_m is 4×8 matrix given by

$$\Lambda_m = \begin{bmatrix} \cos P_m & -i \sin P_m / r_{m-1} & \cos Q_m & -i r_{m-1} \sin Q_m \\ -i r_{m-1} \sin P_m & \cos P_m & i \sin Q_m / r_{m-1} & -\cos Q_m \\ p_m(Y_m-1) \cos P_m & -i p_m(Y_m-1) \sin P_m / r_{m-1} & p_m Y_m \cos Q_m & -i p_m Y_m r_{m-1} \sin Q_m \\ i p_m Y_m r_{m-1} \sin P_m & -p_m Y_m \cos P_m & -i p_m(Y_m-1) \sin Q_m / r_{m-1} & p_m(Y_m-1) \cos Q_m \\ -1 & 0 & -1 & 0 \\ 0 & -1 & 0 & 1 \\ -p_{m+1}(Y_{m+1}-1) & 0 & -p_{m+1} Y_{m+1} & 0 \\ 0 & p_{m+1} Y_{m+1} & 0 & -p_{m+1}(Y_{m+1}-1) \end{bmatrix}$$

$$\dots\dots\dots(3.37)$$

where $P_m = k r_{i,i} \cdot d_i$

$$\dots\dots\dots(3.38)$$

$$Q_m = k r_{i,i} \cdot d_i$$

The submatrix corresponding to (n-1)th interface, Λ_{n-1} , is a 4x6 matrix. Its first four columns are the same as those of Λ_n and the last two columns are $[-1, -r_{i,i}, -p_i(Y_i-1), p_i Y_i r_{i,i}]^T$, $[-r_{i,i}, 1, -p_i Y_i r_{i,i}, -p_i(Y_i-1)]^T$

The dispersion function Δ_n for Rayleigh waves takes the form

$$\Delta_n = T^{(n)} F^{(n-1)} F^{(n-2)} F^{(n-3)} \dots \begin{cases} F^{(n-2)} F^{(n-1)} & \text{if } (n-1) \text{ is even} \\ F^{(n-2)} F^{(n-1)} & \text{if } (n-1) \text{ is odd} \end{cases} \dots\dots\dots(3.39)$$

Where $F^{(n)}$ and $F^{(n-1)}$ are the interface matrices which are obtained from the submatrix Λ_n . Their form is given in Appendix-I(A). The elements of $T^{(n)}$ are obtained from Λ_{n-1} , and are also given in the Appendix-I(B).

The matrix relation(3.39) is the sixth order matrix representation of the Rayleigh wave dispersion relation. A set of manipulations have been suggested by Schwab(1970) which aim at reducing the order of matrices involved. Following these manipulations sixth order matrices are reduced to fourth order matrix multiplications. Original six sixth order multiplications are reduced to two fourth order and three fifth order multiplications per matrix product. The final complete dispersion relation is given by:

$$\Lambda_n = T_{n-1} \begin{cases} H1 & \text{if } (n-1) \text{ is even.} \\ H2 & \text{if } (n-1) \text{ is odd.} \end{cases} \quad \dots\dots\dots(3.40)$$

The full form of H1 and H2 are given in Appendix-I(C).

$$T_{n-1} = [U_{n-1} \ V_{n-1} \ W_{n-1} \ R_{n-1}] \quad \dots\dots\dots(3.41)$$

The elements of T_{n-1} are also given in the Appendix-I(D). Equation(3.40) is identical to equation(44) of Schwab(1970) and equation(68) of Schwab and Knopoff(1972).

3.4 DISCUSSION

In Rayleigh wave dispersion computations, evaluation of the dispersion function is of fundamental importance. The solution of the problem under investigation involves determination of zeroes of the dispersion functions. In Thomson-Haskell method this function is synthesized by constructing layer matrices. These matrices relate components of motion at one interface in a layered earth model to those at the next. The components of motion at deepest interface and at the free surface are then related through the product of these layer matrices. The computation of elements of the layer matrices and the product of these matrices is the most time consuming part in using Thomson-Haskell formulation. In Knopoff's method these computations are simplified and the computation of roots of dispersion function becomes faster. In these formulations only real quantities are used and the use and the manipulations of complex numbers is completely avoided. In the present investigations Knopoff's method has been used to construct phase velocity dispersion curves. For the root finding, the pattern search method has been employed. It is the simplest among all

TABLE - 3.1

MODEL -1
(After Chen and Molnar, 1981)

LAYER NO.	P-WAVE VELOCITY Km/sec.	S-WAVE VELOCITY Km/sec.	DENSITY gm/c.c.	THICKNESS Km.
1.	4.411	2.55	2.41	03.75
2.	5.880	3.40	2.70	16.25
3.	6.055	3.50	2.70	25.00
4.	6.400	3.70	3.00	10.00
5.	7.780	4.50	3.30	-

MODEL - 2
(After Chun, 1986)

LAYER NO.	P-WAVE VELOCITY Km/sec.	S-WAVE VELOCITY Km/sec.	DENSITY gm/c.c.	THICKNESS Km.
1.	4.060	2.34	2.66	04.00
2.	5.310	3.06	2.72	06.00
3.	6.570	3.80	3.00	10.00
4.	6.890	3.98	3.08	20.00
5.	7.830	4.52	3.29	-

MODEL -3
(After Chun and Yoshii, 1977)

LAYER NO.	P-WAVE VELOCITY Km/sec.	S-WAVE VELOCITY Km/sec.	DENSITY gm/c.c.	THICKNESS Km.
1.	4.500	2.60	2.40	03.50
2.	5.980	3.45	2.80	08.50
3.	5.980	3.42	2.80	16.00
4.	5.800	3.37	2.75	10.00
5.	6.300	3.64	2.90	30.00
6.	7.700	4.45	3.30	-



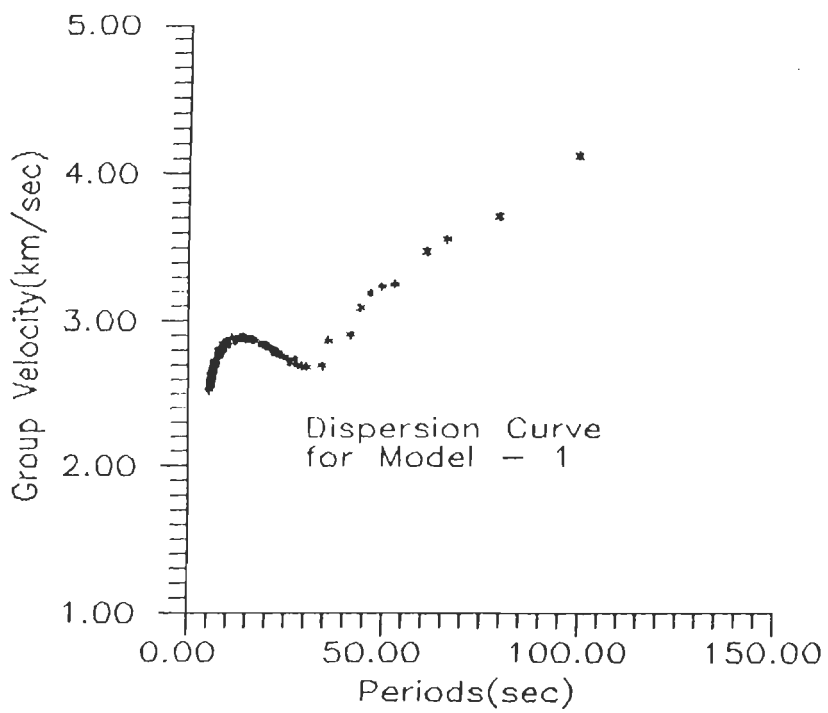


Figure-3.2 Synthetic Group Velocity Dispersion Curve for Model-1.

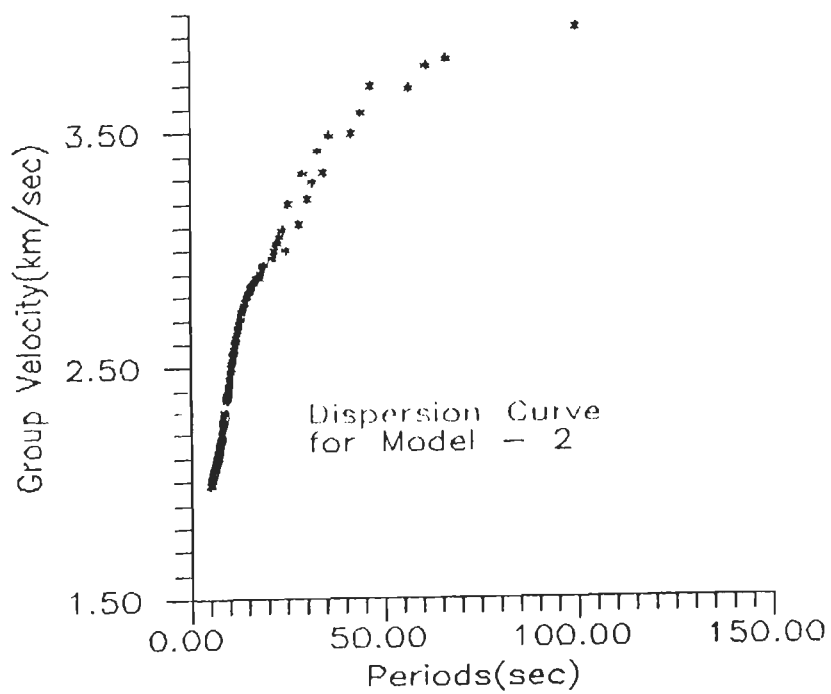


Figure-3.3 Synthetic Group Velocity Dispersion Curve for Model-2.

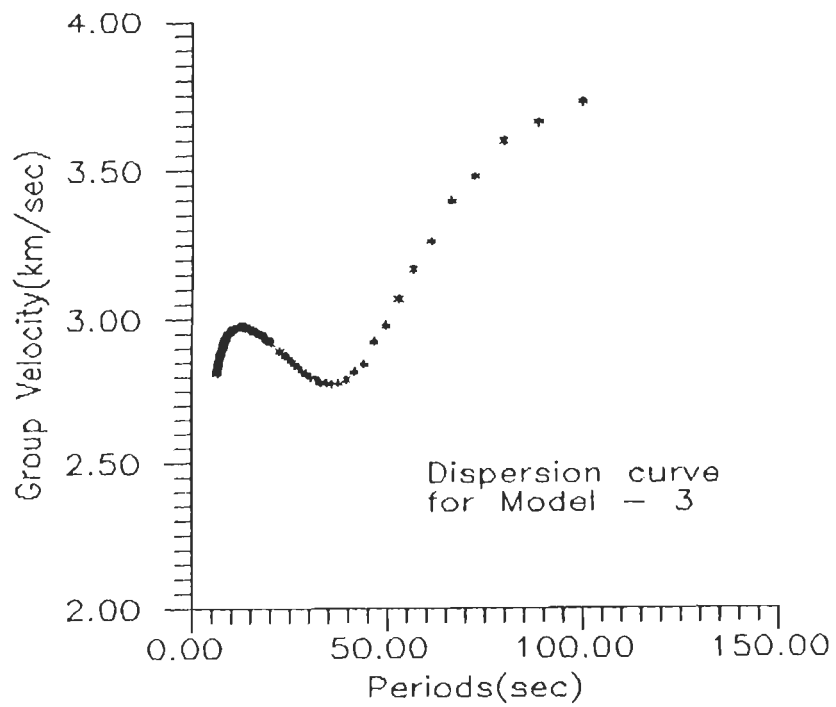


Figure-3.4 Synthetic Group Velocity Dispersion Curve for Model-3.

the other methods. In this method the convergence is always definite. Due to this reason it is slightly slower than the other methods as it searches the global root of the function. It is applied in continuous functions. It is also exhaustive in nature. From the phase velocity dispersion curves, the group velocity dispersion curves are obtained by numerical differentiation using forward difference formula. The centre difference formula has also been tried, but the results obtained using the two formulae are not much different from each other. Hence for the sake of simplicity the forward difference formula has been applied in the present study.

3.5 SYNTHETIC DISPERSION CURVES

For computing synthetic dispersion curves Knopoff's method has been followed and a computer program was prepared based on equation(3.40). The earth models with model parameters given in Table-3.1 were selected. Three actual models were chosen for this purpose. First model was taken from Chen and Molnar(1981) for the Tibet region, which includes a thin layer in lower crust. The second model was selected from Chun(1986) for the Western Ganga Basin. The third one is also for Tibet region given by Chun and Yoshii(1977). The synthetic group velocity dispersion curves for all the three models are shown in Figures 3.2 to 3.4.

CHAPTER - 4

COMPUTATION OF RRAYLEIGH WAVE GROUP VELOCITY DISPERSION CURVES

4.1 INTRODUCTION

In the present study crustal structure in India and adjoining regions has been determined on the basis of group velocity dispersion curves of Rayleigh waves. For this purpose the seismograms recorded at the Wide Band Seismological Observatory, Department of Earth Sciences, University of Roorkee, Roorkee have been used. The computation of group velocity dispersion curves has been carried by multiple filter technique deascribed in Chapter 2. The details of earthquakes used and computational aspects of group velocity dispersion curves have been presented in the following paragraphs.

4.2 THE WIDE BAND SEISMOLOGICAL OBSERVATORY

The Wide Band Seismological Observatory commenced operation at the Department of Earth Sciences, University of Roorkee, Roorkee in October 1982. The seismometers used in the observatory are based on the force balance principle, wherein the boom is always kept close to the centre position by an electrically generated restoring force. This makes it easier to control the linearity, dynamic range and stability of the seismometer. The boom position is sensed by a displacement transducer of the differential transformer type (LVDT). The boom is kept centred by sending

appropriate currents through two moving coil transducers which generate a feedback force. The seismometers act in a broad band configuration where in the output is proportional to ground velocity between a period range of 0.2 to 20.0 seconds. Three seismometers have been installed on a concrete pillar in a ten meter deep vault. The three seismometers have been installed so as to record ground motion in the north, east and vertical directions. The output from the three seismometers is fed into a signal conditioner and recorded on rectilinear ink recorder. Time signals are obtained from a crystal clock, and impinged on the chart. The three component seismograms are written on the same chart.

4.2.1 SEISMOMETER RESPONSE

Each of the three seismometers installed at the Wide Band Seismological Observatory records ground velocity in the period range from 0.2 to 20.0 seconds. Seismographs have a response identical to a system comprising a long period seismometer of natural period 20 seconds and damping 0.712 coupled to a short period Galvanometer of natural period 0.2 seconds and damping 0.623.

The velocity response of the wide band seismograph system can be represented by the following relation.

$$T(\omega) = \frac{-i.\omega^3.S}{(\omega_s^2 - \omega^2 - 2h_s\omega_s\omega).(\omega_g^2 - \omega^2 - 2h_g\omega_g\omega)} \dots(4.1)$$

where w_s = natural frequency of seismometer
 = $2\pi / T_s$, T_s being natural period of seismometer
 T_s = 20.0 seconds in our case
 w_g = natural frequency of galvanometer
 = $2\pi / T_g$, T_g being natural period of galvanometer
 T_g = 0.2 seconds in our case
 h_s = damping of the seismometer
 = 0.712 in our case
 h_g = damping of the galvanometer
 = 0.623 in our case
 S = generator constant which has the value
 2400 volt.sec/meter in the present case.

Figure 4.1 shows velocity response of the wide band seismograph system along with its displacement response and acceleration response. It is observed from Figure 4.1 that the velocity response of the wide band seismograph system is flat between 0.2 seconds and 20.0 seconds and rolls off at shorter and longer periods, at a rate of 6 db/octave.

The seismograms obtained at the wide band seismological observatory provide a unique data set for carrying out body wave and surface wave studies. The typical nature of the response of the seismometers makes it possible to record local as well distant events. The Rayleigh waves recorded by these seismographs span a period range from 2.0 seconds to 20.0 seconds as seen on analog records. This affords a unique opportunity to include short period Rayleigh waves in the analysis of group velocity dispersion data.

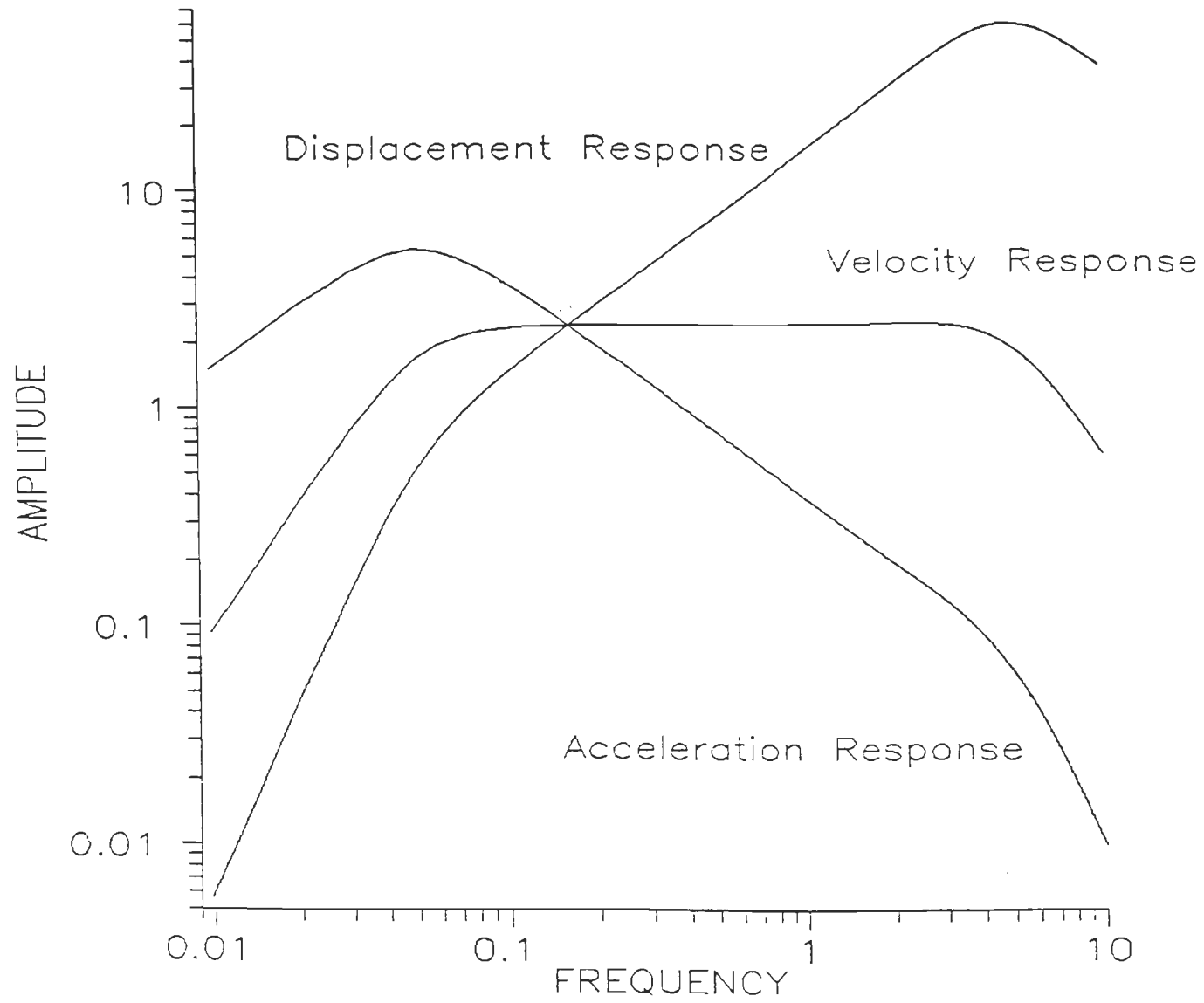


Figure-4.1 Velocity Response of the Wide Band Seismograph System. The Displacement and Acceleration Response are also given in the figure.

TABLE 4.1

LIST OF EARTHQUAKES SELECTED FOR THE STUDY

Sr. No.	Date dd mm yr	Origin Time hh mm sec.	Epicenter		Depth km.	Magnitude		Epc. Dist.	
			Lat. °N	Long. °E		mb	Ms		
INDIA BANGLADESH BORDER									
1.	13 04 89	12 55 36.70	24.472	92.505	33.0	5.1	5.0	14.08	
CHINA									
2.	06 01 87	04 22 46.55	41.964	81.319	16.5	5.9	5.8	12.42	
3.	25 04 89	07 43 20.83	30.048	99.419	7.7	6.2	6.0	18.66	
4.	03 05 89	11 23 1.17	30.091	99.475	14.0	6.1	6.1	18.71	
5.	03 05 89	21 11 30.88	30.053	99.499	7.5	5.8	5.9	18.73	
TIBET									
6.	31 10 82	00 10 52.69	35.847	82.494	33.0	5.2	5.0	7.00	
7.	15 06 85	20 47 42.98	34.620	82.992	43.2	5.4	5.2	6.43	
AFGHANISTAN TADZHAKISTAN BORDER									
8.	27 02 83	01 37 49.99	38.841	70.727	49.2	5.3	5.2	10.74	
9.	07 04 83	03 48 47.63	38.853	71.472	33.0	5.2	4.7	10.43	
TADZHAKISTAN									
10.	20 07 88	11 50 51.57	37.028	72.914	40.6	5.5	5.0	8.28	
11.	23 01 89	04 32 07.15	38.465	68.694	33.0	5.3	-	11.48	
KIRGHIZKSTAN									
12.	16 12 83	18 45 57.32	39.326	72.926	37.2	5.7	5.6	10.31	
HINDUKUSH									
13.	07 12 83	17 41 31.89	36.035	69.044	48.6	5.4	4.8	9.65	
14.	22 12 83	11 01 45.47	35.994	69.115	33.0	5.6	4.6	9.58	
15.	28 01 84	06 19 16.73	36.053	69.069	33.0	5.3	4.2	9.64	
16.	03 07 84	06 28 15.35	36.295	69.522	53.5	5.2	5.1	9.51	
IRAN									
17.	12 07 83	17 04 17.57	27.606	56.381	25.0	5.9	5.8	18.99	
18.	30 03 88	07 42 42.86	30.890	50.194	32.9	5.4	5.7	23.85	

-Origin time for all the events is in IST.

-Location were taken from Earthquake Data Reports of USGS.

TABLE - 4.2
REGIONWISE DISTRIBUTION OF EARTHQUAKES

Name of the Region	Number of Earthquakes
India Bangladesh Border	1
China Region	4
Tibet Region	2
Tadzhakistan, Kirghizkstan,	3
Afghanistan Tadzhakistan Border	2
Hindukush Region	4
Iran Region	2

4.3 SELECTION OF DATA SET

The seismograms recorded at the wide band seismological observatory over a period of seven years from October 1982 to May 1989 were examined for good quality Rayleigh wave records. Only the vertical component seismograms were selected for the purpose of present study. After a careful examination of all available records, seismograms of 18 earthquakes were selected. Table 4.1 shows the earthquake parameters of the selected events and Table 4.2 shows their region wise distribution. Figure 4.2 shows the location of selected events. The earthquakes selected in this study are distributed from east to west in seven distinct source regions.

The dispersed wave trains of Rayleigh waves of all selected earthquakes were digitised in order to compute group velocity dispersion curves. The digitisation of analog records was carried out on Calcom Digitiser at the Department of Earthquake Engg, University of Roorkee, Roorkee. The digitised data was subjected to further processing to obtain equispaced amplitude readings and to remove d.c. shift if any present in the data. The data for further analysis consisted of amplitude in centimeters at a sampling interval of 0.5 seconds which was considered adequate for computation of group velocity dispersion curves. The duration of dispersed wave trains selected for digitisation varied from 360 seconds to 600 seconds. The digitisation was done for the group velocity range from 4.0 km/sec. to 1.5 km/sec.

4.4 COMPUTATIONAL ASPECTS OF MULTIPLE FILTER TECHNIQUE

A computer program MFT has been written to carryout Multiple Filter Technique

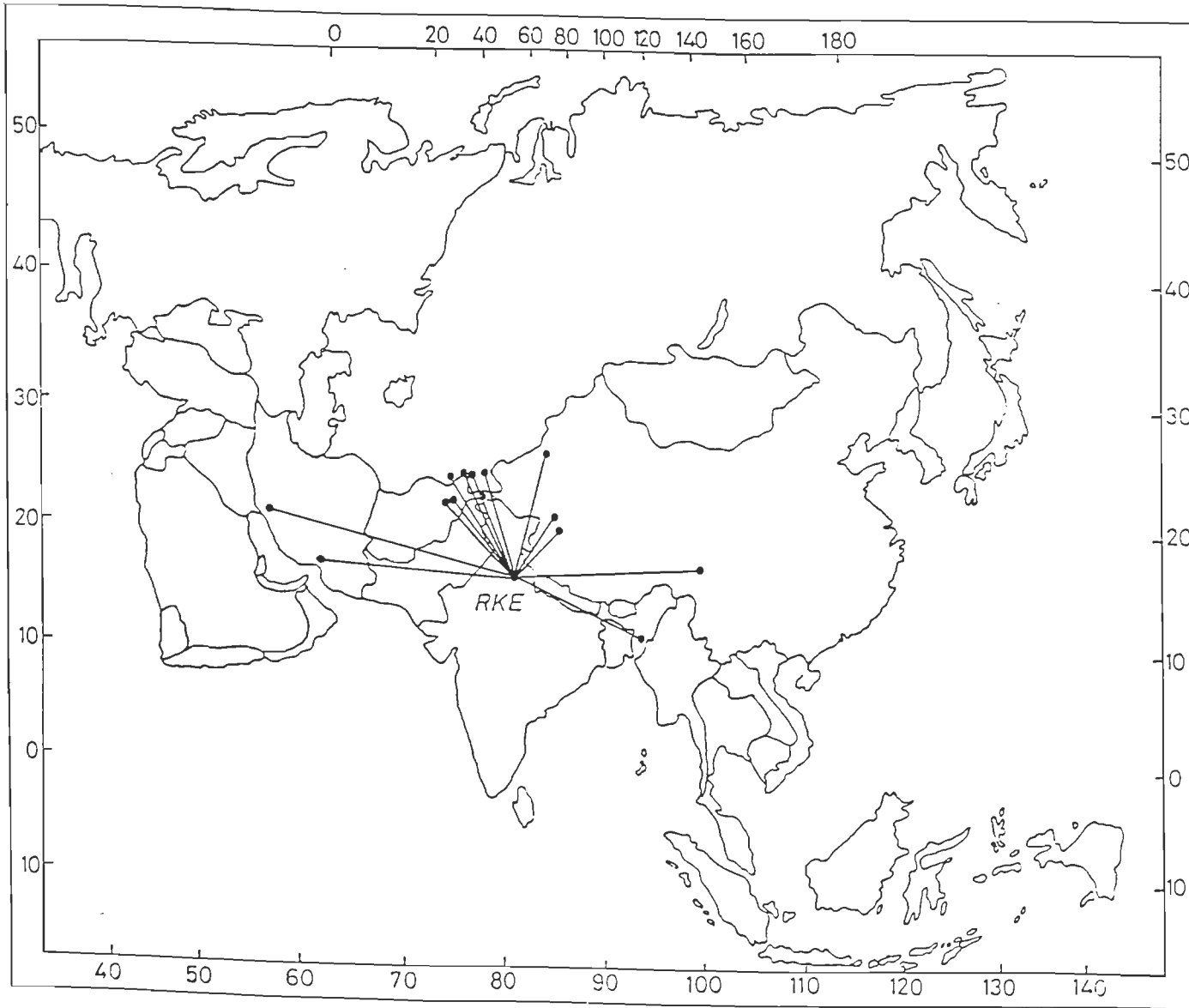


Figure-4.2 Epicentre Map of events selected in the present study.

to compute group velocity dispersion curves. Figure 4.3 shows a flowchart of the technique. This program produces a matrix of instantaneous amplitudes for a number of group velocity values and a number of central frequencies. The steps in the procedure for computation of group velocity dispersion curves are given below.

- a. The given record is Fourier Transformed using an FFT Algorithm given in Aki and Richards(1980). This algorithm uses complex arithmetic. The number of data points for this purpose are taken to be 2^N where N is an integer.
- b. Instrumental correction is applied to the spectrum of records based on equations 4.1 This has been done by dividing the observed spectrum with the instrumental response function. Complex arithmetic has been followed for this purpose. The corrected data yields ground velocity spectrum which is then converted into ground displacement spectrum. The digitized seismogram and the displacement seismogram after applying the instrumental correction for the Tibet earthquake of October 31st, 1982(one of the earthquakes used in present study) is shown in Figure 4.4.
- c. A set of central frequencies are selected based on the frequency content of the observed spectrum corrected for instrumental effect. The central frequencies selected are usually those which are closer to the frequencies present in the observed spectrum. The frequency resolution obtained in the observed spectrum depends on the length of the time series, and can be increased by padding zeroes to the time series.

FLOW CHART OF MULTIPLE FILTER TECHNIQUE

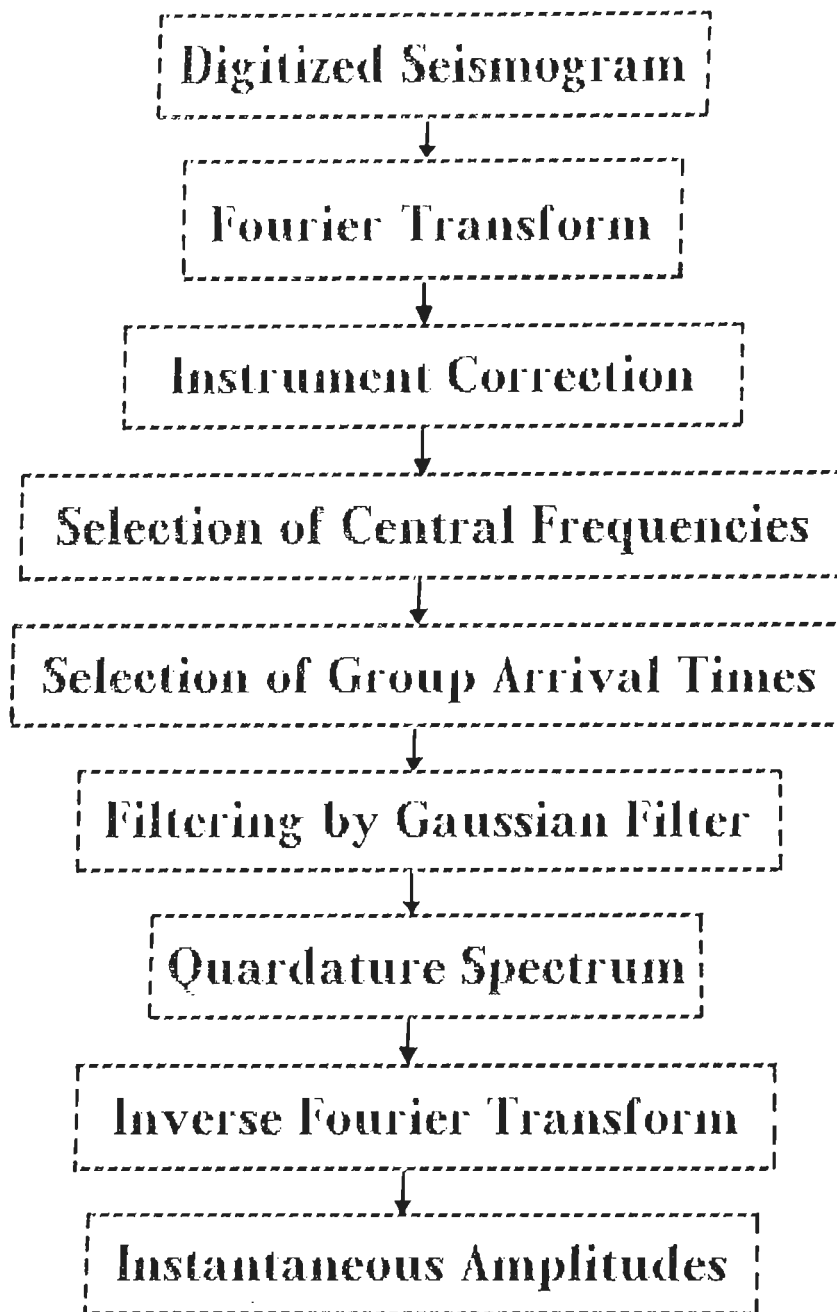


Figure-4.3 Flow chart for Multiple Filter Technique.

TIBET EARTHQUAKE OF 31.10.82

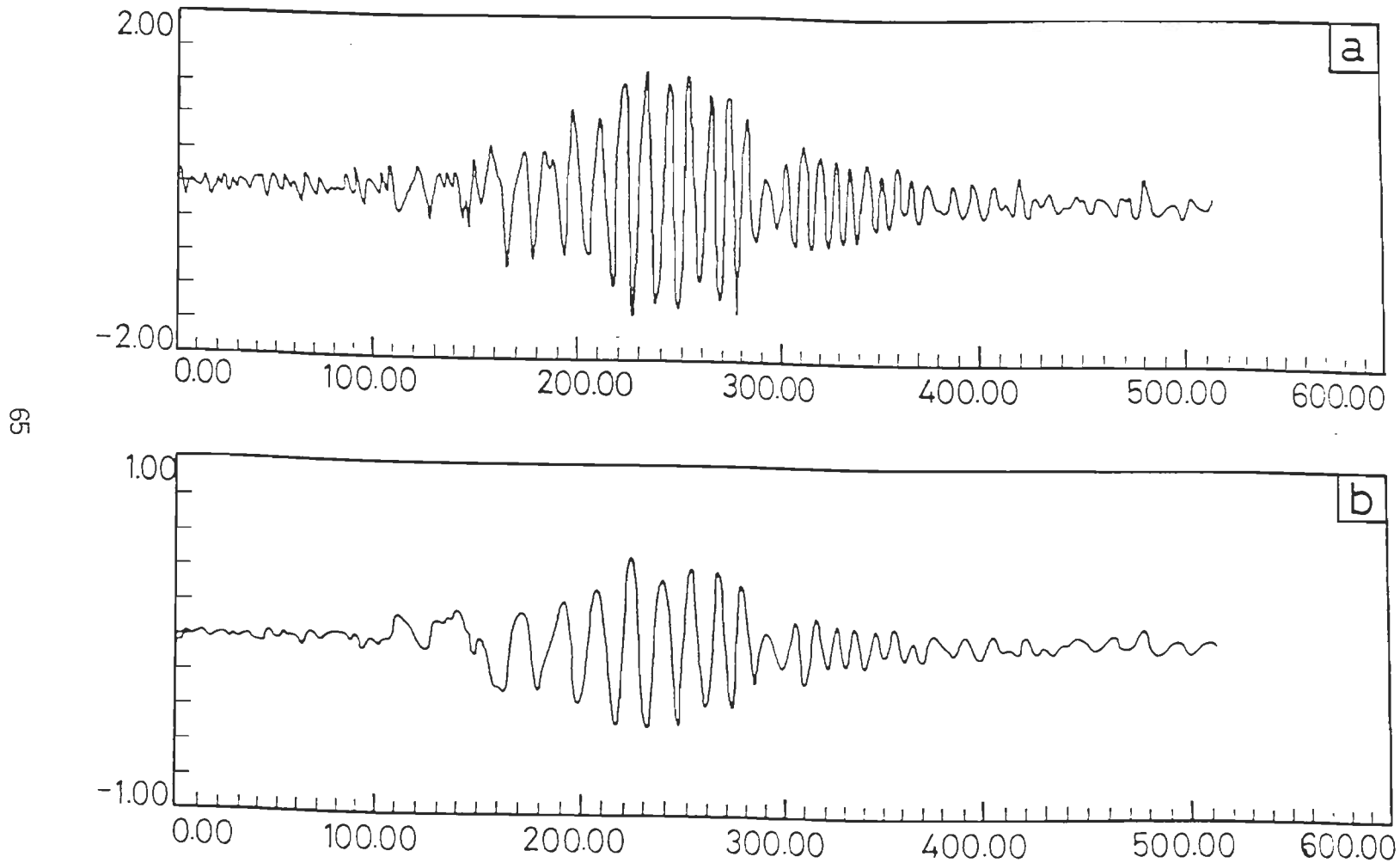


Figure-4.4 (a) The digitized seismogram for Tibet earthquake of October, 31st, 1982. (b) Seismogram after instrumental correction.

d. Narrow band Gaussian filters are applied in frequency domain centred at the frequencies selected in step (c). The form of the Gaussian filter used in the present study is given by equation(2.21). In time domain this filter is represented by

$$h_n(t) = \frac{1}{2\pi} \int_0^{\infty} A(\omega) \cdot \cos[k(\omega) \cdot r - \omega t] \cdot \exp\{-\alpha[(\omega - \omega_n)^2 / \omega_n^2]\} \cdot d\omega.$$

.....(4.2)

The parameter α in equation (4.2) controls the resolution of the filter and its value is dependent on the nature of the dispersion present in the Rayleigh wave train, and the level of noise present. Generally a value of α between 40 and 50 is chosen. In the present study a value of 50 has been chosen for α .

Another parameter β is related to the band width of the filter in the frequency domain. In equation (2.18) the lower limit of the filter is denoted by $\omega_n - \Delta \omega$ which can be rewritten as $(1 - b_r)\omega_n$. The upper limit can be similarly expressed as $(1 + b_r)\omega_n$. The parameter b_r is the relative band width. The parameter β is obtained from the desired value of the filter response at the lower and upper limits of the filter. It is given by

$$\beta = \ln \left| \frac{H_n(\omega_n)}{H_n(\omega_i)} \right| = \ln \left| \frac{H_n(\omega_n)}{H_n(\omega_o)} \right| \dots\dots(4.3)$$

The two parameters α , β are related by

$$\alpha = \beta / b^2_w \dots\dots(4.4)$$

- e. After filtering the observed spectrum the quadrature spectrum is obtained. This is done by multiplying the windowed spectrum by i where $i = (-1)^{1/2}$ which is equivalent to increasing the phase of windowed spectrum by $\pi/2$. In practice, the quadrature spectrum is obtained using the following relation

$$\text{Re} [Q_n(\omega)] = -\text{Im} [H_n(\omega)] \dots\dots(4.5a)$$

$$\text{Im} [Q_n(\omega)] = \text{Re} [H_n(\omega)] \dots\dots(4.5b)$$

where Re, Im denote real and imaginary parts respectively, and $Q_n(\omega)$ is the complex quadrature spectrum.

- f. The windowed spectrum $H_n(\omega)$ and the quadrature spectrum $Q_n(\omega)$ are inverse Fourier transformed. This yields $h_n(t)$ and $q_n(t)$, the two time series.
- g. The two time series $h_n(t)$ and $q_n(t)$ are used to get instantaneous

amplitudes and instantaneous phase. In the present study only the instantaneous amplitudes have been computed. The instantaneous amplitudes for each group arrival time selected earlier. The procedure is repeated for all central frequencies.

- h. The dispersion curve is then plotted by joining maximum amplitudes for all frequencies(or periods). A typical dispersion curve obtained in the present study is shown in Figure.4.5.

4.5 TEST OF COMPUTER PROGRAM MFT

The computer program written to compute group velocity dispersion curves was tested on synthetic data. For this purpose another computer program SDC was written to generate synthetic seismogram for a given dispersion curve. To test the program the synthetic seismogram was filtered using MFT for a number of selected frequencies and a group velocity dispersion curve was computed and compared with the dispersion curve assumed to generate the synthetic seismogram.

4.5.1 SYNTHETIC SEISMOGRAM

In the following two methods of generating a synthetic seismogram simulating a dispersed wave train for which dispersion curves are assumed to be available have been presented here.

4.5.1.1 First Method: This method is based on Chander et al. (1968). Synthetic waveform is computed by the superposition of dispersed sinusoidal waves. The relation used is as follows.

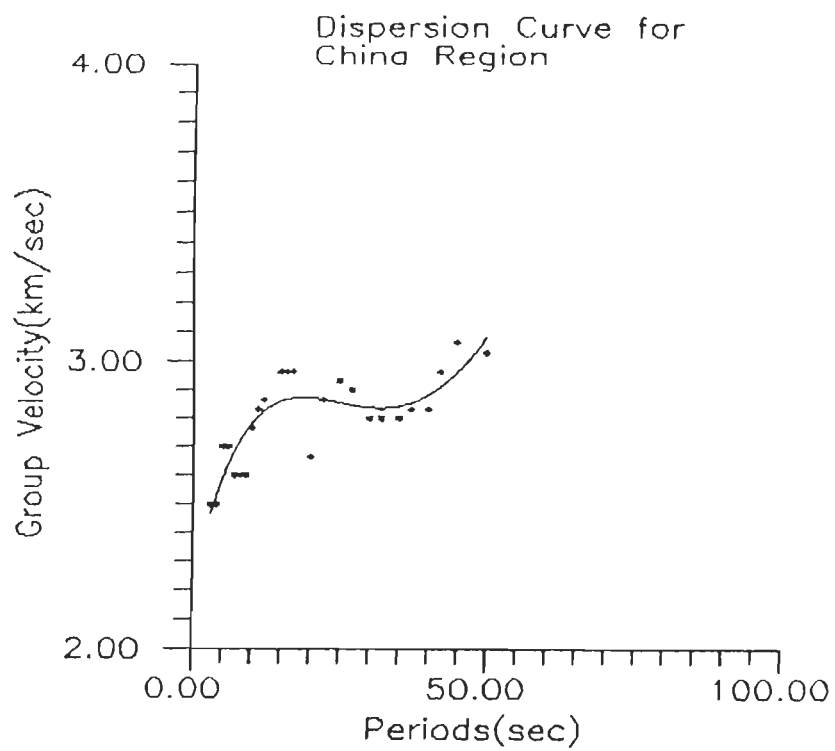


Figure-4.5 Group Velocity Dispersion Curve for China Region obtained in the present study. The solid line shows the best fit line of the fourth order polynomial. * represents the observational points.

$$f(t) = \int_{w_1}^{w_2} A(w) \cdot \cos(wt) dw \quad \dots\dots(4.6)$$

where

$$A(w) = A_{c_p}(w) \cdot A_{i_{nc}}(w) \cdot \exp(-w(X_{s_{tn}} - X_{c_p}(w))/2QU(w)) \quad \dots\dots(4.7)$$

$$t' = t - tt_{s_{tn}} - tt_{c_p}(w) - (X_{s_{tn}} - X_{c_p}(w))/C(w) + (\phi_{i_{nc}}(w) + \phi_{c_p}(w))/w \quad \dots\dots(4.8)$$

Here w_1 and w_2 are the lower and upper limits of the frequencies being used in the synthesis. $A_{i_{nc}}(w)$ and $\phi_{i_{nc}}(w)$ are the amplitude and phase response of the seismograph. $X_{c_p}(w)$ is the epicentral distance of the point where the coupling of shear and PL waves took place. $X_{s_{tn}}$ is the epicentral distance of the station. The $tt_{c_p}(w)$ is the travel time of shear waves to the coupling point and $tt_{s_{tn}}$ to the recording station. $C(w)$ and $U(w)$ are phase and group velocities of the PL waves. Q is the factor taking account of the attenuation. t is the running time. $A_{c_p}(w)$ and $\phi_{c_p}(w)$ are the amplitudes and phase of the PL waves at the coupling point.

With the aim of testing the MFT the following simplifications were introduced.

$$A_{c_p}(w) = 1 \quad ; \quad \phi_{c_p}(w) = 0 \quad ; \quad X_{c_p}(w) = 0$$

$$tt_{s_{tn}} = 0 \quad ; \quad tt_{c_p}(w) = 0$$

Initially a synthetic wave train was generated before being recorded by the

seismograph. Towards this end following simplifications were made.

$$A_{1n2}(w) = 1 \text{ and } \phi_{1n2}(w) = 0$$

With these simplifications the equation(4.6) is reduced to;

$$A(w) = \exp(-w(X_{stn}/2QU(w))) \quad \dots(4.9)$$

$$t' = t - X_{stn}/C(w) \quad \dots(4.10)$$

The assumed phase and group velocity dispersion curves are shown in Figure 4.6, based on which the synthetic seismogram was constructed and has been shown in Figure 4.7.

4.5.1.2 Second Method: According to Bullen and Bolt(1985).

$$yr(x,t) = \frac{A(Kr) \cdot \cos(KrX_{stn} - Yrt - \pi/4)}{[\pi/2 \cdot |dU/dK| \cdot t]^{1/2}} \quad \dots(4.11)$$

For our purpose we have put $A(Kr)=1$. Other terms are-

dU/dK = derivative of group velocity w.r.t. wave number

X = epicentral distance

Yr = $C \cdot Kr$ where C is phase velocity

Kr = wave number

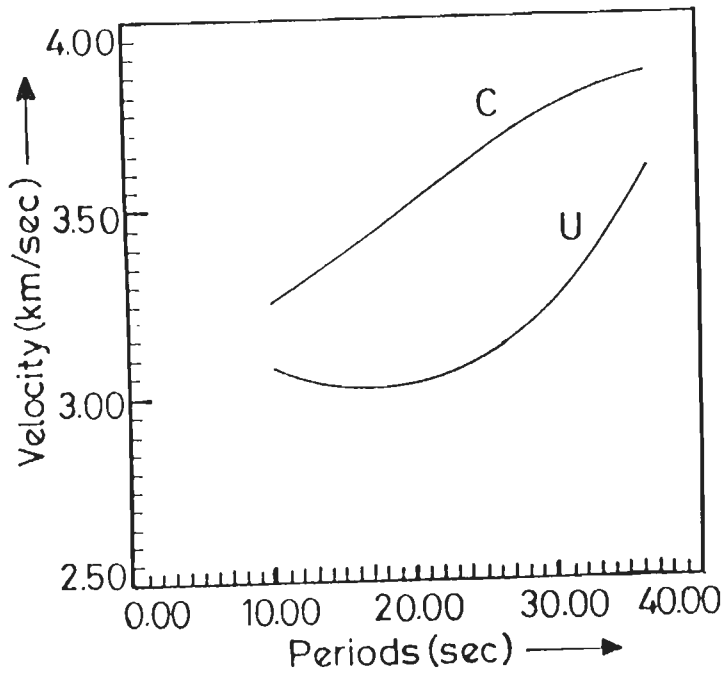


Figure-4.6 Assumed Phase and Group velocity dispersion curve for generating synthetic seismogram for the test of program MFT.

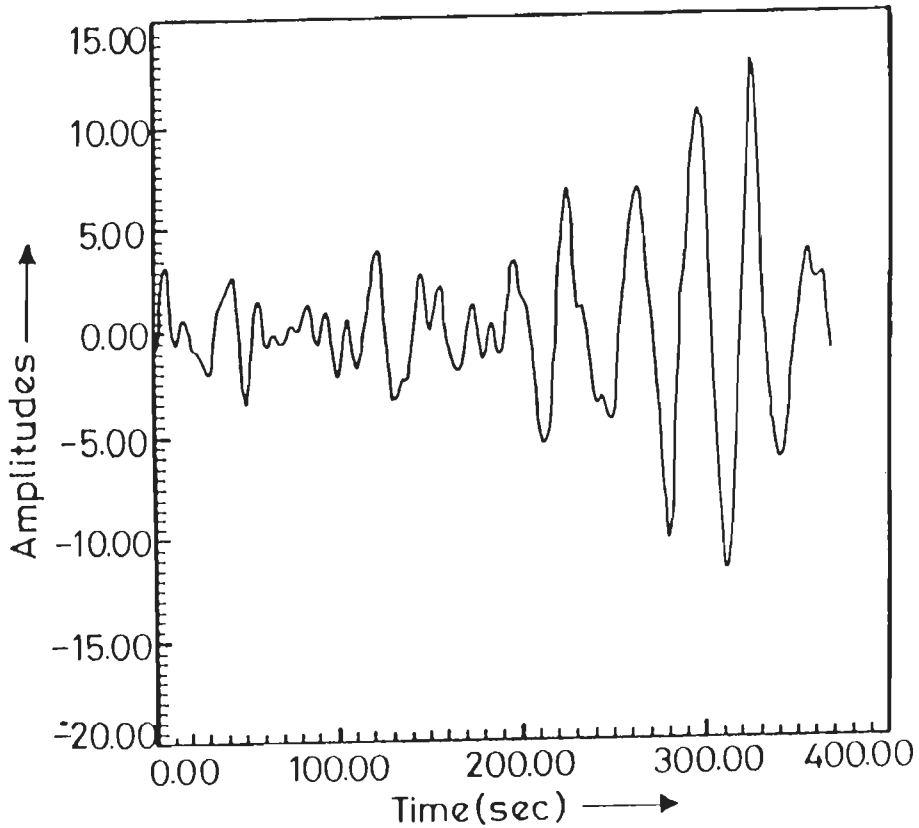


Figure-4.7 Synthetic Seismogram using Chander et al.(1968) formula. For the dispersion curve given in figure 4.6. The seismogram is generated without taking instrument effect into account.

TABLE - 4.3
 Error Analysis for Synthetic Dispersion Sets

Dispersion set No.	Match (%)	Absolute Error (%)	R.M.S. Error (%)
1.	89.59	1.50	1.91
2.	90.19	1.53	1.95
3.	93.85	2.54	2.73
4.	82.12	2.69	4.12
5.	98.81	3.58	3.82

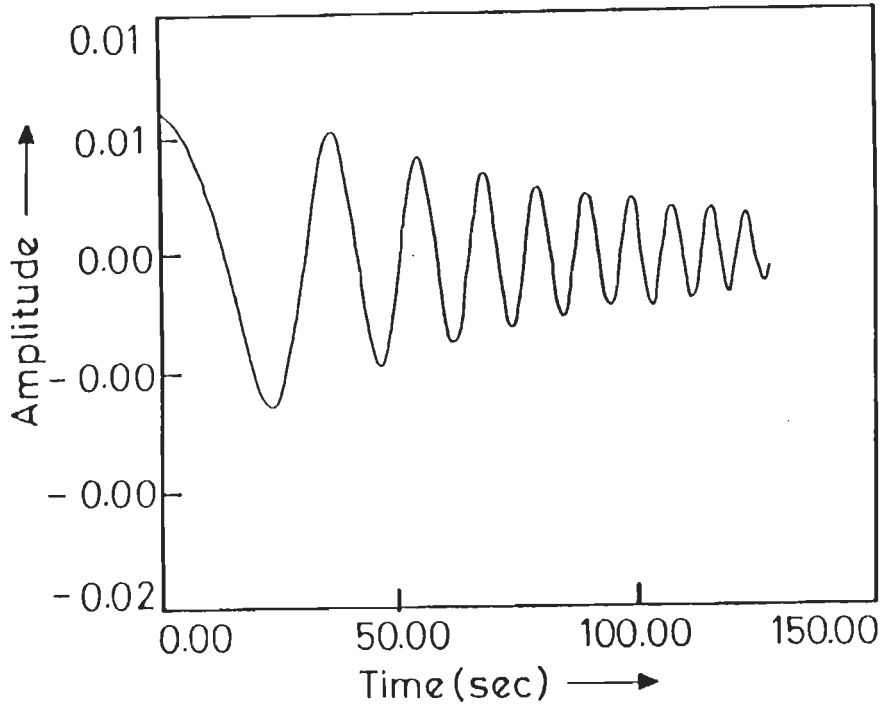


Figure-4.8 Synthetic Seismogram without taking instrument effect into account, using Bullen and Bolt(1985) Formula. The assumed dispersion curve for this seismogram is shown in figure 4.9

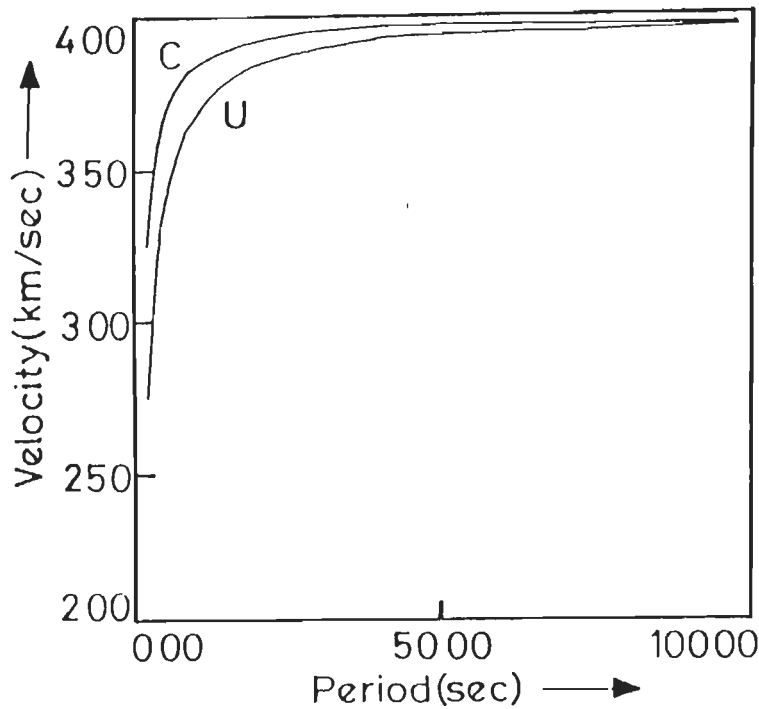


Figure-4.9 Assumed Phase and Group velocity Dispersion Curve for generating Synthetic seismogram for testing the program MFT.

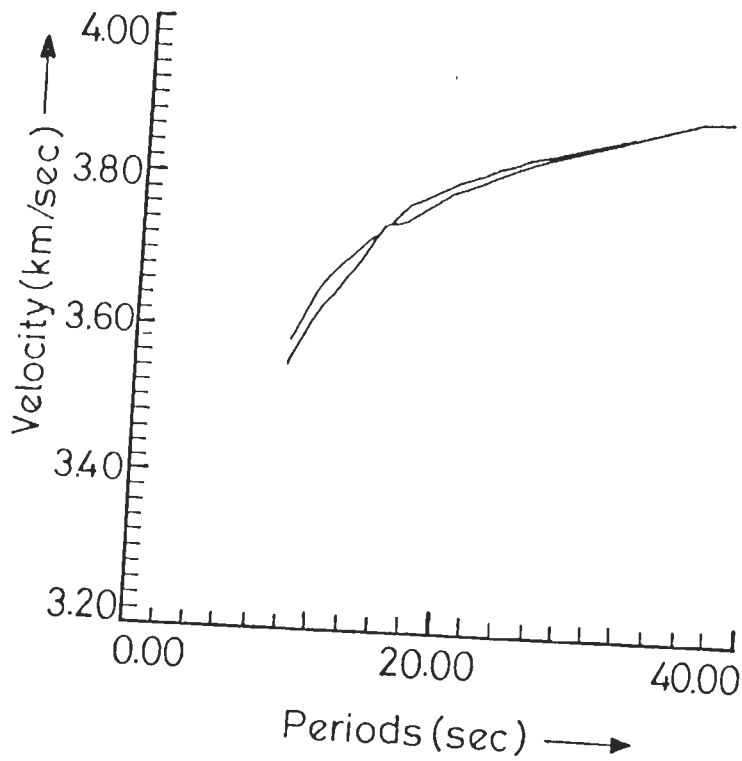


Figure-4.10 Comparison of computed and assumed dispersion curves. The computed dispersion curve is obtained after applying the program MFT.

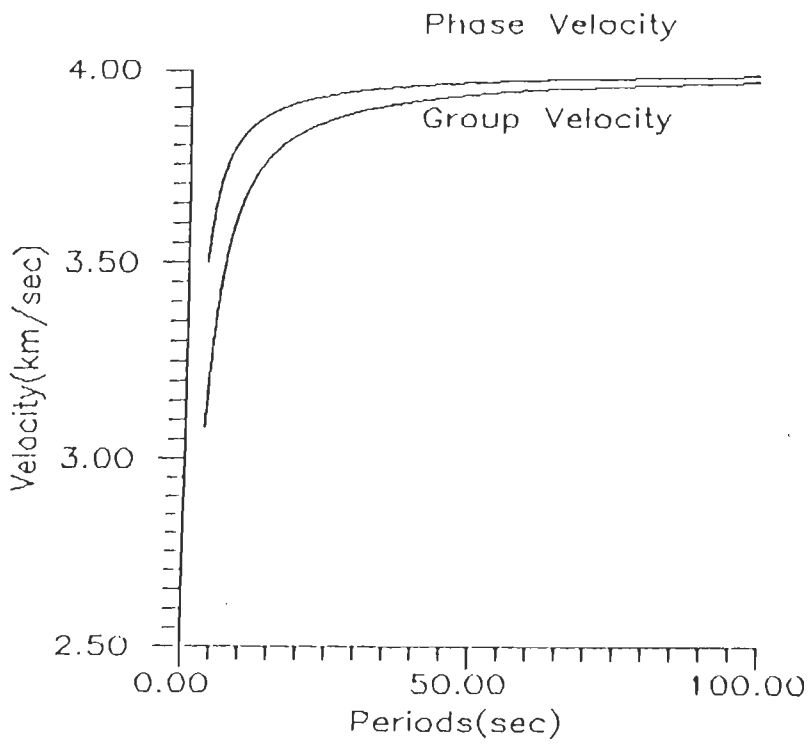
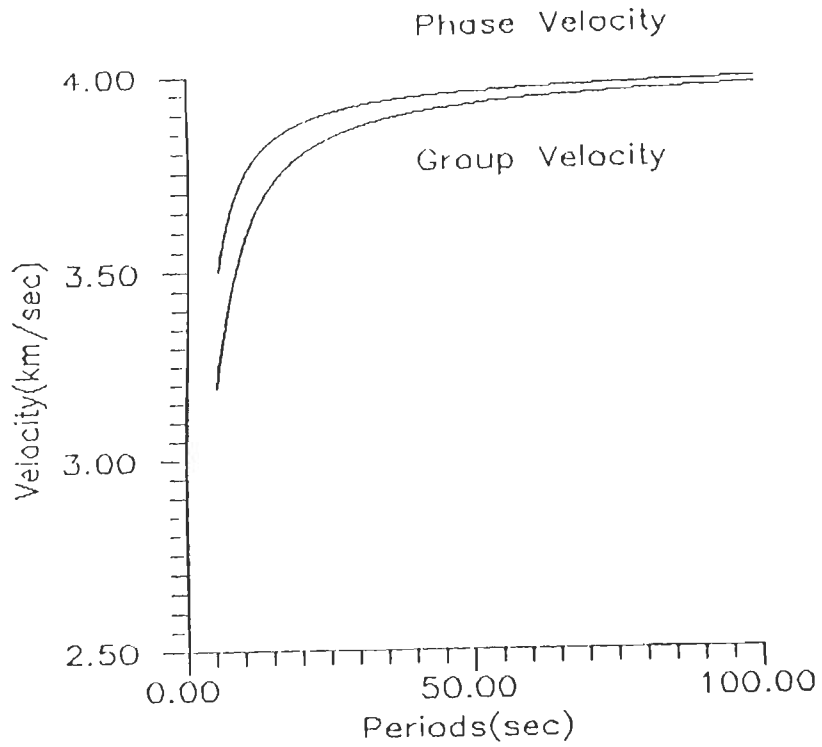


Figure-4.11 Assumed Phase and Group velocity dispersion Curves set (ii) and (iii) used in the construction of Synthetic Seismograms for the test of program MFT.

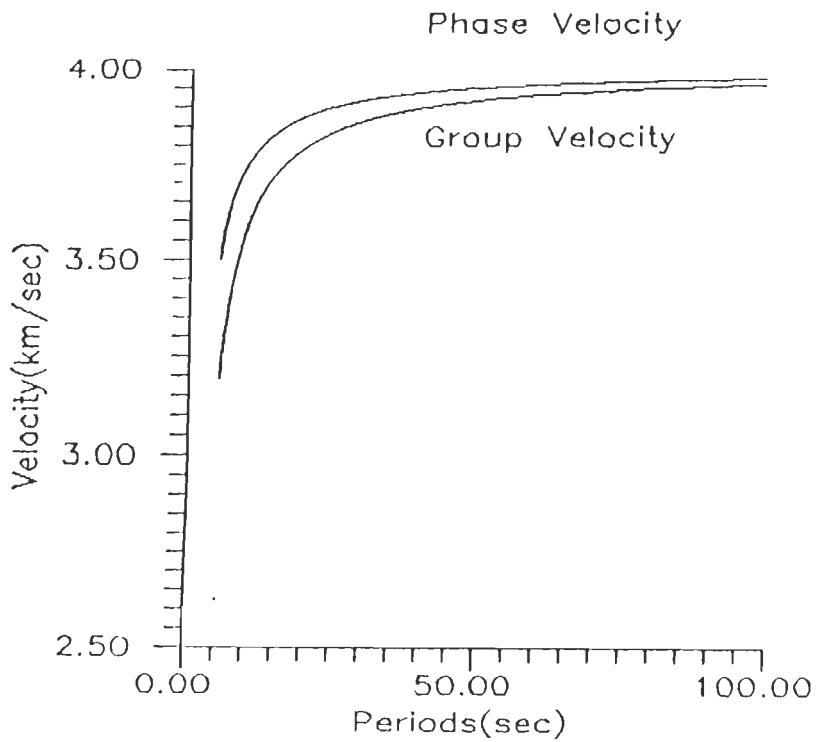
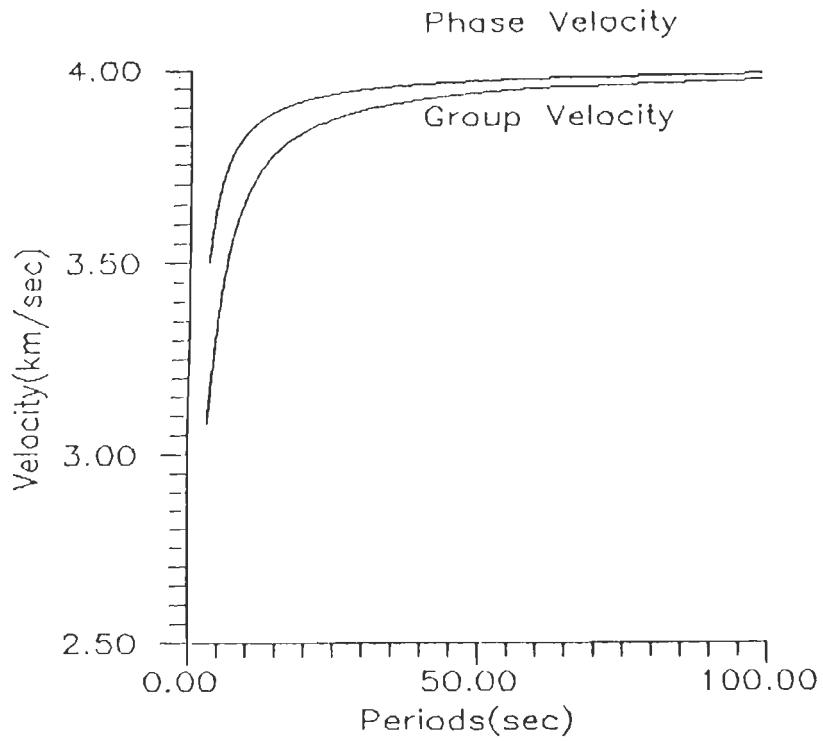


Figure-4.12 Assumed Phase and Group velocity dispersion Curves set (iv) and (v) used in the construction of Synthetic Seismograms for the test of program MFT.

t = running time

Using the above relation a synthetic seismogram has been constructed. The synthetic seismogram and assumed dispersion curve is shown in Figure 4.8 and Figure 4.9 respectively. For the purpose of present study the second method was adopted due to its simplicity.

4.5.2 RESULTS OF THE TESTS

The free field synthetic seismogram generated above was convolved with the instrument transfer function (equation 4.1) in the frequency domain. This gives the synthetic seismogram which would have been recorded by the seismograph. This seismogram was processed further to remove the effect of the instrument. The resulting time series was filtered using MFT to obtain the group velocity dispersion curve. One set of two dispersion curves assumed and computed are shown in Figure 4.10. Table 4.3 shows the degree of fit between the two sets of dispersion curves. The Figure 4.11 and Figure 4.12 show the assumed dispersion curves used in the construction of synthetic seismograms for the test of MFT. It is observed that both the absolute error and the RMS error are below 5% for the dispersion curves test. This establishes the validity of the program MFT. The inclusion of instrumental effect to get recorded seismogram and its removal has been done in frequency domain throughout.

CHAPTER - 5

ANALYSIS AND INTERPRETATION OF RESULTS

5.1 INTRODUCTION

In the studies presented herein a set of 18 earthquakes has been selected for computing group velocity dispersion curves of Rayleigh waves and deducing the crustal structure in different regions.

The vertical component seismograms of these 18 earthquakes recorded by seismographs at the Wide Band Seismological Observatory at the Department of Earth Sciences, University of Roorkee, Roorkee were obtained. In fact many earthquakes were recorded at this observatory since it started operation in October 1982. The selection of earthquakes for further studies was based on their location in the vicinity of India and the quality of Rayleigh wave records obtained. The epicentral parameters of these earthquakes have been obtained from Earthquakes Data Reports of the United States Geological Survey and are given in Table 4.1. The origin times of these earthquakes have been given in Indian Standard Time (IST).

All the earthquakes have their foci in the crust, the depths ranging from 7.5 km to 49 km. Their surface wave magnitudes lie in the range 4.2-6.0. For the purpose of the present study these earthquakes have been grouped regionwise depending upon the location of their epicentres which lie in six geographic regions. The regionwise distribution is given in Table 5.1.

The dispersed Rayleigh wave trains of the selected earthquakes have been

TABLE - 5.1
 REGIONWISE DISTRIBUTION OF EARTHQUAKES
 IN SIX REGIONS UNDER PRESENT STUDY

Name of the Region	Earthquakes
India Bangladesh Border	1 Earthquake of India Bangladesh Border
China Region	3 Earthquakes of China
Tibet Region	2 Earthquakes of Tibet 1 Earthquake of China
Afghanistan Region	2 Earthquakes of Afghanistan- Tadzhakistan Border 1 Earthquake of Tadzhakistan 1 Earthquake of Kirghizkstan
Hindukush Region	4 Earthquakes of Hindukush 1 Earthquake of Tadzhakistan
Iran Region	2 Earthquakes of Iran

digitized on a Calcomp digitizer. The digitized wave trains have been analysed for computing group velocity dispersion curves of fundamental mode Rayleigh waves using the Multiple Filter Technique (Dziewonski et al., 1969). The instrumental correction has been applied using the formulation given in Chapter 4.

The Rayleigh wave paths of all earthquakes considered in this study are continental in nature, and traverse regions of moderate to intense tectonic activity. The group velocity dispersion data in each region have been plotted over average dispersion curves for mid continental and Alpine type crust given by Brune (1969). These crustal types have emerged from surface wave studies. The parameters used are crustal thickness, upper mantle (P_1) velocity, tectonic characteristics and sediment thickness.

For interpreting the observed dispersion data, theoretical dispersion curves have been generated using Knopoff's (1964) method. All plausible models of crustal structures in different regions have been examined and the theoretical dispersion curves generated. The two types of dispersion curves, observed and computed, have been compared to find the degree of their goodness of fit. The degree of fit between the observed and computed dispersion curves has been examined quantitatively by computing total absolute error and percentage of the goodness of fit. The maximum error has been found to be 9.8 % (absolute), and the goodness of fit has a minimum value of 67.8 %.

In the following paragraphs the results of the present study have been presented regionwise and the interpretation of the results has been discussed in the light of available information from other studies.

5.2 ANALYSIS OF RESULTS AND THEIR INTERPRETATION

5.2.1 INDIA BANGLADESH BORDER REGION

In this region only one earthquake has been found which occurred on April 13, 1989. It had a magnitude of 5.0(Ms) and had its focus at a depth of 33 km. The epicentral distance of this earthquake from Roorkee is 1577 km. The path of Rayleigh wave from this earthquake passes through East Ganga basin and runs close to India-Nepal border near Himalayan foothills (Figure 5.1). The seismogram exhibits Rayleigh waves upto a period of 30 seconds. The group velocity dispersion data plotted over average dispersion curve for mid-continental type of crust is shown in Figure 5.2. It is seen that the observed group velocities are less than those for mid continental type crust. This may be explained by lower crustal and upper mantle velocities.

To interpret this dispersion curve the crustal velocity model suggested by Chaudhary(1966) was selected as the starting point. This model consists of a three layered crust underlain by a uniform half space. The top layer consists of a sedimentary layer with a thickness of 3 km. The thickness of crust is 40 km. The theoretical curve which fits the observed dispersion data is shown in Figure 5.3. and the velocity model is given in Figure 5.4. This is similar to initial model except for the fact that the thickness of sedimentary layer is 5 km with a shear wave velocity of 2.3 km/s which is 1 km/s less than that in the earlier model. The difference in the properties of earth materials along the path of propagation may explain the slight difference in the top layer of two crustal models. The path in the present case lies close to foothills zone of Himalayas characterized by deep sedimentary basins which

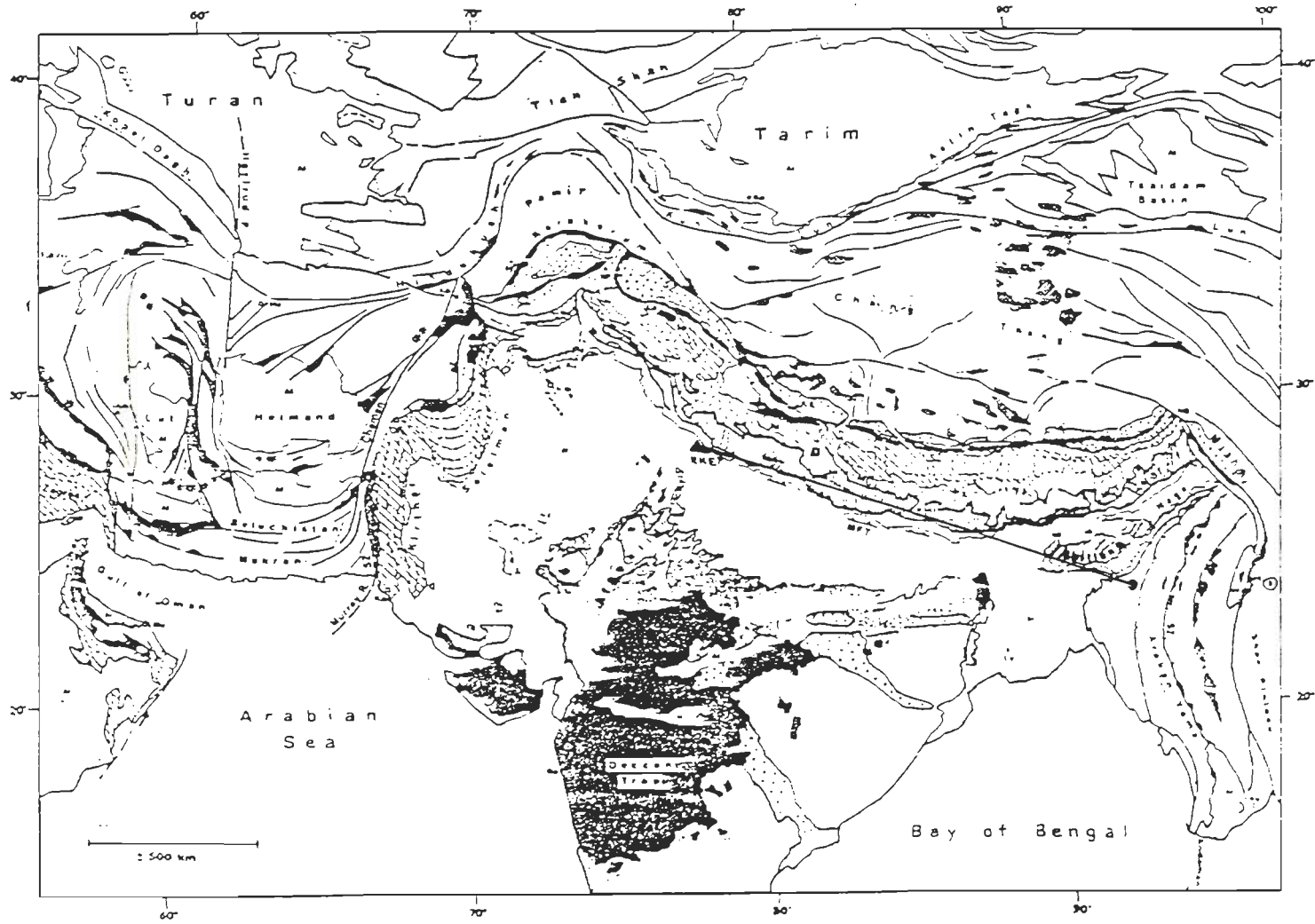


Figure-5.1 Wave path for Rayleigh waves in East Ganga Basin region. (Map modified after (Gansser, 1993))

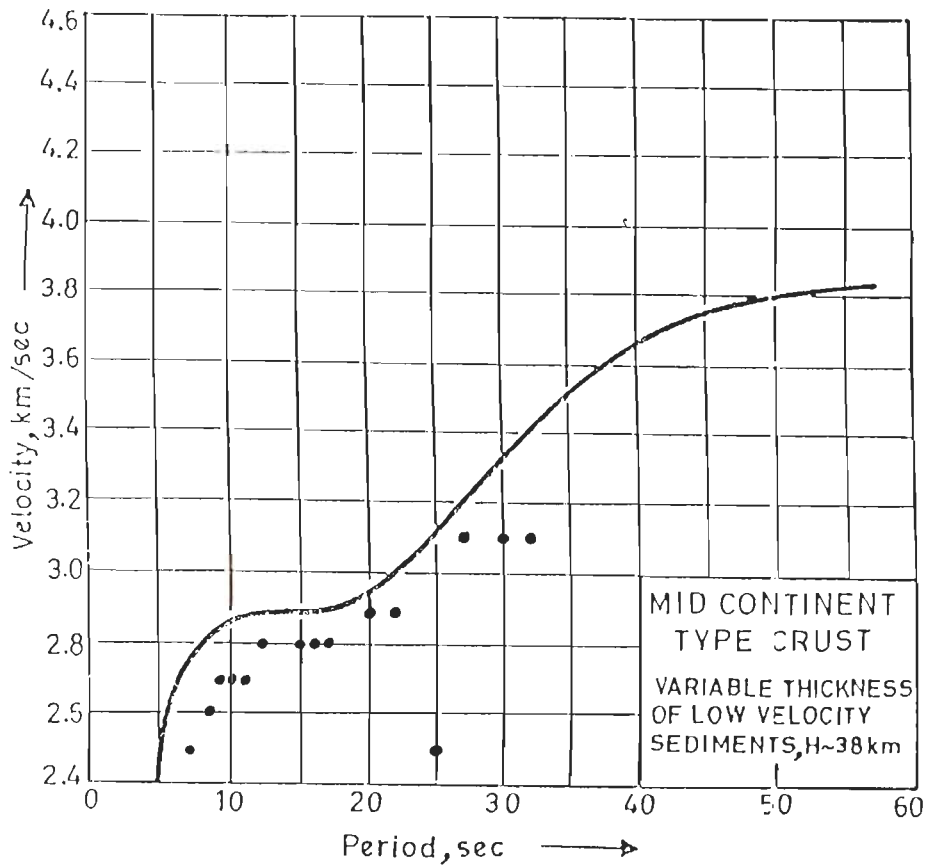


Figure-5.2 Group velocity dispersion data of East Ganga Basin is plotted over average dispersion curve for Mid Continental type of Crust (After Brune, 1969)

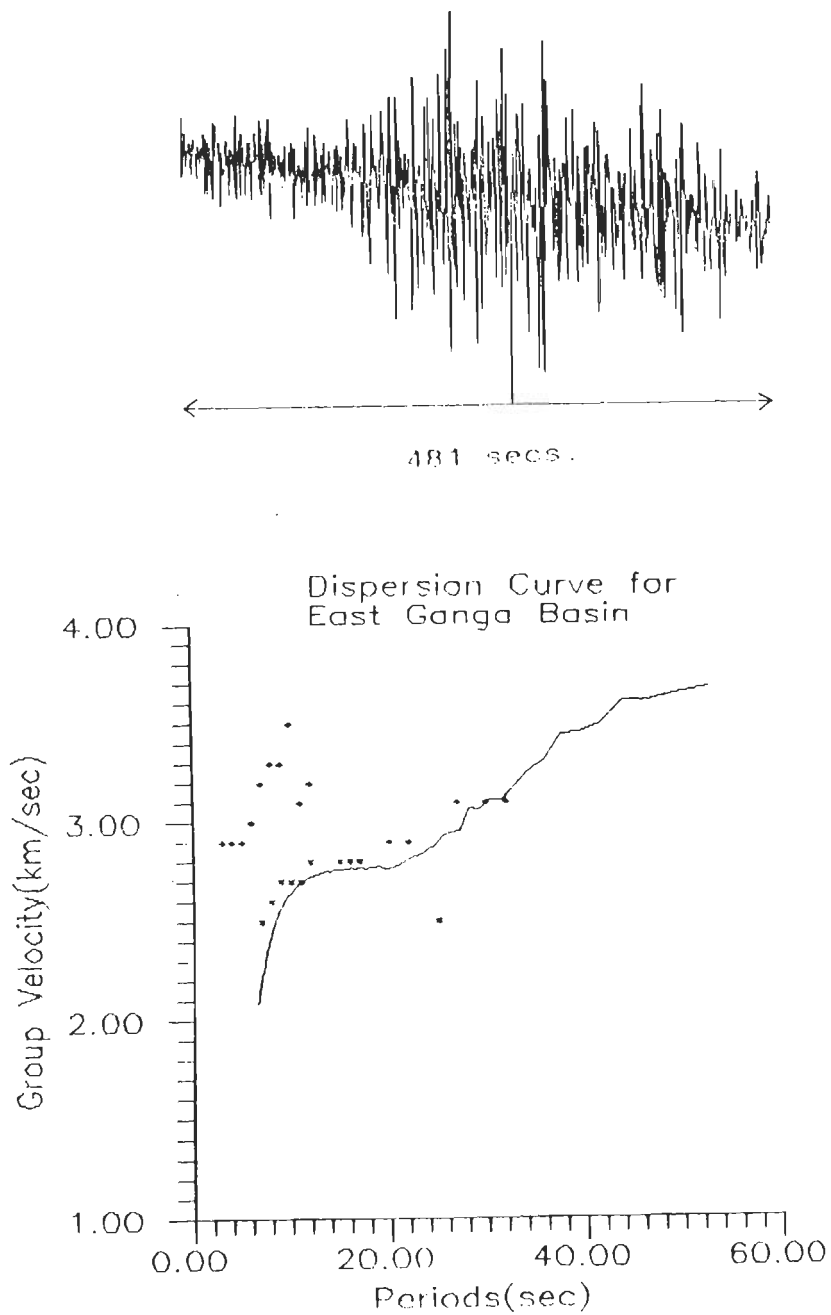


Figure-5.3 (a) The seismogram for India Bangladesh Border region earthquake of April, 13 1989, for 481 sec. duration. (b) Group velocity dispersion curve for East Ganga Basin. * represents the observed data and solid line represents the theoretical model.

REGION - 1
MODEL FOR EAST GANGA BASIN

LAYER NO.	P-WAVE VELOCITY Km/sec.	S-WAVE VELOCITY Km/sec.	DENSITY gm/c.c.	THICKNESS Km.
1.	3.980	2.30	2.340	05.00
2.	6.150	3.55	2.817	15.00
3.	6.580	3.80	2.922	20.00
4.	7.830	4.52	3.290	-

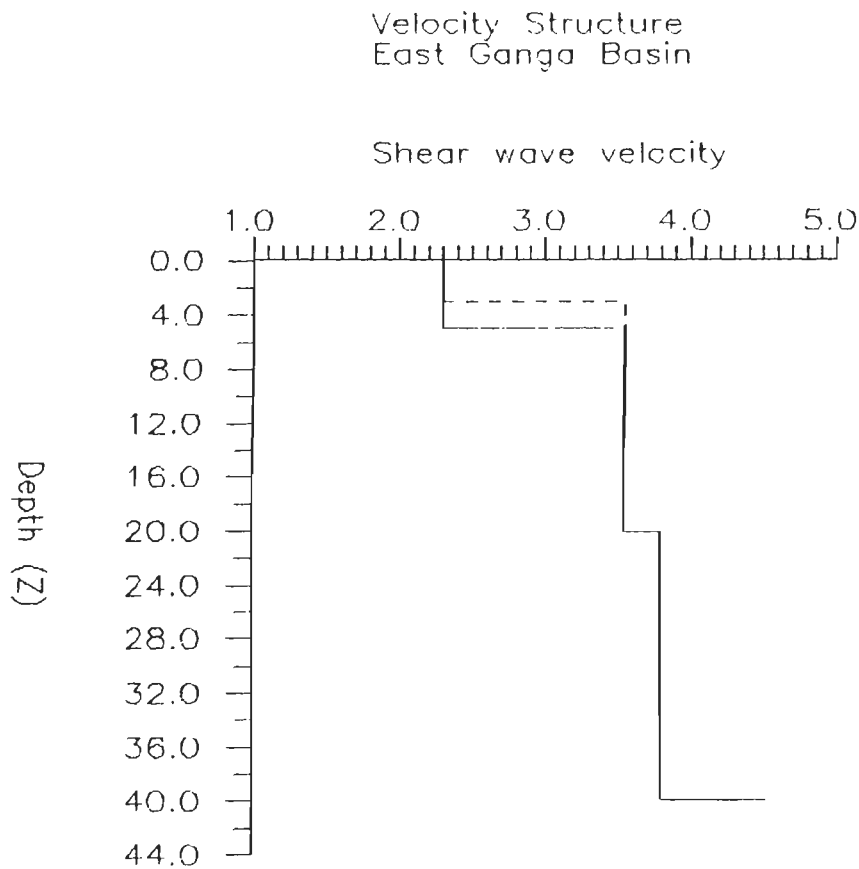


Figure-5.4 Proposed shear velocity model for East Ganga Basin. Complete model for this region is shown in the upper part of the figure. Dashed line shows the velocity model given by Chaudhary(1966).

have been explored for hydrocarbon accumulations by the Oil and Natural Gas Corporation Limited, India. This also explains low shear wave velocities in the top layer. The upper mantle P-wave velocity of 7.83 km/s is less than 8.2 km/s, the value beneath mid continent type crust. Chun(1986) has remarked on the similarity between the crust in East Ganga Basin below the sedimentary layer and that of Canadian shield. However the P-wave velocity is less than that for a typical shield type crust for upper mantle of Brune(1969). The S-wave velocity of 4.52 km/s is likewise less than 4.6 km/s under this crustal type.

5.2.2 CHINA REGION

The three earthquakes belonging to this region lie in Sichuan province in China. The epicenters of these earthquakes are so close to each other that the paths of Rayleigh waves from these events to Roorkee, which have a mean distance of nearly 2090 km, can be taken to be coincident (Figure 5.5). The surface wave magnitudes of these earthquakes vary from 5.9 to 6.1. Two of these earthquakes are very shallow (focal depth 7.5 km) and the third has a focal depth of 14 km.

The combined group velocity data for the three earthquakes is shown in Figure 5.6 plotted over mid-continental type crust. It is seen that lower group velocities are observed especially for periods exceeding 17 seconds. For shorter periods the velocity value straddle the curve. There is decrease in the velocity between 28 to 40 second period. The longest periods obtained in this case are nearly 60 seconds. The path of Rayleigh waves for these earthquakes traverses part of Tibetan plateau and Himalayan ranges. To interpret the dispersion data the crustal model proposed by Chun and Yoshii(1977) was adopted as the initial model which includes a low velocity layer in the crust. The theoretical curve for interpreted model is

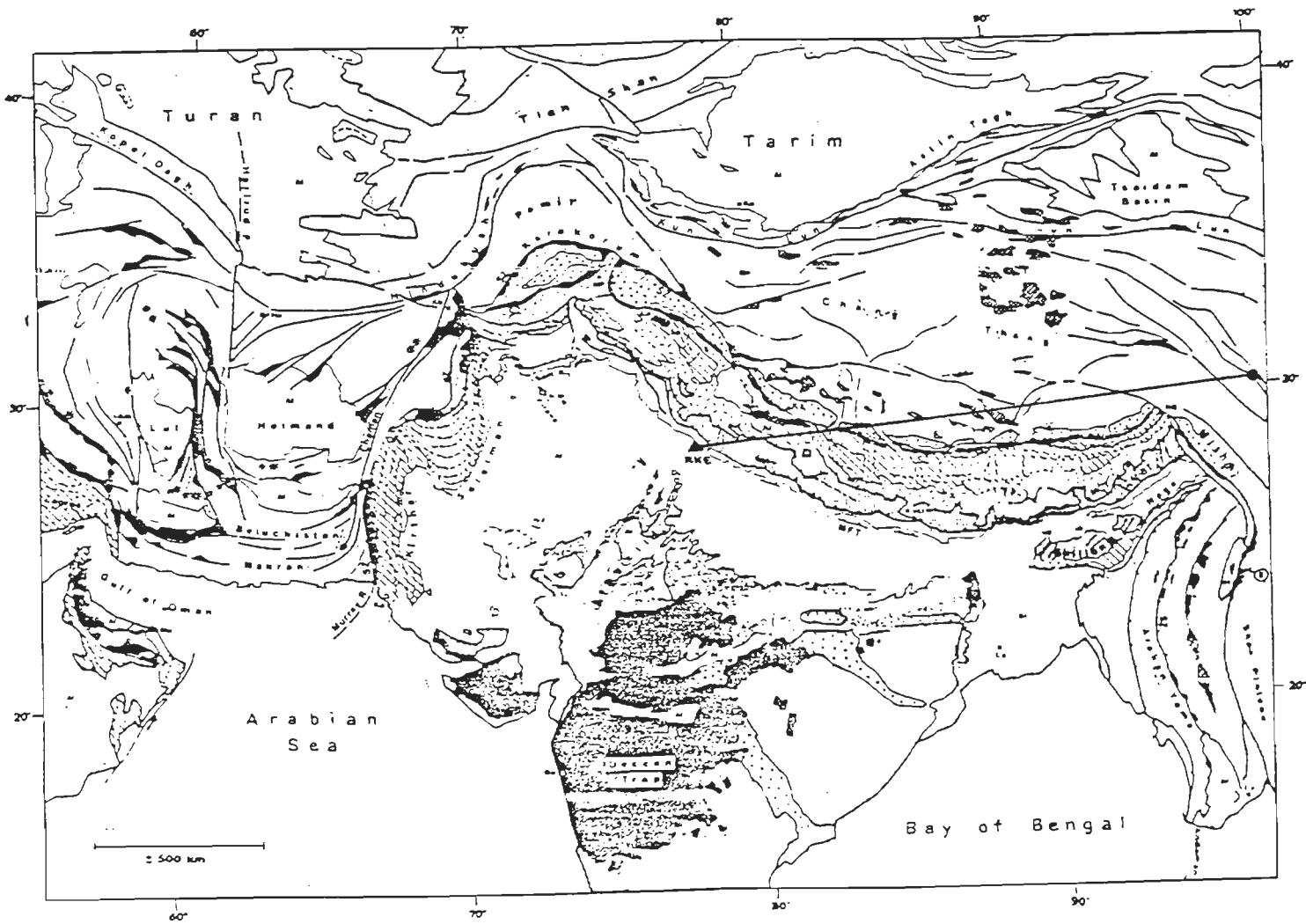


Figure-5.5 Wave path for Rayleigh waves in China region. (Map modified after Gansser, 1993)

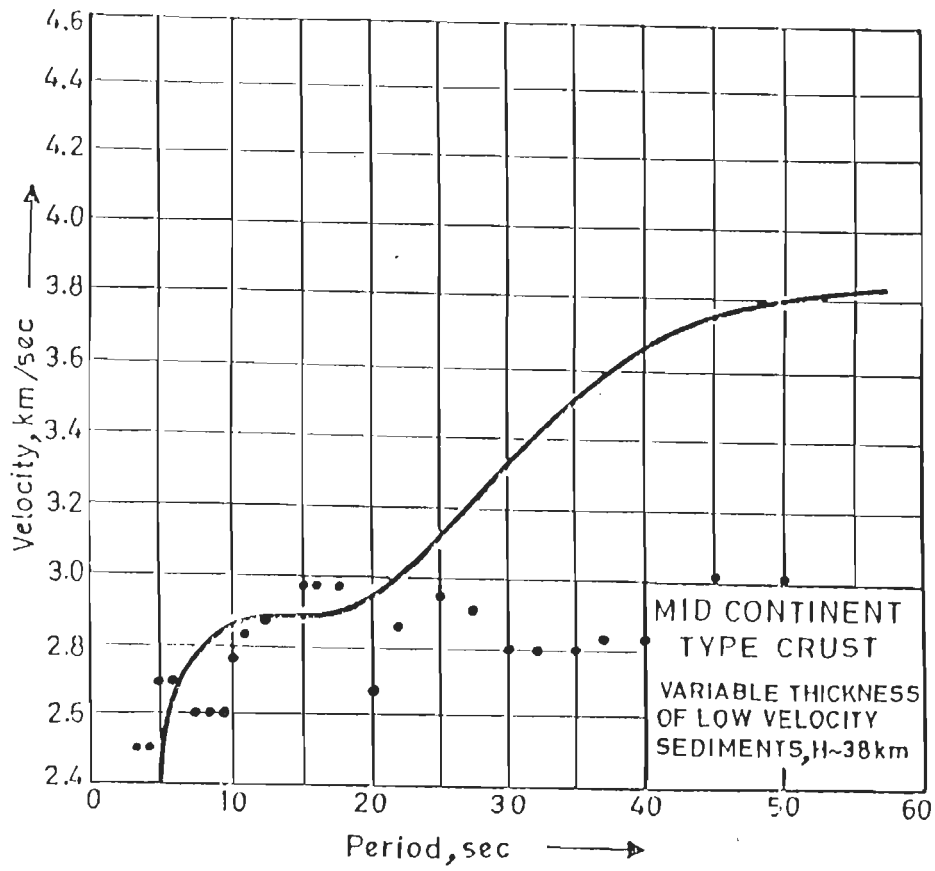


Figure-5.6 Average Group velocity dispersion data of China Region is plotted over average dispersion curve for Mid Continental type of Crust(After Brune, 1969)

shown in Figure 5.7. and the crustal model is given in Figure 5.8. The low velocity layer is 15 km thick at a depth of 21 km. from the surface. The shear wave velocity in this layer is 3.37 km/sec which is slightly less than that in the upper layer, the difference being 3.7%. The upper mantle P-wave velocity (7.78 km/s) is less than the value for mid continent type crust indicating substantial departure from an average continental crust.

The epicentres of these earthquakes fall in the Chinghai- Tibet subplate of Pines et al.(1980). This subplate consists of the areas north of the Himalayas including the Kun Lun mountains. It extends towards the east till longitude 105° E. The western boundary is less well defined extending approximately 500 km to the west of the border of China. It is characterised by high seismicity. The Rayleigh wave paths used in surface wave study of Pines et al.(1980) cross most of Tibet plateau and part of Hindukush whereas in the present case the paths cross Tibet plateau and Himalayan ranges. The group velocity of Rayleigh waves determined in the present study ranges from 2.5 km/s at 2 second period to little more than 3 km/s at 44 second period. The variation in group velocity obtained in the earlier study was from 2.60 to 3.65 km/s over a period range of 10 to 120 seconds. The interpreted models in the two cases differ in the presence of a low speed layer at the top (shear wave velocity 4.11 km/s) and a low velocity layer at 21 km depth. The crust is found to be 61.25 km thick and consists of four layers. The three crustal layers of thickness 16.25 km, 15 km and 25 km have shear wave velocities of 3.50 km/sec, 3.37 km/sec and 3.64 km/sec. Pines et al. also found similar velocities and considered all these layers to have granitic composition. The upper mantle shear wave velocity of 4.5 km/s is smaller than that which characterizes average continental crust.

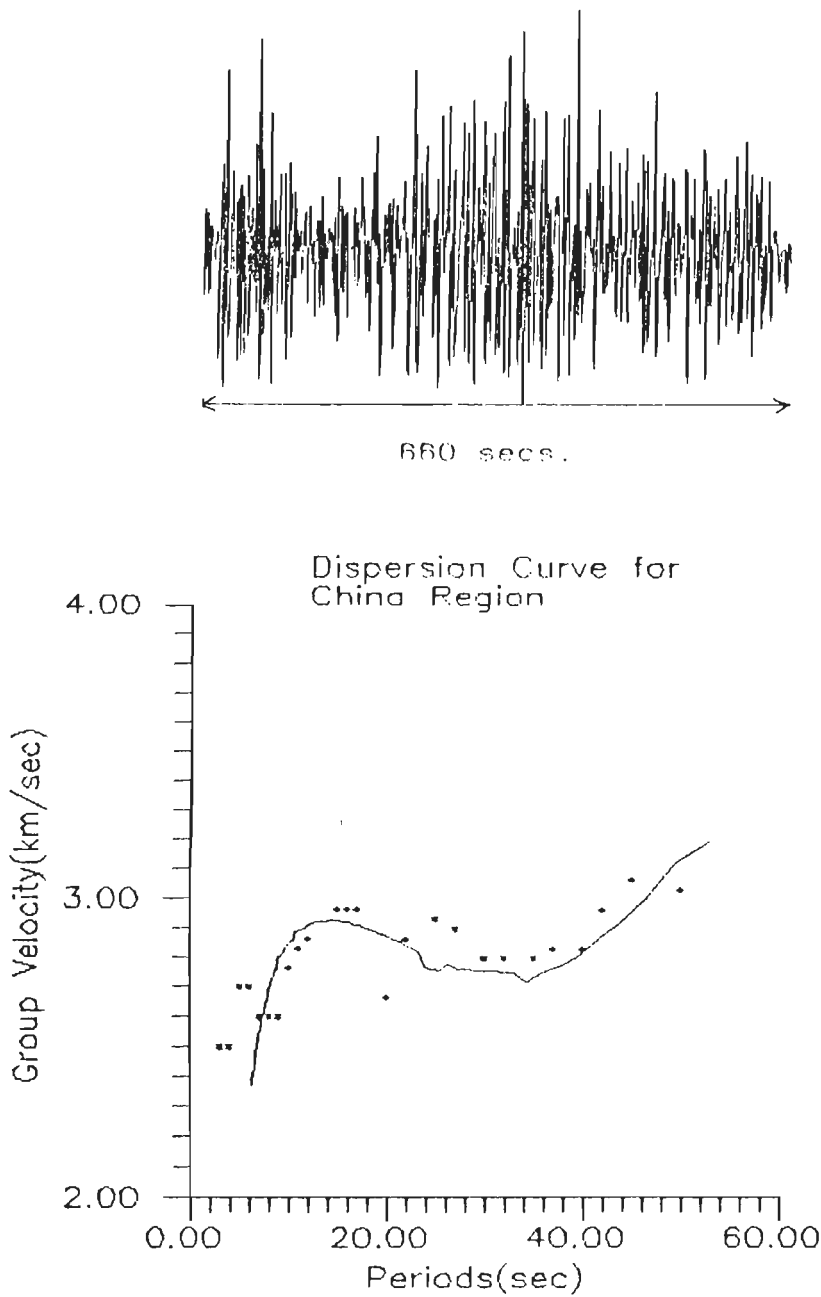


Figure-5.7 (a) The seismogram for China region earthquake of April, 25 1989, for 660 sec. duration. (b) Average Group velocity dispersion curve for China Region. * represents the observed data and solid line represents the theoretical model.

REGION - 2
MODEL FOR CHINA REGION

LAYER NO.	P-WAVE VELOCITY Km/sec.	S-WAVE VELOCITY Km/sec.	DENSITY gm/c.c.	THICKNESS Km.
1.	4.411	2.55	2.41	05.00
2.	6.055	3.50	2.70	16.25
3.	5.800	3.37	2.75	15.00
4.	6.300	3.64	2.90	25.00
5.	7.780	4.50	3.30	-

Velocity Structure
Roorkee-China Path

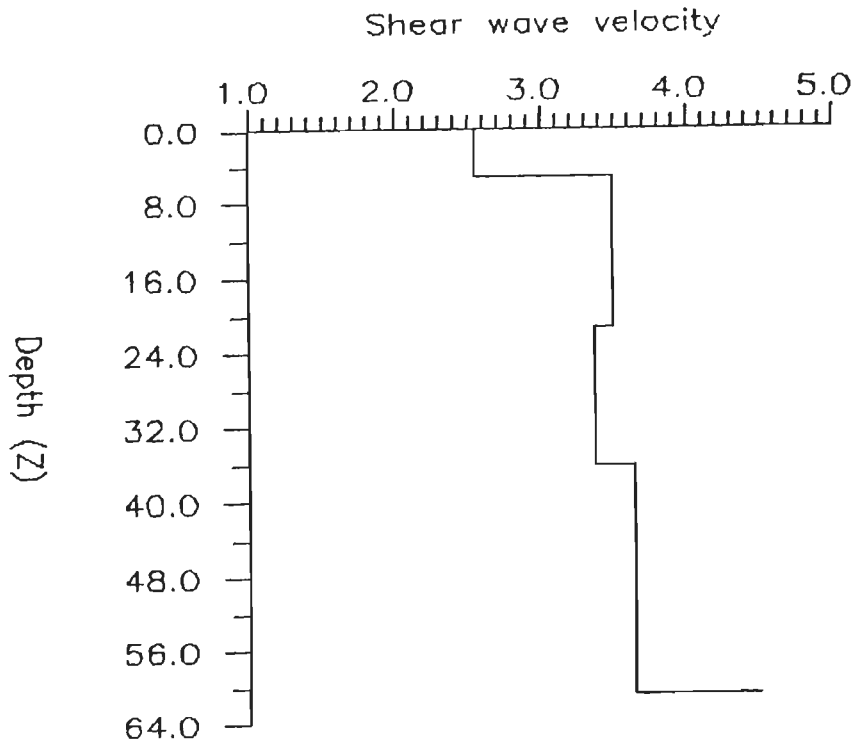


Figure-5.8 Proposed shear velocity model for China Region. Complete model for this region is shown in the upper part of the figure.

5.2.3 TIBET REGION

Tibetan plateau is one of the most conspicuous topographic features on earth. Its average elevation above sea level is about 5 km over an area of 7×10^6 sq km. It is bounded by Himalayan convergent zone to the south and Altyn Tagh and Kun Lun left lateral strike slip faults to the north. Because of its unusual elevation and the limited geological data the crustal structure in this region has been the subject of investigation by many workers who have applied a variety of techniques. Surface wave dispersion studies to deduce the crustal structure in this region has been carried out, among others, by Chen and Molnar(1975,81), Chun and Yoshii(1977), and Chun and McEvelly(1986). Seismic refraction and wide angle reflection profiles for elucidating crustal structure have been carried out by Chinese scientists and jointly by French and Chinese scientists. The results of a study of gravity anomalies have also been described (Molnar, 1988).

According to Molnar(1988) the data from explosion seismology studies in Tibet which consist of refraction profiles and wide angle reflection profiles, show a complex crustal structure, with dipping interfaces that could well be the manifestations of major thrust faults.

Results of surface wave dispersion studies by earlier workers indicate a crustal thickness of 70 km. and low shear wave velocities (4.4 - 4.5 km/s or less) for the mantle immediately below the Moho. Chen and Molnar(1981) suggested a crustal thickness of 55 to 85 km. on the basis of surface wave dispersion studies. The corresponding shear wave velocities in the upper mantle vary between 4.4 km/s to 4.9 km/s respectively. When data on S' velocities (4.8 km/s) determined from travel time data was combined with surface wave studies the most likely estimates of

crustal thickness lie between 65–80 km. Chun and McEvilly(1986) found a very thick crust(74 ± 10 km) and a prominent low velocity channel at mid crustal depth.

For this region three earthquakes have been used. Two of these earthquakes are from Tibet with the epicentral distances of 719 and 783 km. Another event which falls north of Tibet plateau has an epicentral distance of 1388 km. The paths of these three events are nearly coincident (Figure 5.9). The paths of Rayleigh waves traverse the western part of Tibetan plateau and also cross Himalayan region. The combined dispersion data are shown in Figure 5.10, on which average dispersion curve for mid continental type crust is plotted and in Figure 5.11 on which the curve for the Alpine type crust is plotted. From these figures no firm conclusions can be drawn with respect to the type of crusts with which dispersion data agree. For periods shorter than 22 seconds, the data seems to match mid continental type crust. The group velocities are higher in the period range where low group velocities for Alpine type crust are indicated. The observed group velocities are lower than those for the latter type of crust for periods longer than 27 seconds. It can be surmised that the Tibetan crust is somewhat continental type for periods shorter than 22 seconds but is not typically Alpine for longer periods. To interpret the dispersion curve in the present study the crustal model proposed by Chen and Molnar(1981) was adopted. The comparison of observed dispersion data with the theoretical dispersion curve for the final velocity model is shown in Figure 5.12 and the crustal model is given in Figure 5.13. A four layer crustal model was arrived at with an upper mantle shear wave velocity of 4.5 km/s immediately below Moho which lies at a depth of 67 km. This value of shear wave velocity is quite small when compared with that of upper mantle below average continental crust. A 20 km thick low velocity layer was found at a depth of 22 km and a 3.75 km thick low velocity layer at the top. The presence of a 10 km thick low velocity zone is also suggested

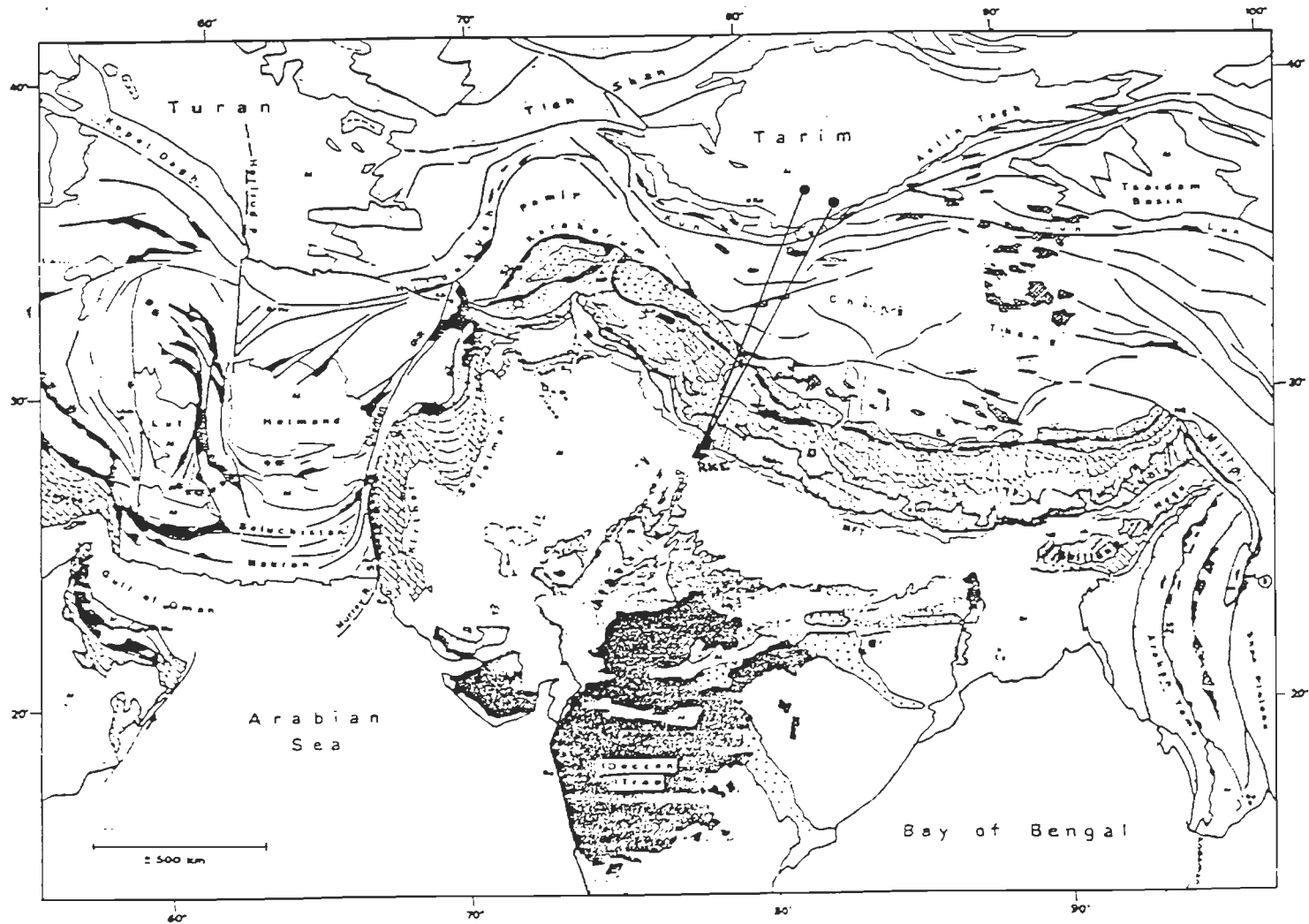


Figure-5.9 Wave path for Rayleigh waves in Tibet region.(Map modified after Gansser, 1993)

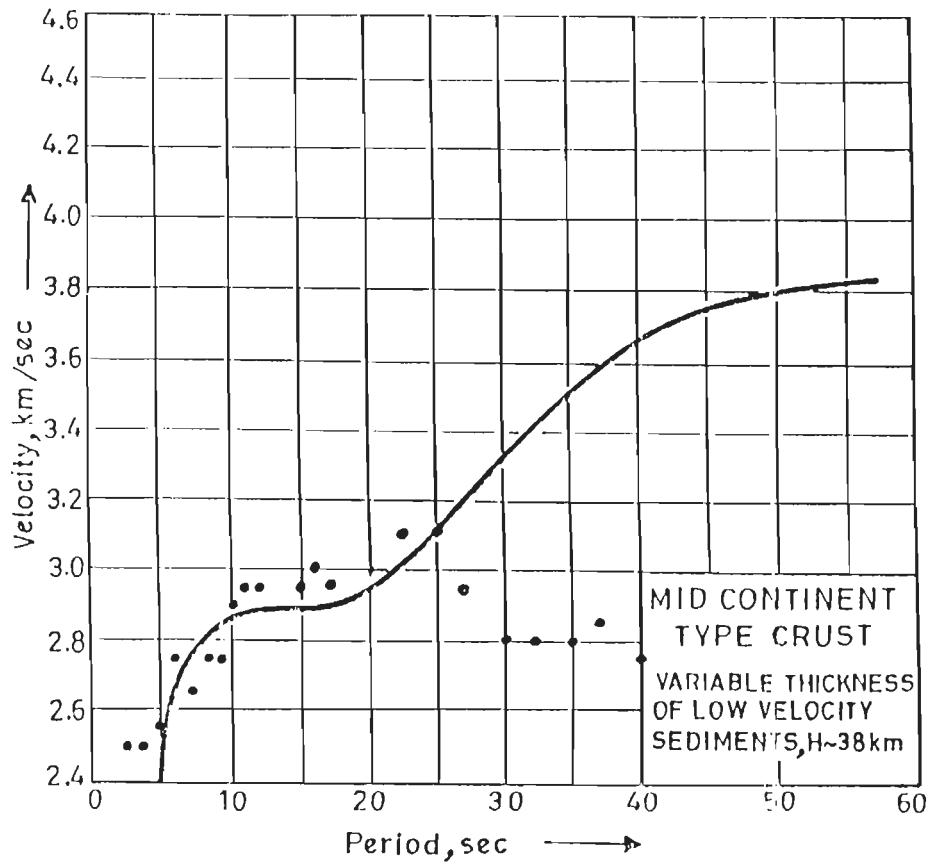


Figure-5.10 Average Group velocity dispersion data of Tibet Region is plotted over average dispersion curve for Mid Continental type of Crust (After Brune, 1969)

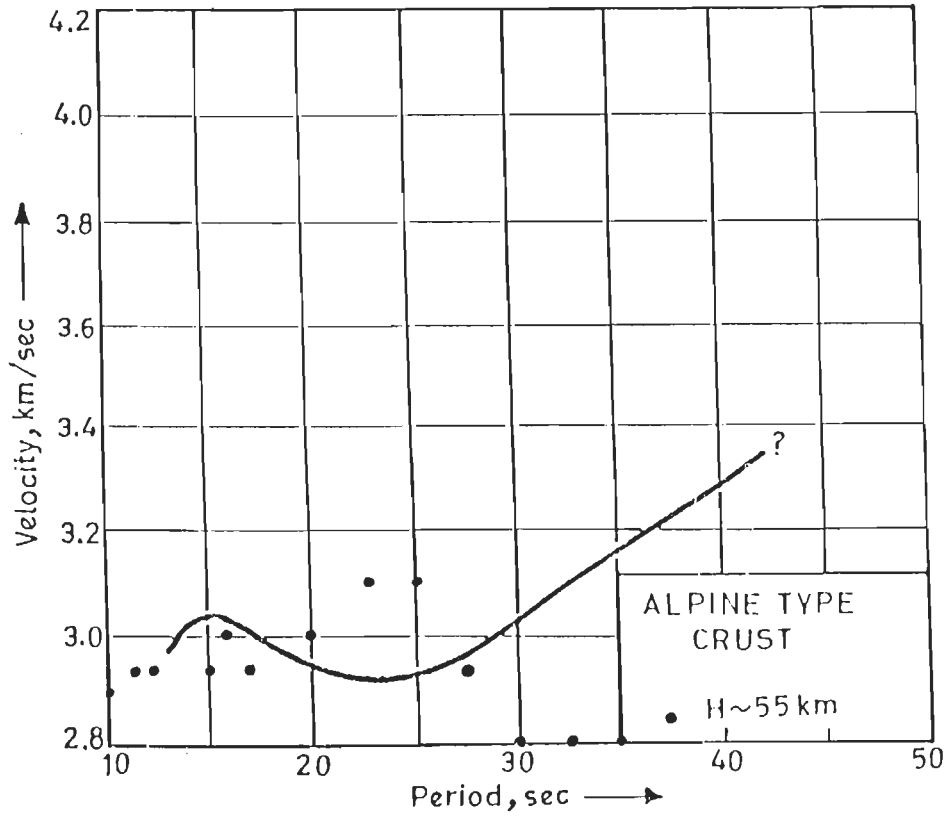


Figure-5.11 Average Group velocity dispersion data of Tibet Region is plotted over average dispersion curve for Alpine type of Crust (After Brune, 1969)

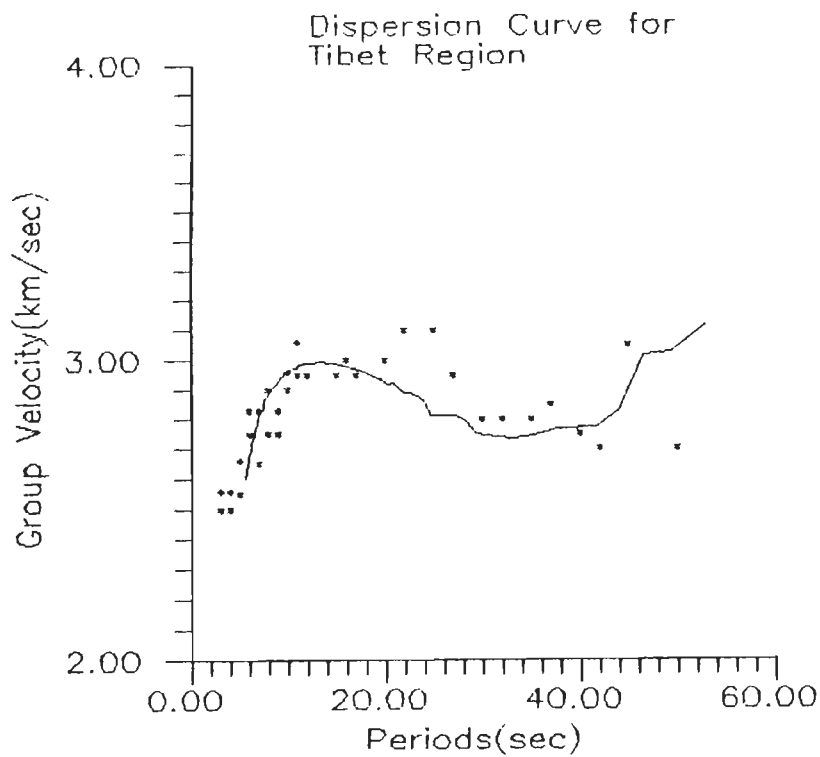
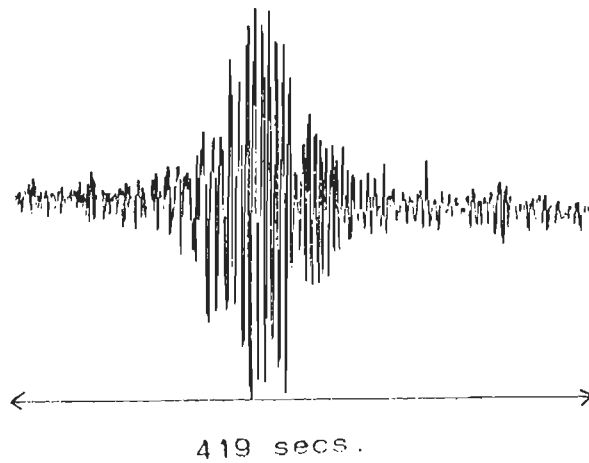


Figure-5.12 (a) The seismogram for Tibet Region earthyquake of October, 31 1982, for 419 sec. duration. (b) Average Group velocity dispersion curve for Tibet Region. * represents the observed data and solid line represents the theoretical model.

REGION - 3
MODEL FOR TIBET REGION

LAYER NO.	P-WAVE VELOCITY Km/sec.	S-WAVE VELOCITY Km/sec.	DENSITY gm/c.c.	THICKNESS Km.
1.	4.411	2.55	2.41	03.75
2.	6.055	3.50	2.70	16.25
3.	5.800	3.37	2.75	20.00
4.	6.300	3.64	2.90	25.00
5.	7.780	4.50	3.30	-

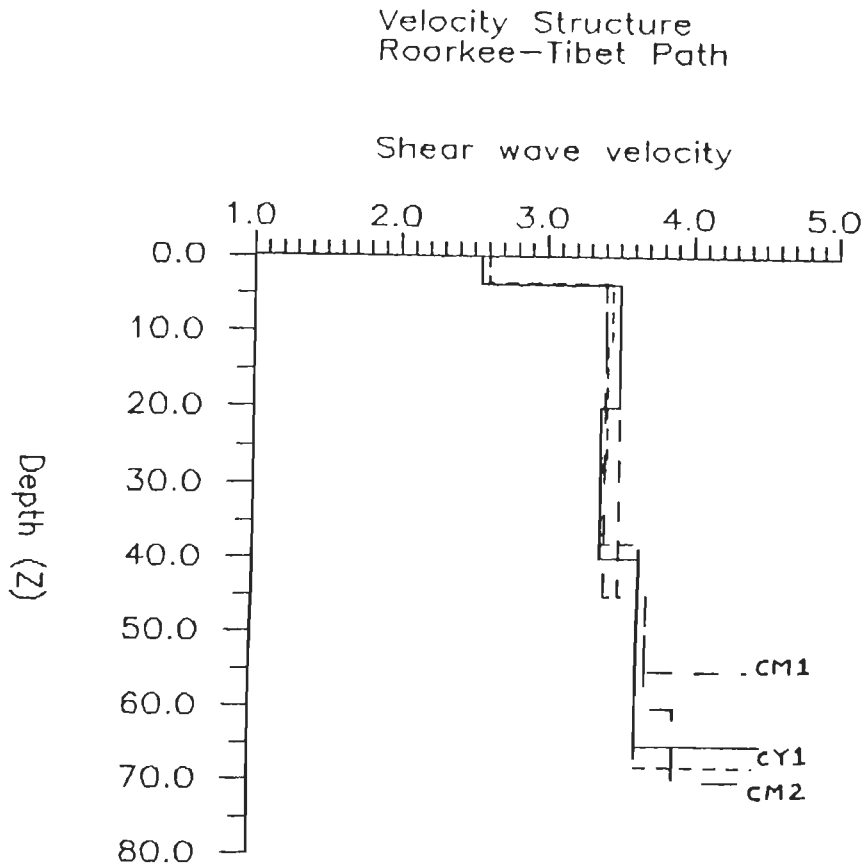


Figure-5.13 Proposed shear velocity model for Tibet Region. Complete model for this region is shown in the upper part of the figure. Dashed lines show the velocity models given by Chen and Molnar(1981) and Chun and Yoshii(1977). CM1 corresponds to 55 km crust, CM2 corresponds to 70 km crust while CY1 is for 68 km crust.

by Romanowicz(1982) and Chun and McEvelly(1986). The crustal model has been found in the present study for the mixed paths whereas Chun and McEvelly used 100% pure paths in their study. Various mechanisms have been put forward by different workers to explain the presence of low velocity zone e.g., partial melting in the lower crust, high pore water pressure, dehydration of hydrated minerals in the crustal rocks, etc. The presence of a very low resistivity zone in the depth range of 20-30 km has been suggested on the basis of magnetotelluric studies(Van Ngol et al.,1984, Yuan et al., 1984) in south Tibet. This low resistivity zone falls in the depth range of the low velocity zone found in the model arrived at in this study.

5.2.4 AFGHANISTAN REGION

This region does not seem to have received much attention from seismologists. The importance of this region cannot be underestimated because it is an important seismic zone representing last phase of collision between Eurasia and India.

Of the four events which have been selected from this region, two have originated at the border region of Afghanistan and former Soviet Republics, one in Tadzhikstan and one in Kirghizstan. The epicentral distances of these events from Roorkee range from about 925 km to 1200 km (Figure 5.14). Their surface wave magnitudes lie in the range 4.2 to 5.6. The combined dispersion data is shown plotted over the average mid continent type crust in Figure 5.15 and on Alpine type crust in Figure 5.16. Observed group velocities lie between 2.6 km/s to 3.0 km/s and they indicate affinity with continental type of crust for periods shorter than 20 seconds and to Alpine type crust for longer periods.

To interpret the observed dispersion data, the crustal structure for Tibet as

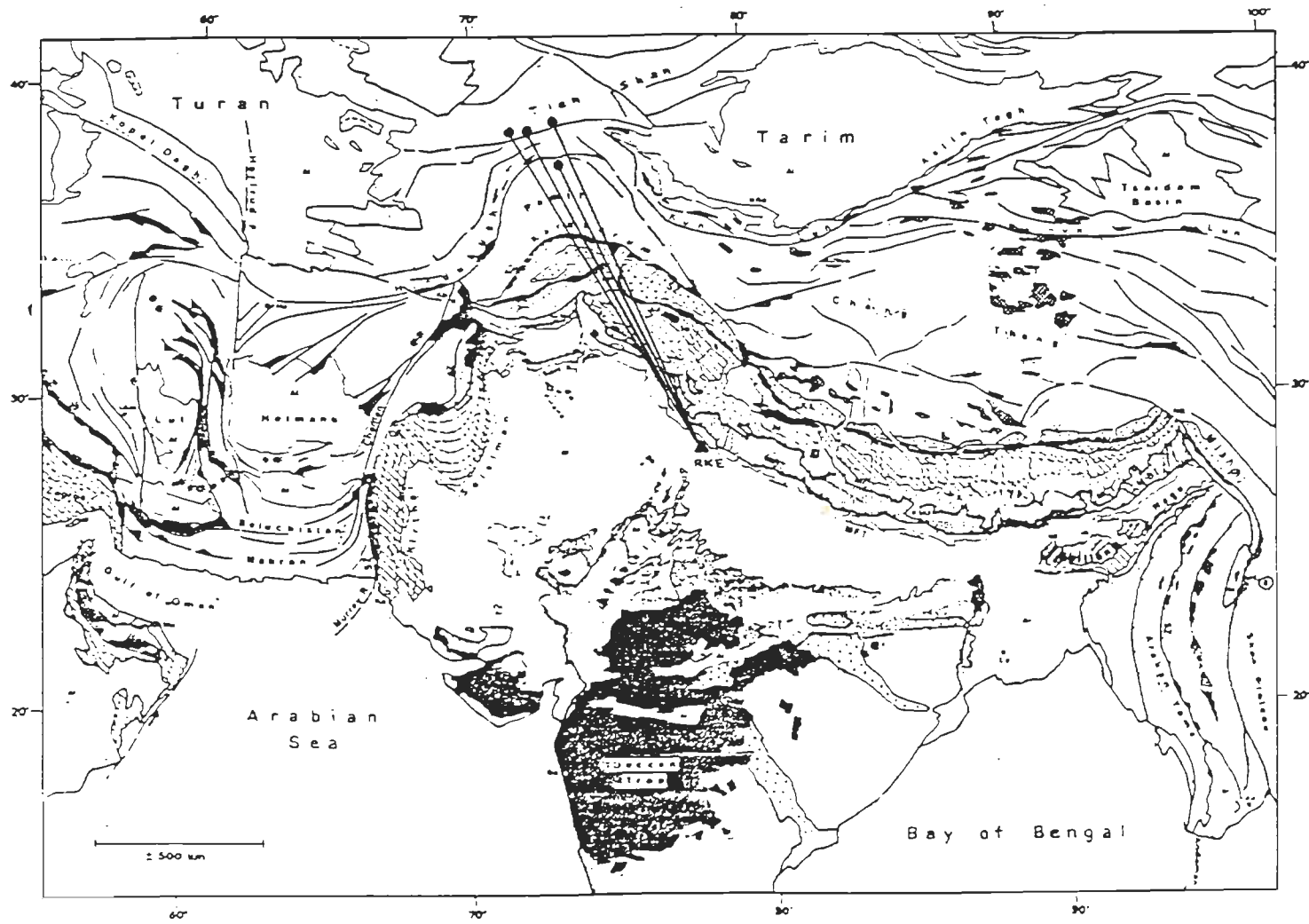


Figure-5.14 Wave path for Rayleigh waves in Afghanistan region.(Map modified after (Gansser, 1993)

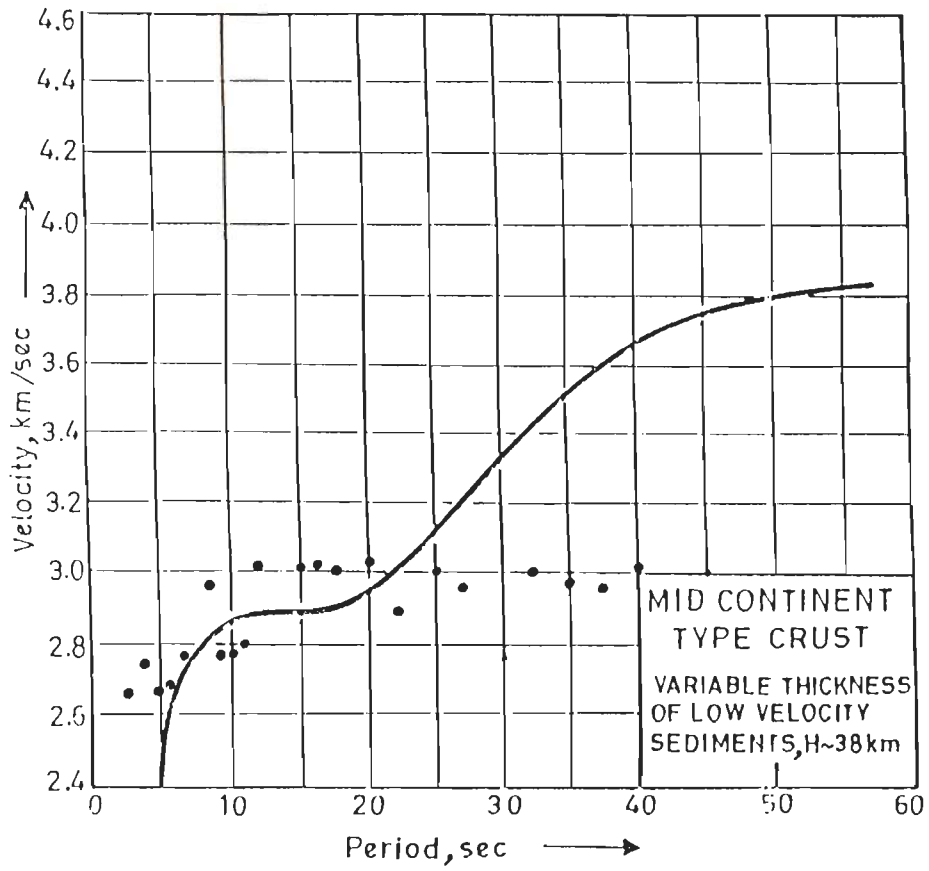


Figure-5.15 Average Group velocity dispersion data of Afghanistan Region is plotted over average dispersion curve for Mid Continental type of Crust (After Brune, 1969)

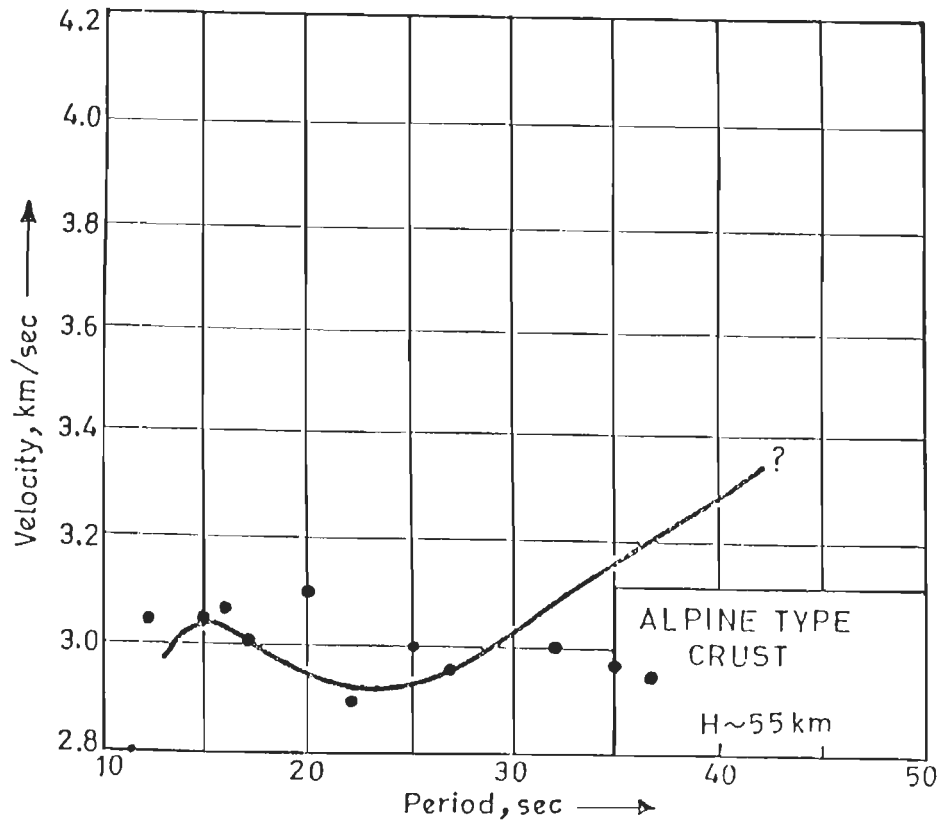


Figure-5.16 Average Group velocity dispersion data of Afghanistan Region is plotted over average dispersion curve for Alpine type of Crust(After Brune, 1969)

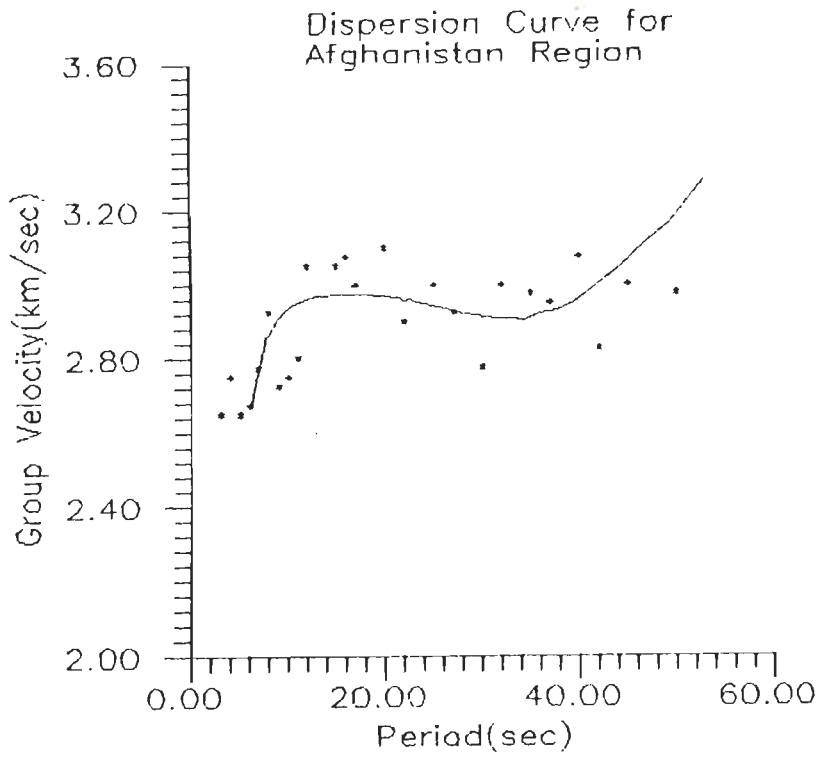
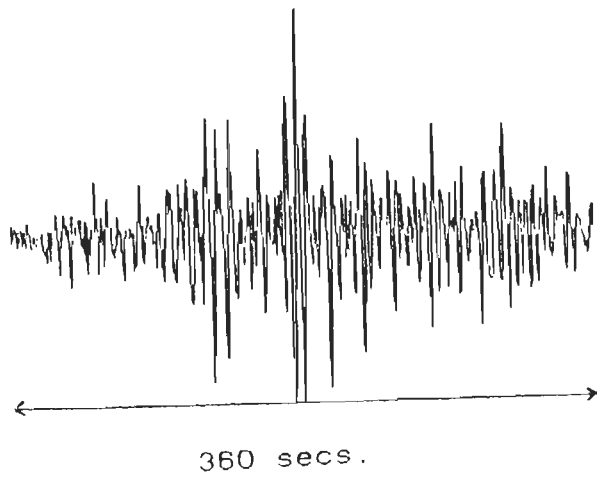


Figure-5.17 (a) The seismogram for Afghanistan- Tadzhakistan Border region earthquake of February, 27 1983, for 360 sec. duration. (b) Group velocity dispersion curve for Afghanistan Region . * represents the observed data and solid line represents the theoretical model.

REGION - 4
MODEL FOR AFGHANISTAN REGION

LAYER NO.	P-WAVE VELOCITY Km/sec.	S-WAVE VELOCITY Km/sec.	DENSITY gm/c.c.	THICKNESS Km.
1.	4.411	2.550	2.41	04.00
2.	6.140	3.550	2.75	27.00
3.	6.410	3.747	3.00	35.00
4.	8.080	4.630	3.30	-

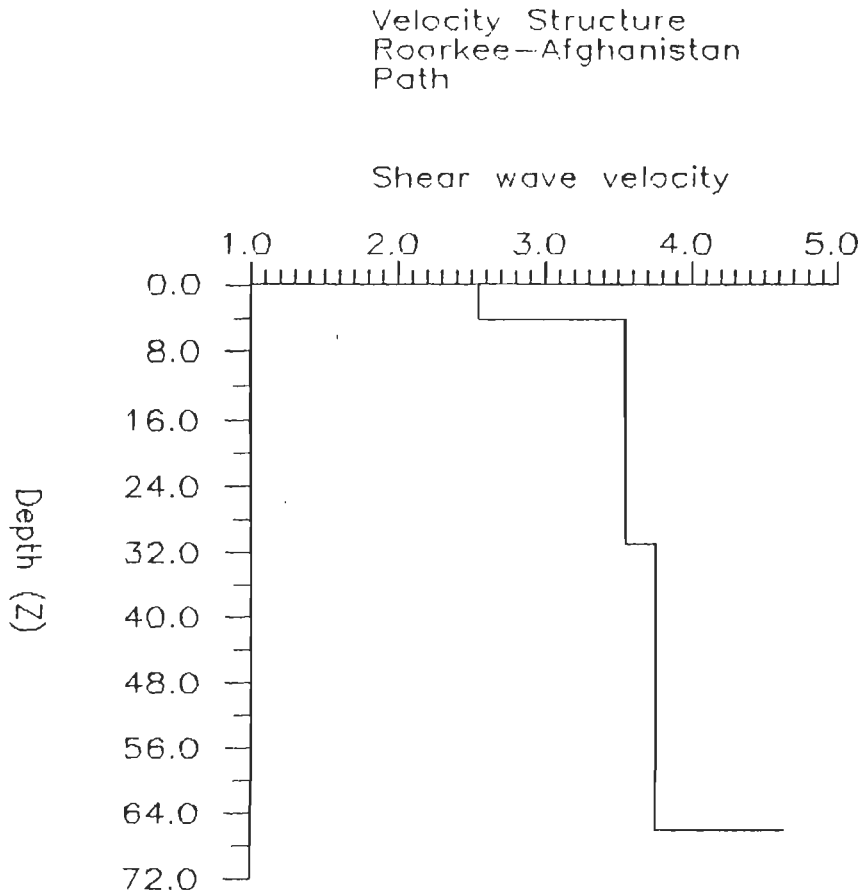


Figure-5.18 Proposed shear velocity model for Afghanistan Region. Complete model for this region is shown in the upper part of the figure.

determined in this study was taken as the starting model. The dispersion curve for the final crustal model is shown in Figure 5.17 and the model itself is given in Figure 5.18. A three layer crust is obtained with a total thickness of 66 km and a 4 km thick sedimentary layer at the top. The P-wave velocity in the upper mantle is found to be 8.08 km/s which is quite close to that found under continental type crust. The model represents the average crustal structure of over the path crossing different mountainous regions, which have undergone intense tectonic activity.

5.2.5 HINDUKUSH REGION

Hindukush region is a very well known seismic region of the world characterised by many earthquakes in the intermediate depth range.

Rayleigh wave records of five earthquakes have been analysed from this region one of which falls in the territory of Tadzhakistan, and the rest in Afghanistan. The epicentral distance are in the range 1065 to 1283 km. The paths of Rayleigh waves cross regions of different tectonic activity (Figure 5.19). The combined dispersion data are plotted over average group velocity dispersion curves for mid-continental crust (Figure 5.20) and for Alpine crust (Figure 5.21). The observed group velocity is seen to be less than 3 km/sec for periods upto 40 seconds beyond which an increase is observed. The low group velocities indicate low shear wave velocities in the crust. It is seen that the observed dispersion data compares better with Alpine type crust than for mid continental type crust.

No previous study of crustal structure in this region has been done which makes use of surface wave dispersion. Rucker (1982) investigated the crustal and upper mantle crustal structures in this region based on microearthquake investigations

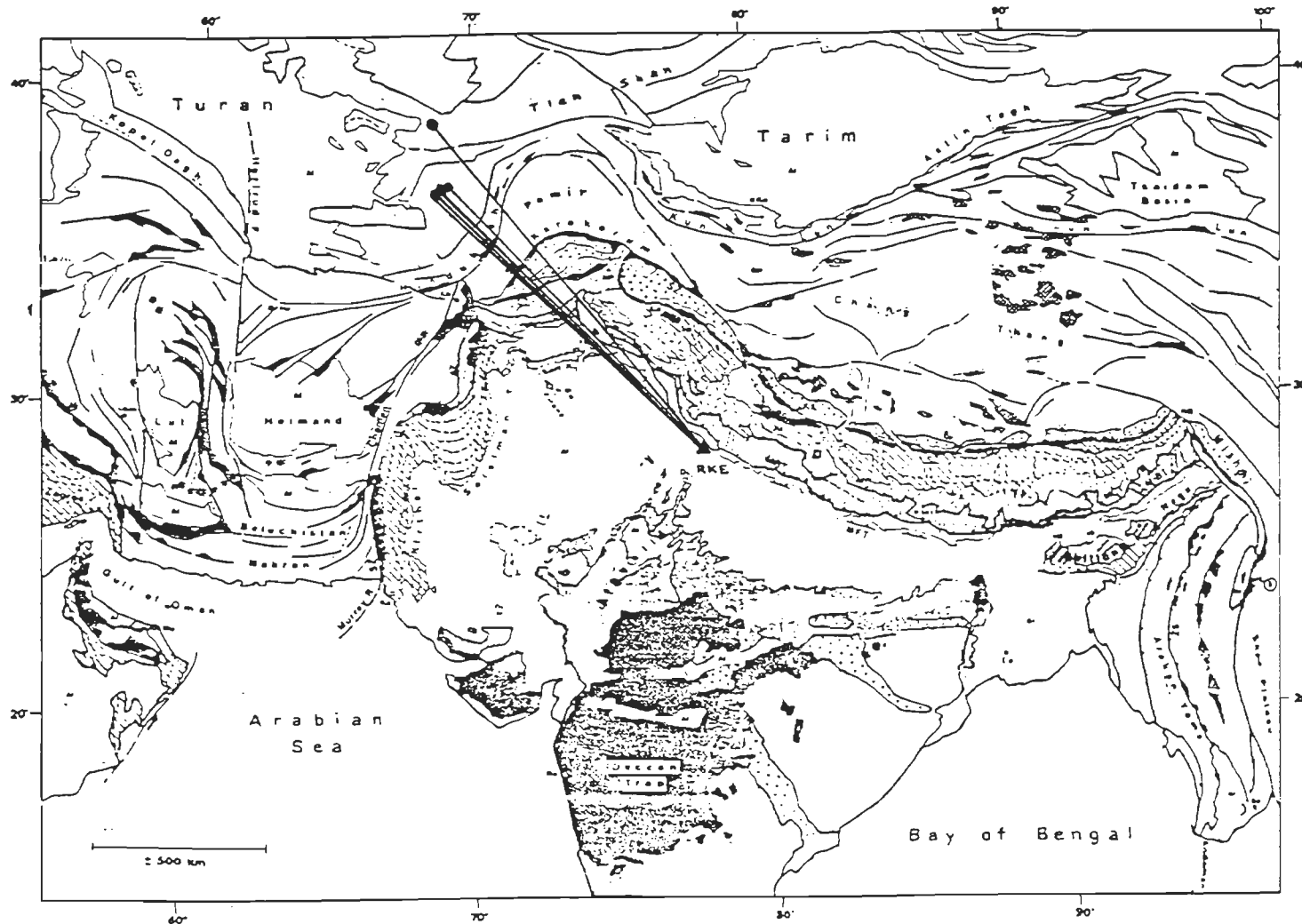


Figure-5.19 Wave path for Rayleigh waves in Hindukush region. (Map modified after (Gansser, 1993))

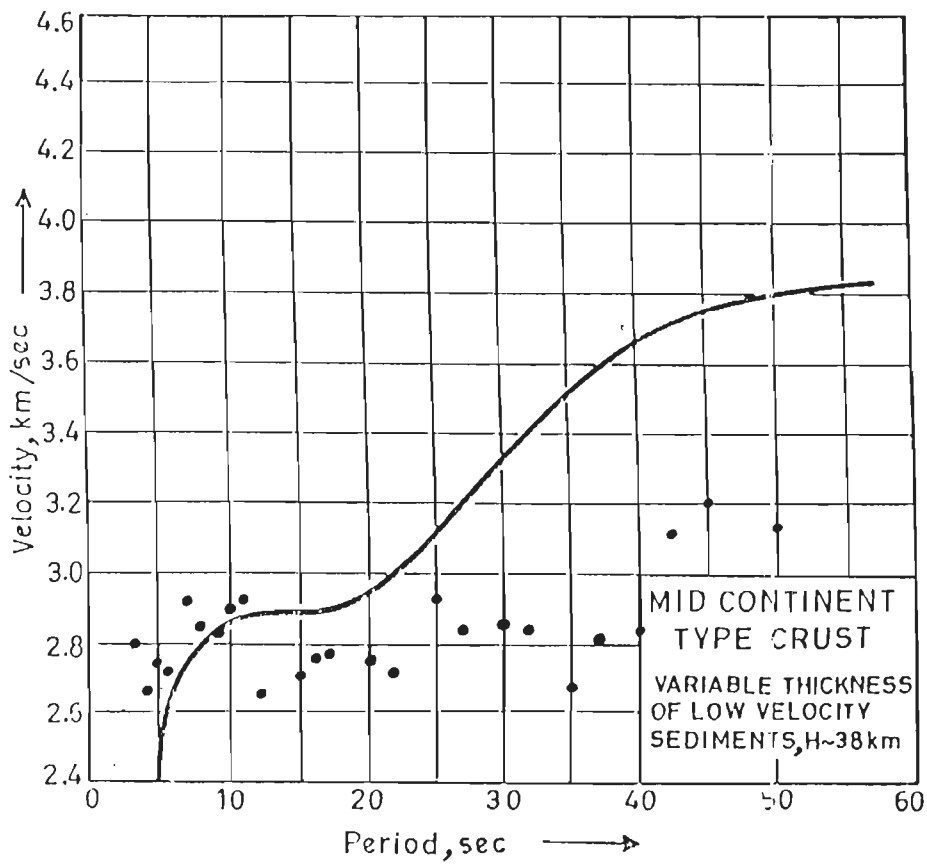


Figure-5.20 Average Group velocity dispersion data of Hindukush Region is plotted over average dispersion curve for Mid Continental type of Crust (After Brune, 1969)

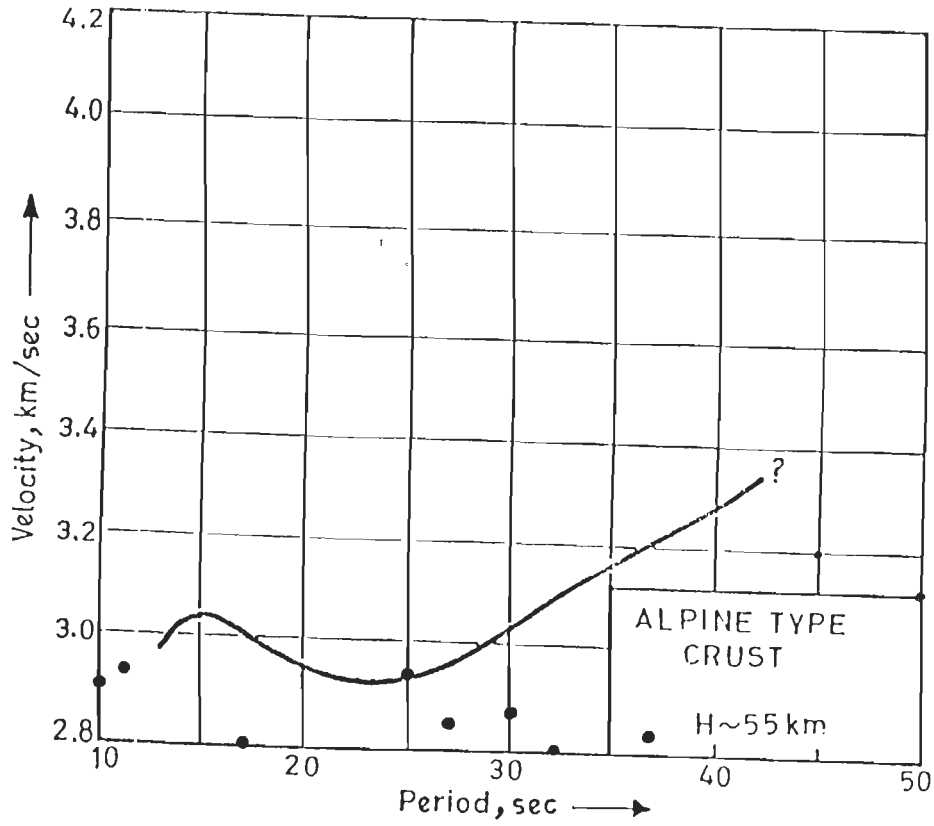


Figure-5.21 Average Group velocity dispersion data of Hindukush Region is plotted over average dispersion curve for Alpine type of Crust (After Brune, 1969)

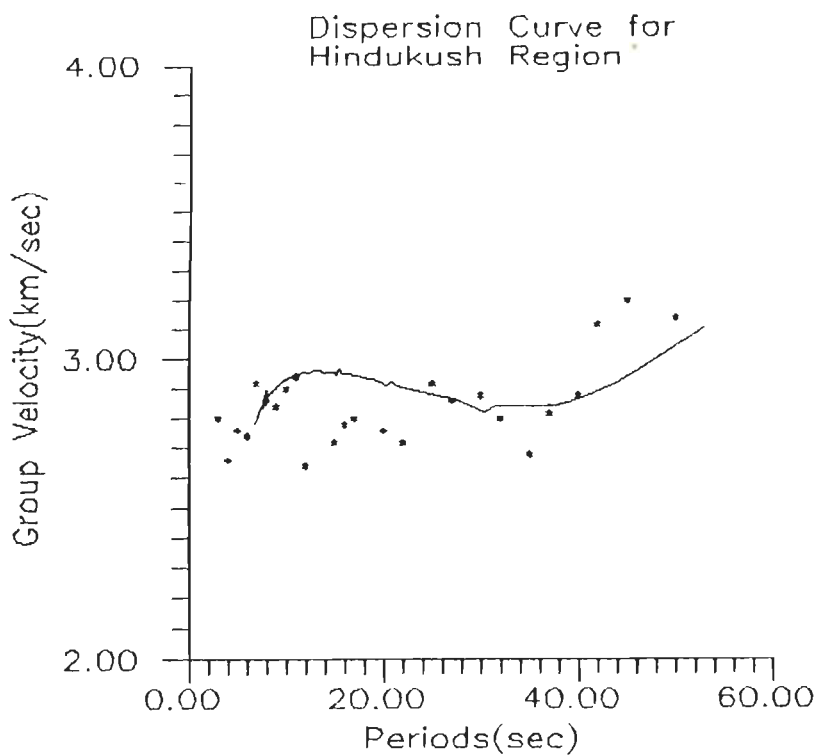
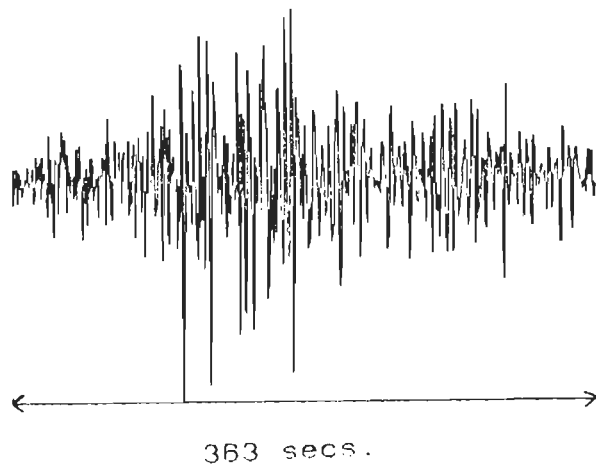


Figure-5.22 (a) The seismogram for Hindukush Region earthquake of July, 03 1984, for 363 sec. duration. (b) Group velocity dispersion curve for Hindukush Region * represents the observed data and solid line represents the theoretical model.

REGION - 5
MODEL FOR HINDUKUSH REGION

LAYER NO.	P-WAVE VELOCITY Km/sec.	S-WAVE VELOCITY Km/sec.	DENSITY gm/c.c.	THICKNESS Km.
1.	4.411	2.55	2.41	03.75
2.	5.930	3.48	2.80	27.00
3.	5.800	3.37	2.75	06.00
4.	6.410	3.71	3.10	35.00
5.	7.900	4.56	3.30	-

Velocity Structure
Roorkee-Hindukush Path

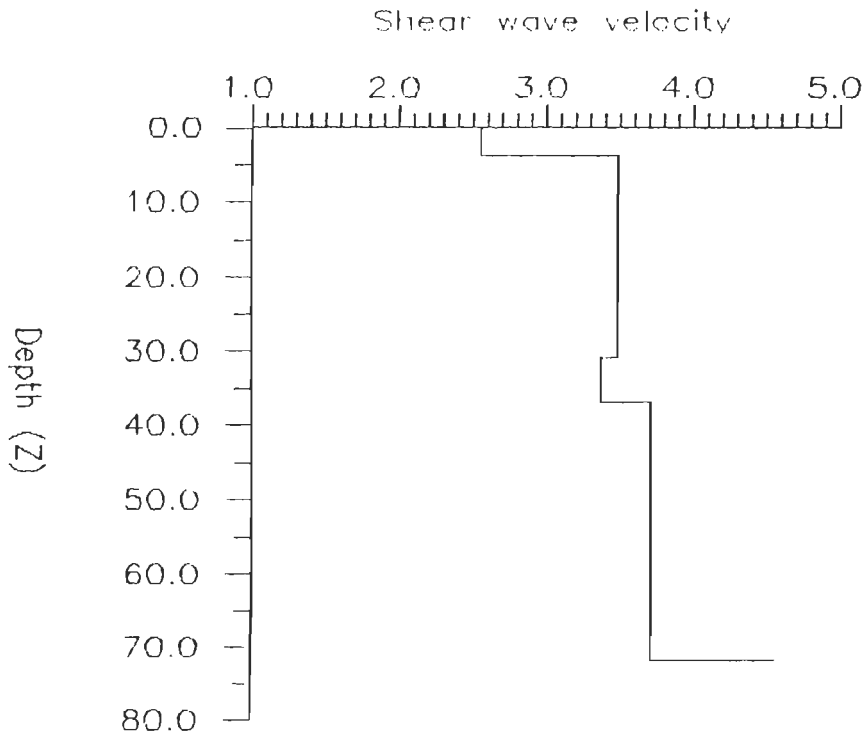


Figure-5.23 Proposed shear velocity model for Hindukush Region. Complete model for this region is shown in the upper part of the figure.

and proposed a two layered crustal structure. In the present study a four layered crustal model with a total thickness of 72 km and a near surface low velocity layer is proposed based on interpretation of Rayleigh wave dispersion data. The theoretical curve fitting the dispersion data is shown in Figure 5.22 and the model is given in Figure 5.23. A six km thick low velocity layer at a depth of about 31 km has also been found. The presence of such a thin low velocity layer was speculated by Røcker(1982). The upper mantle compressional wave velocity of 7.9 km/s is compares quite favourably with 8 km/s under the Alpine type crust.

5.2.6 IRAN REGION

Two earthquakes with their epicentres in Iran have been used in the present study. One of these earthquakes occurred in southern Iran and has its epicentre at a distance of 2123 km. The other earthquake occurred in western Iran at an epicentral distance of 2666 km. The two earthquakes had surface wave magnitudes of 5.7 and 5.8 and their depth of foci was 32.9 km and 25 km respectively. Since the difference in the paths is not much when these enter Afghanistan and then Indian subcontinent, both paths are considered coincident (Figure 5.24). The group velocity data when plotted over dispersion curve for the average mid-continental type crust as shown in Figure 5.25 reveals that the group velocities over this path which vary from 2.5 km/s to 3.2 km/s are substantially lower than the group velocities for the average continental structure over periods longer than 10 seconds. According to Brune the thickness of the crust in the Alpine region is of the order of 45 to 55 km. In the present case the thickness of crust is found to be about 46 km with a three km thick sedimentary layer at the top. The theoretical curve fitting the dispersion data is shown in Figure 5.26 and the model is shown in Figure 5.27. The upper mantle P-wave velocity of 7.7 km/s is substantially lower than that

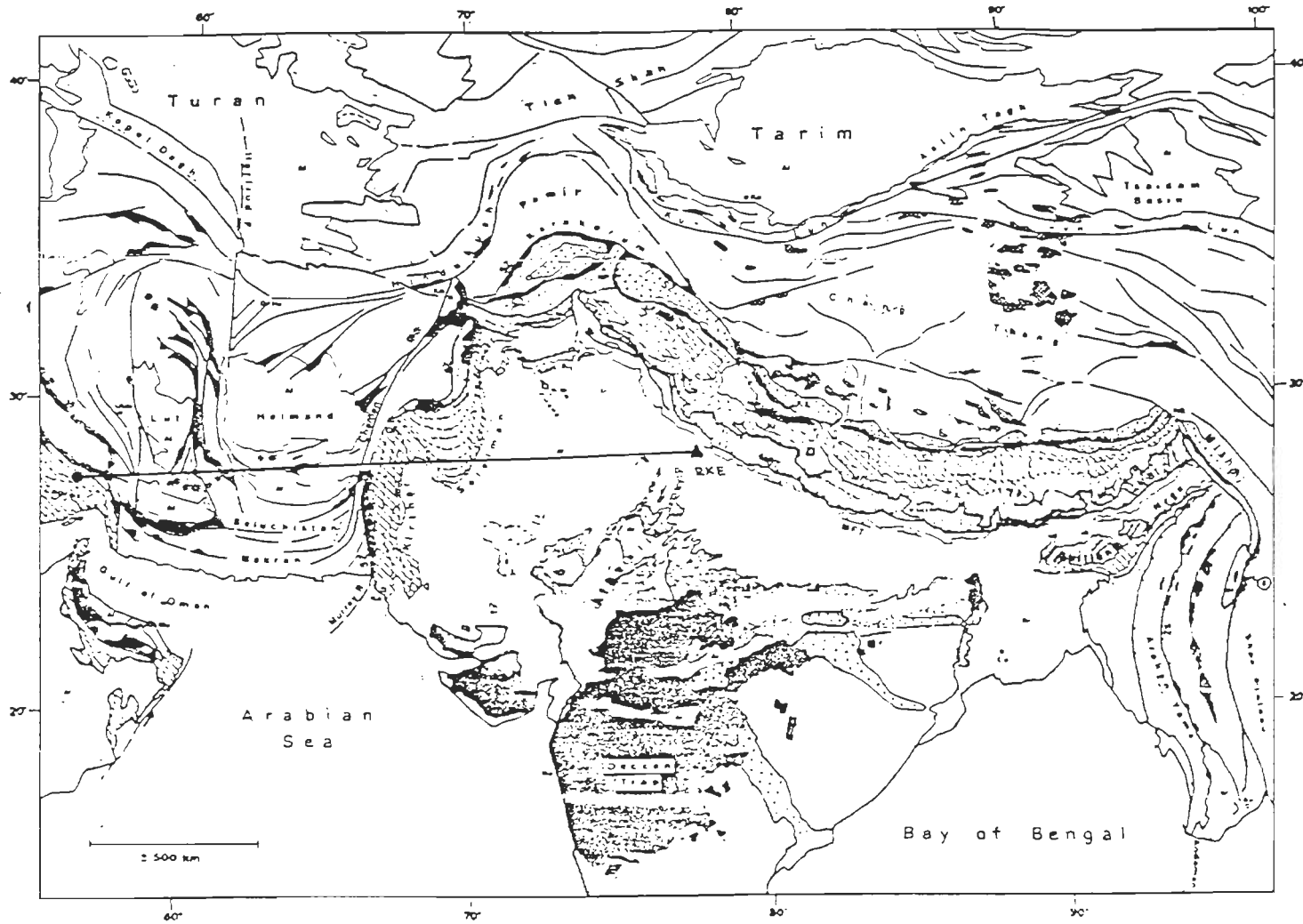


Figure-5.24 Wave path for Rayleigh waves in Iran region.(Map modified after (Gansser, 1993)

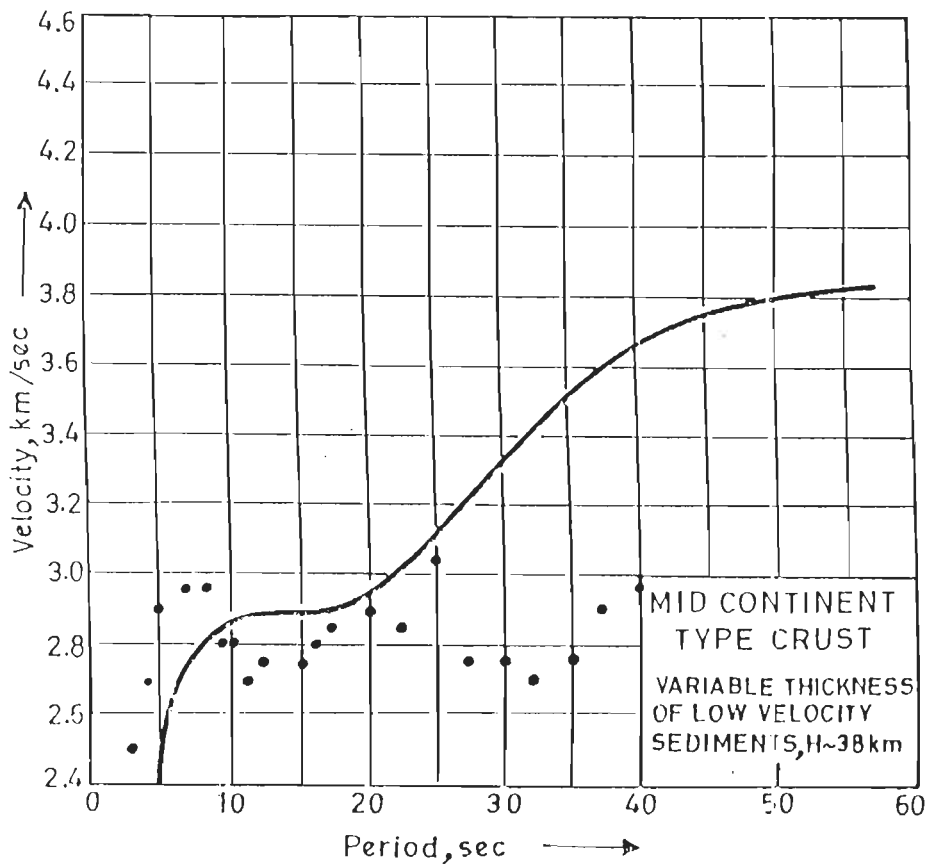


Figure-5.25 Average Group velocity dispersion data of Iran Region is plotted over average dispersion curve for Mid Continental type of Crust (After Brune, 1969)

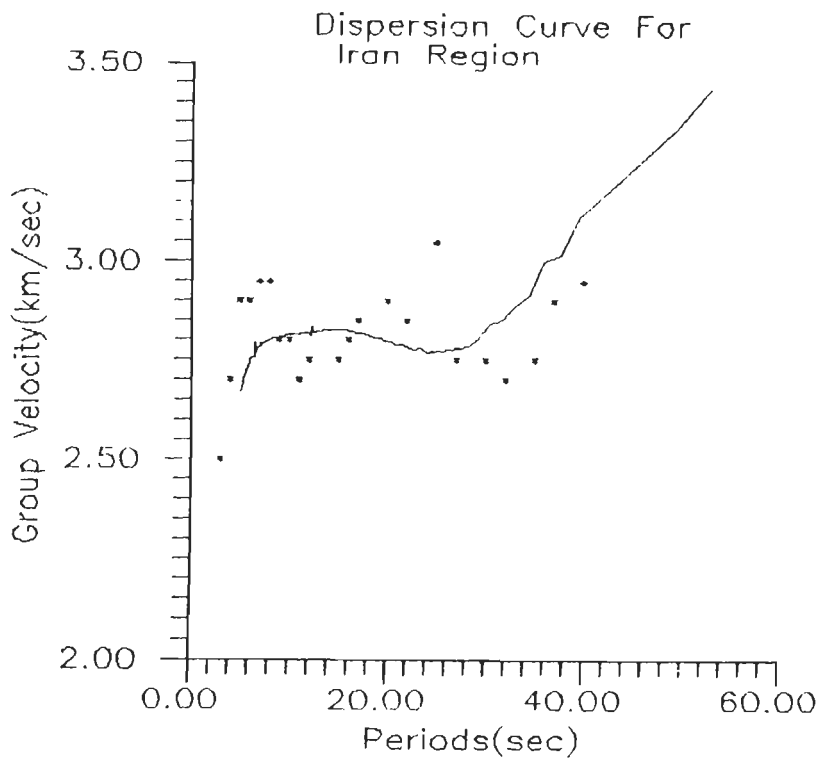
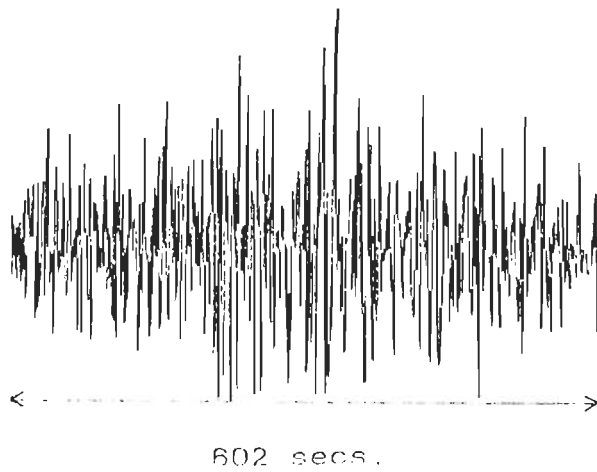


Figure-5.26 (a) The seismogram for Iran earthquake of July, 12 1983, for 602 sec. duration. (b) Group velocity dispersion curve for Iran Region. * represents the observed data and solid line represents the theoretical model.

REGION - 6
MODEL FOR IRAN REGION

LAYER NO.	P-WAVE VELOCITY Km/sec.	S-WAVE VELOCITY Km/sec.	DENSITY gm/c.c.	THICKNESS Km.
1.	4.411	2.55	2.41	03.00
2.	5.700	3.31	2.90	15.00
3.	6.100	3.56	2.90	28.00
4.	7.700	4.35	3.30	-

Velocity Structure
Roorkee-Iran Path

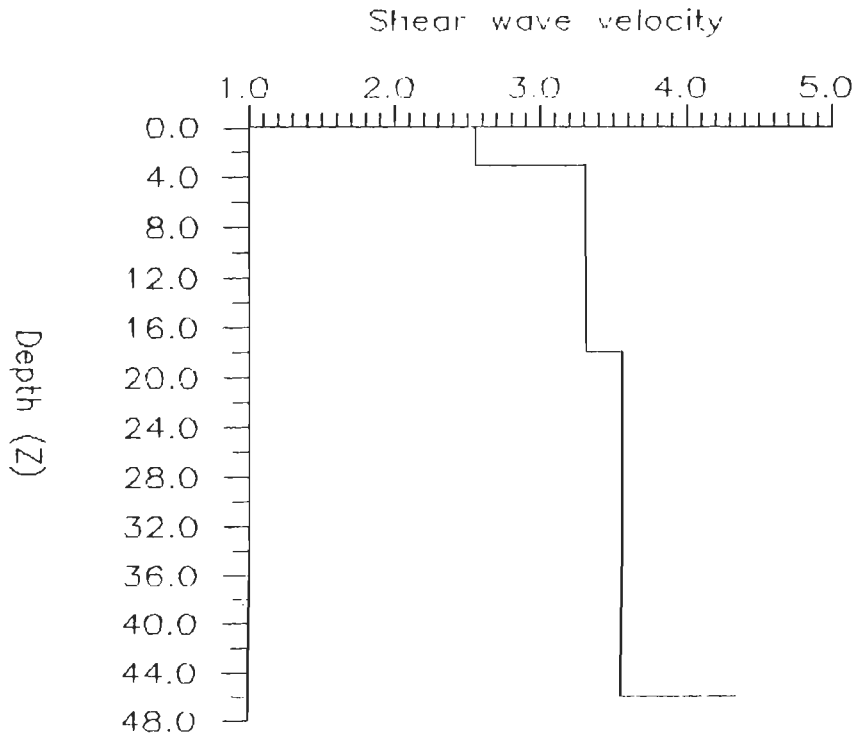


Figure-5.27 Proposed shear velocity model for Iran Region. Complete model for this region is shown in the upper part of the figure.

under typical continental crust.

5.3 COMMENTS

The crustal models derived from observed dispersion data presented above for all regions are for mixed paths between the source and Roorkee. A low velocity layer, at the top, of varying thickness but not more than 5 km is found in all models. The velocity structures derived are neither typically continental nor Alpine but incorporate features of both. In regions of intense tectonic activity the dispersion data come closer to continental type crusts at short periods (periods less than 20 seconds). At longer periods however the group velocities become substantially lower indicating lower velocities in the lower crust and upper mantle. The present study is based on dispersion data for 18 earthquakes which accounts for approximate nature of interpretations. The results obtained indicate some interesting features indicated above.

The interpretations given above apply to the total path between the epicentral regions of the earthquakes investigated and Roorkee. The paths of Rayleigh waves traverse regions of widely varying crustal types with both vertical and lateral inhomogeneities and intense deformation due to prolonged tectonic activity. Thus the interpretations depict varying degrees of approximation which also explains in part the observed scatter.

CHAPTER - 6

CONCLUSIONS

On the basis of the analysis of group velocity dispersion data of 18 earthquakes recorded at the Wide Band Seismological Observatory, Department of Earth Sciences, University of Roorkee, Roorkee which have been presented and discussed in previous chapters, following conclusions have emerged:

- (1) The crustal velocity models derived for mixed paths in the six regions are neither typical continental nor Alpine in the sense of crustal models of Brune(1969).
- (2) The crustal structure in the Afghanistan, Tibet and China regions are quite similar in that they approach continental type for periods shorter than 20 seconds. The same is the case with Iran region. For Hindukush region this feature is observed for periods shorter than 10 seconds. At longer periods the group velocities are lower and approach Alpine crustal types.
- (3) In East Ganga Basin, the observed data show departures from continental type crust at all periods.
- (4) A low velocity layer at the top is found for all crustal models. Its thickness varies from 3.75 km to 5 km and the shear wave velocity from 2.3 km/s to 2.55 km/s in most cases. This top layer is most probably sedimentary in character.
- (5) Low velocity layers in the crust are found for China and Tibet regions. A thin low velocity layer has been found for Hindukush region. This is due to the

appearance of short period Rayleigh waves on seismograms of Wide Band Observatory and establishes the usefulness of these records for refining crustal models at shallow depth.

(6) The crustal thicknesses found in the present work compare favourably well with those found by other workers for all six regions.

(7) The upper mantle P and S-wave velocities immediately below Moho are less than those for continental type of crust in all regions.

(8) The theoretical dispersion curves derived for the crustal models have total absolute error less than 9.8 % and the degree of goodness of fit with observed dispersion data is better than 67.8 % .

(9) The present study establishes the superiority of Multiple Filter Technique in unravelling the fine structure in observed dispersion data especially in the short period range.

Limitations

The study presented herein is by no means exhaustive because not many earthquakes could be found with good quality recording of dispersion data. Paucity of data is also the reason for not attempting formal inversion of observed data. The interpretations obtained apply for mixed paths and observed scatter in data is due to vertical inhomogeneities in crustal structure as well as different types of crustal structure in the path of propagation.

APPENDIX - I

(A)

The elements of the matrix $F^{(*)}$ and $F^{(**)}$ are given below in detail form (Schwab,1970);

$$F^{(*)} = \begin{bmatrix} (m) & (m) & (m) & (m) & (m) & (m) \\ F1212 & F1213 & F1214 & F1223 & F1224 & F1234 \\ F1312 & F1313 & F1314 & F1323 & F1324 & F1334 \\ F1412 & F1413 & F1414 & F1423 & F1424 & F1434 \\ F2312 & F2313 & F2314 & F2323 & F2314 & F2334 \\ F2412 & F2413 & F2414 & F2423 & F2414 & F2434 \\ F3412 & F3413 & F3414 & F3423 & F3424 & F3434 \end{bmatrix}$$

$$F^{(**)} = \begin{bmatrix} (m) & (m) & (m) & (m) & (m) & (m) \\ F3434 & -F3424 & F3423 & F3414 & -F4313 & F3412 \\ -F2434 & F2424 & -F2423 & -F2414 & F2413 & -F2412 \\ F2334 & -F2324 & F2323 & F2314 & -F2313 & F2312 \\ F1434 & -F1424 & F1423 & F1414 & -F1413 & F1412 \\ -F1334 & F1324 & -F1323 & -F1314 & F1313 & -F1312 \\ F1234 & -F1224 & F1223 & F1214 & -F1213 & F1212 \end{bmatrix}$$

APPENDIX - I

(B)

The elements of $T^{(4)}$ are obtained from $\wedge_{(4)}$, using following relations (Schwab, 1970):

$$T_{11}^{(4)} = \wedge_{11(4)} \wedge_{22(4)} - \wedge_{21(4)} \wedge_{12(4)}$$

$$T_{12}^{(4)} = \wedge_{11(4)} \wedge_{23(4)} - \wedge_{21(4)} \wedge_{13(4)}$$

$$T_{13}^{(4)} = \wedge_{11(4)} \wedge_{24(4)} - \wedge_{21(4)} \wedge_{14(4)}$$

$$T_{14}^{(4)} = \wedge_{12(4)} \wedge_{23(4)} - \wedge_{22(4)} \wedge_{13(4)}$$

$$T_{15}^{(4)} = \wedge_{12(4)} \wedge_{24(4)} - \wedge_{22(4)} \wedge_{14(4)}$$

$$T_{16}^{(4)} = \wedge_{13(4)} \wedge_{24(4)} - \wedge_{23(4)} \wedge_{14(4)}$$

Thus

$$T^{(4)} = [1, -q, 0, 0, 0, 0]$$

APPENDIX - I

(C)

The full form of H1 and H2 are given below as discussed by Schwab(1970).

$$\begin{array}{l}
 \text{H1} \\
 \left[\begin{array}{l}
 \begin{array}{ll}
 (n-1) & (n-1) \\
 \text{F1212} & - \text{F3412}
 \end{array} \\
 (n-1) \\
 - \text{Im}(\text{F1312}) \\
 (n-1) \\
 \text{F1412} \\
 (n-1) \\
 \text{F2312} \\
 (n-1) \\
 - \text{Im}(\text{F2412})
 \end{array} \right]
 \end{array}$$

$$\begin{array}{l}
 \text{H2} \\
 \left[\begin{array}{l}
 \begin{array}{ll}
 (n-1) & (n-1) \\
 \text{F3412} & - \text{F3412}
 \end{array} \\
 (n-1) \\
 \text{Im}(\text{F2412}) \\
 (n-1) \\
 \text{F2312} \\
 (n-1) \\
 \text{F1412} \\
 (n-1) \\
 \text{Im}(\text{F1312})
 \end{array} \right]
 \end{array}$$

The complete expression for the quantities $F^{(m)}(ijkl)$ for $1 < m < n-2$ are given in the table below.

TABLE
Expressions for the quantities F_{ijkl}

kl	12	13	14	23	24	34
ij						
12	$-e_8(m)$	0	$e_{13}(m)$	$e_6(m)$	0	$e_{10}(m)$
13	$-i(e_{11}z_9 + e_7z_{10})$	$e_{15}z_{14}$	$i(e_{14}z_9 + e_{12}z_{10})$	$i(e_9z_9 + e_5z_{10})$	$-e_{15}z_7$	$i(e_{11}z_9 + e_7z_{10})$
14	$e_{11}z_7 - e_7z_{12}$	$i(e_{15}z_{10})$	$-e_{14}z_7 + e_{12}z_{12}$	$-e_9z_7 + e_5z_{12}$	$i(e_{15}z_8)$	$-e_{11}z_7 + e_7z_{12}$
23	$-e_{11}z_{15} + e_7z_7$	$i(e_{15}z_9)$	$e_{14}z_{15} - e_{12}z_7$	$e_9z_{15} - e_5z_7$	$i(e_{15}z_{11})$	$e_{11}z_{15} - e_7z_7$
24	$-i(e_{11}z_{11} + e_7z_8)$	$-e_{15}z_7$	$i(e_{14}z_{11} + e_{12}z_8)$	$i(e_9z_{11} + e_5z_8)$	$e_{15}z_{13}$	$i(e_{11}z_{11} + e_7z_8)$
34	e_{10}	0	$-e_{13}$	$-e_6$	0	$-e_8$

$e_0(m) = p_{m+1}/p_m$	$e_8(m) = e_1(m)e_4(m)$	$z_1(m) = \cos P_m$	$z_9(m) = z_1(m)z_6(m)$
$e_1 = Y_m - e_0 Y_{m+1}$	$e_9 = e_2 z_2$	$z_2 = \cos Q_m$	$z_{10} = z_2 z_3$
$e_2 = e_1 - 1$	$e_{10} = e_2 e_3$	$z_3 = r_{Lm} \sin P_m$	$z_{11} = z_2 z_4$
$e_3 = e_1 + e_0$	$e_{11} = e_2 e_4$	$z_4 = \sin P_m / r_{Lm}$	$z_{12} = z_3 z_5$
$e_4 = e_2 + e_0$	$e_{12} = e_3 z_2$	$z_5 = r_{Bm} \sin Q_m$	$z_{13} = z_4 z_5$
$e_5 = e_{12}$	$e_{13} = e_3 e_4$	$z_6 = \sin Q_m / r_{Bm}$	$z_{14} = z_3 z_6$
$e_6 = e_1 e_2$	$e_{14} = e_4 z_2$	$z_7 = z_1 z_2$	$z_{15} = z_4 z_6$
$e_7 = e_1 e_3$	$e_{15} = -e_0$	$z_8 = z_1 z_5$	
	$e_{16} = e_8 + e_{10}$		

APPENDIX - I

(D)

The elements of the matrix $T_{i,j}$ are given here in complete form Schwab(1970).

For $m + 1$ even

$$\begin{aligned}
 U &= e_{16} U + e_{11} K + e_7 L \\
 V &= e_{15} (z_{14} V + z_{10} W + z_9 R - z_7 S) \\
 W &= -e_{14} K - e_{12} L + 2e_{13} U \\
 R &= -e_9 K - e_5 L + 2e_6 U
 \end{aligned}$$

where

$$\begin{aligned}
 K &= z_9 V + z_7 W - z_{15} R + z_{11} S \\
 L &= z_{10} V - z_{12} W + z_7 R + z_8 S
 \end{aligned}$$

and for $m+1$ odd,

$$\begin{aligned}
 U &= -e_{16} U + e_{11} X + e_7 Z \\
 V &= e_{15} (z_{13} V - z_{11} W - z_8 R - z_7 S) \\
 W &= e_9 X + e_5 Z - 2e_6 U \\
 R &= e_{14} X + e_{12} Z - 2e_{13} U
 \end{aligned}$$

where

$$\begin{aligned}
 X &= z_{11} V + z_{15} W - z_7 R + z_9 S \\
 Z &= z_8 V - z_7 W + z_{12} R + z_{10} S
 \end{aligned}$$

REFERENCES

01. Aki, K. and P. G. Richards,(1980). Quantitative Seismology, W. H. Freeman and Company, San Francisco. Vol. I.
02. Bath, M.,(1974). Spectral analysis in Geophysics, Elsevier Scientific Publishing Company. Amsterdam-Oxford-NewYork. 563p.
03. Bhattacharya, S.N.,(1971). Seismic surface wave dispersion and crust mantle structure of Indian peninsula. Ind. J. Met. Geoph., 22:179-86.
04. Bhattacharya, S.N.,(1974). The crust mantle structure of the Indian peninsula from surface wave dispersion. G.J.R.A. Soc., 36:273-83.
05. Bhattacharya, S.N.,(1981). Observation and inversion of surface wave group velocities across central India. Bull. Seismol. Soc. Am., 71:1489-1501.
06. Bloch, S. and A. L. Hales,(1968). New techniques for the determination of surface wave phase velocities. Bull. Seismol. Soc. Am., 58:1021-34.
07. Bloch, S.,A. L. Hales and M. Landisman,(1969). Velocities in the crust and upper mantle of Southern Africa from multi-mode surface wave dispersion. Bull. Seismol. Soc. Am., 59:1599-1629.
08. Brune, J.N., J. E. Nafe and J. Oliver,(1960). A simplified method for the analysis

and synthesis of dispersed wave trains. *J. Geophys. Res.*, 65: 287-304.

09. Brune, J.N.,(1969). Surface waves and crustal structure . Ed. Pembroke J. Hart, Am. Geophysical Union, Washington, D.C. Reprinted from Geophysical Monograph, 13,The Earth Crust and Upper Mantle:230-42.

10. Brune, J.N. and D.D. Singh,(1986). Continent like crustal thickness beneath the Bay of Bengal sediments. *Bull. Seismol. Soc. Am.*, 76:191-203.

11. Bullen, K.E., and Bruce A. Bolt,(1985). An introduction to the theory of seismology. Cambridge University Press, Cambridge, London. 499p.

12. Chander, R., L. E. Alsop and Jack Oliver,(1968). On the synthesis of shear coupled PL waves. *Bull. Seismol. Soc. Am.*, 58:1849-1877.

13. Chatterjee, S.N.,(1971). On the dispersion of Love waves and crust mantle structure in the Gangetic basin. *G,J,R.A. Soc.*, 23: 129-38.

14. Chaudhary, H.M.,(1966). Seismic surface waves dispersion and the crust across the Gangetic basin. *Ind. J. Met. Geoph.*, 17: 385-93.

15. Chaudhary, H.M.,(1967). Sedimentary Rayleigh waves across the Gangetic basin_A preliminary study. *Ind. J. Met. Geoph.*, 18: 273- 78.

16. Chen, W.P. and P. Molnar,(1975). Short period Rayleigh wave dispersion across the Tibetan plateau. *Bull. Seismol. Soc. Am.*, 65:1051-57.

17. Chen, W.P. and P. Molnar,(1981). Constraints on the seismic wave velocity structure beneath the Tibetan plateau and their tectonic implications. J.G.R.,86,N0.B7:5937-62.
18. Chun, K.Y. and T. Yoshii,(1977). Crustal structure of the Tibetan plateau : A surface-wave study by a moving window analysis. Bull. Seismol. Soc. Am., 67:735-50.
19. Chun, K.Y.(1986). Crustal block of the western Ganga basin: A fragment of oceanic affinity? Bull. Seismol. Soc. Am., 76:1687- 98.
20. Chun, K.Y. and T.V. McEvelly,(1986). Crustal structure in Tibet: High seismic velocity in the lower crust. J.G.R.,91, No. B10:10405-411.
21. Dorman, J., M. Ewing and J. Oliver,(1960). Study of shear velocity distribution in the upper mantle by mantle Rayleigh waves. Bull. Seismol. Soc. Am., 50:87-115.
22. Dzicwonski, a., S.Bloch and M. Landisman,(1969). A technique for the analysis of transient seismic signals. Bull. Seismol. Soc. Am., 59:427-44.
23. Dziewonski, A.M. and A. L. Hales,(1972). Numerical analysis of dispersed seismic waves. Methods in Computational Physics, Advances in Research and Applications, Academic Press, 11:39-84.
24. Ewing, W. M., W.S. Jardetzky and Frank Press,(1957). Elastic waves in layered media. McGraw-Hill Book Company,Inc. NewYork Toronto London. 380p.

25. Ewing M., S. Mueller, M. Landisman and Y. Satô,(1959). Transient analysis of earthquake and explosion arrivals. *Geofis. Pura Appl.*, 44:83-118.
26. Gansser, A.,(1993). Facts and theories on the Himalaya. *Jour.of the Geol. Soc. of India.* 41: No.6: 487-508.
27. Goodman,N.R.,(1960).Measuring amplitude and phase, *J. Franklin Inst.*, 260, 437-450 pp
28. Grant, F.S. and G.F. West,(1965). Interpretation theory in applied geophysics. McGraw-Hill Book Co., NewYork. 583p.
29. Gupta, H.K. and H. Narain,(1967). Crustal structure in the Himalayan and the Tibet plateau region from surface wave dispersion. *Bull.Seismol. Soc. Am.*, 57:235-48.
30. Haskell, N.A.,(1953). The dispersion of surface waves on multi-layered media. *Bull. Seismol. Soc. Am.*, 43:17-34.
31. Iyer, H.M.,(1964). A frequency-velocity-energy diagram for the study of dispersive surface waves. *Bull. Seismol. Soc. Am.*, 54:183-90.
32. Knopoff, L.,(1964). A matrix method for elastic wave problems. *Bull. Seismol. Soc. Am.*, 54:431-438.
33. Kanamori, H. and K. Abe,(1968). Deep structure of island areas as revealed by surface waves. *Bull. Earthquake Res. Inst.*, 46 : 1001-25.

34. Landisman, M., A. Dziewonski and Y. Sato, (1969). Recent improvement in the analysis of surface wave observations. *Geophys. J. R. Astron. Soc.*, 17:369-403.
35. Levshin, A. L., V. F. Pisarenko and G. A. Pogrebinsky, (1972). On a frequency-time analysis of oscillations. *Ann. Geophys.*, 28:211-218.
36. Linville, A. F. and S.J. Laster,(1967). Near-surface dispersion studies at Tonto Forest Seismological Observatory. *Bull. Seismol. Soc. Am.*, 57:311-340.
37. Meissner, R.,(1986). *The continental crust: A Geophysical approach*, London: Academic Press, 426p.
38. Molnar, P.,(1988). A review of geophysical constraints on the deep structure of the Tibetan plateau, the Himalaya and the Karakoram and their tectonic implecation. In *Tectonic Evolution of the Himalaya and Tibet*, edited by R. M. Shackleton, J. F. Dewey and B. F. Windley. Published by Royal Society, London.
39. Nag, S.K.,(1967). Surface wave dispersion and Crustal structure in the Indian ocean. *Ind. J. Met. Geoph.*, 18:119-22.
40. Negi, J.B. and V.P. Singh,(1973). Love wave dispersion analysis for the crustal structure of laterally inhomogeneous Himalayas. *Bull. Seismol. Soc. Am.*, 63:1163-72.
41. Papoulis, A., (1962). *The Fourier Integral and Its Applications*. McGraw-Hill, 318 pp.

42. Pilant, W.L.,(1979). Elastic waves in Earth, Elsevier Amsterdam-Oxford-NewYork. 493p.
43. Pines, I., Ta-Liang Teng and R. Rosenthal,(1980). A surface wave dispersion study of the crustal and upper mantle structure of China. J. Geoph. Res., Vol 85, No. B7:3829-3844.
44. Press, F.,(1956b). Determination of crustal structure from phase velocity of Rayleigh waves. Part I: Southern California. Bull. Geol. Soc. Am., 67:1647-58.
45. Press, F., A. Ben-Menahem and M.N. Toksöz,(1961). Experimental determination of earthquake fault length and rupture velocity. J. Geophys. Res., 66:3471-85.
46. Randall, M.J.,(1967). Fast programs for layered half-space problems. Bull. Seismol. Soc. Am., 57:1299-1316.
47. Rocker, S.W.,(1982). Velocity structure of the Pamir- Hindukush region: possible evidence of subducted crust. J. Geophys. Res., 87;B2: 945-959.
48. Romanowicz, B.A.,(1982). Constraints on the structure of the Tibetan plateau from pure path phase velocities of Love and Rayleigh waves. J.G.R.,87, B8:6865-83.
49. Santo, T.A.,(1963). Division of the Pacific area into seven regions in each of which Rayleigh waves have the same group velocities. Bull. Earthquake Res. Inst.,Tokyo Univ., 41:719-41.

50. Satô, Y.,(1955). Analysis of dispersed surface waves by means of Fourier Transform(I). Bull. Earthquake Res. Inst.,33:33-48.
51. Schwab, F.A.,(1970). Surface wave dispersion computations: Knopoff's method. Bull. Seismol. Soc. Am., 60:1491-1520.
52. Schwab, F.A. and L. Knopoff,(1970). Surface wave dispersion computations. Bull. Seismol. Soc. Am., 60:321-344.
53. Schwab, F.A. and L. Knopoff,(1972). Fast surface wave and free mode computations. Methods in Computational Physics, Advances in research and application, Academic Press, 11:87-180.
54. Singh, D.D.,(1987). Crustal and upper mantle velocity structure beneath north and central India from the phase and group velocity of Rayleigh and Love waves. Tectonophysics,139: 187-203.
55. Singh, D.D.,(1988). Crustal and upper mantle velocity structure beneath the northern and central Indian ocean from the phase and group velocity of Rayleigh and Love waves. Phys. of the Earth and planet interiors, 50:230-39.
56. Souriau, A.,(1981). The upper mantle beneath Ninety east ridge and Broken ridge, Indian ocean, from surface waves. Geoph. J. R. Astron. Soc., 67: 359-374.
57. Tandon, A.N.,(1973). Average thickness of the Deccan traps between Bombay and Koyna from dispersion of short period Love waves. Pure and Applied Geoph.,

109:1693-99.

58. Thomson, W.T.,(1950). Transmission of elastic waves through a stratified solid medium. J. Appl. Phys., 21:89-93.

59. Tokhi, S.,(1987).Rayleigh wave dispersion using Multiple Filter Technique and crustal structure of West Ganga Basin (M.Tech. Dissertation) University of Roorkee,42 pp

60. Van Ngoc, P.,D. Boyer,P. Therme,X. C. Yuan,L. Li, and J. G. Yuan,(1984). Relationship between the existence of intracrustal partial melting zone and deep crustal structure in southern Tibet from magnetotelluric sounding result, in Proceedings of International Symposium on Geology of the Himalayas (abstract in English),p.11, Organizing Committee,Beijing.

61. Watson, T.H.,(1970). Fast computation of Rayleigh wave dispersion in a layered half space. Bull. Seismol. Soc. Am., 60, (in Press).

62. Yuan, X. C., L. Li, J. G. Yuan, Y. P. Feng, C. H. Zhu, K. Lu, P. Van Ngoc, D. Boyer, P. Therme and J. L. Miel,(1984). Geophysical study of the formation and evolution of the earth crust and upper mantle of the Qinghai-Xizang(Tibet) plateau, in proceedings of International Symposium on Geology of the Himalaya(abstract in Chinese), p.267. Organizing committee, Beijing.(in Chun and McEvelly, 1986).

